

Research Article

Ralph M. Kaufmann and Yongheng Zhang

Permutohedral structures on E_2 -operads

DOI: 10.1515/forum-2016-0052

Received February 26, 2016; revised September 21, 2016

Abstract: There are two interesting families of E_2 -operads, those that detect double loop spaces, and those that solve Deligne's conjecture on Hochschild cochains. The first family deformation retracts to Milgram's model obtained by gluing together permutohedra along their faces. We show how the second family can be covered by permutohedra as well, shedding new light on several proposed solutions of Deligne's conjecture. In particular, our approach induces an explicit homotopy equivalence between the models of the two families. The permutohedra and partial orders play a central role providing direct links to other fields of mathematics. We for instance find a new cellular decomposition of permutohedra using partial orders and that the permutohedra give the cells for the Dyer–Lashof operations.

Keywords: Permutohedra, little discs, E_2 , configuration spaces

MSC 2010: 55P48, 55P35, 55R80, 52B12

Communicated by: Frederick R. Cohen

Introduction

Over several decades different models of E_2 -operads suitable for different purposes have been introduced: the little 2-cubes operad \mathcal{C}_2 (see [8, 30]), the little 2-discs operad \mathcal{D}_2 , the Steiner operad $\mathcal{H}_{\mathbb{R}^2}$ (see [31, 40]) which combines the good properties of \mathcal{C}_2 and \mathcal{D}_2 , and more recently the Fulton–MacPherson operad FM_2 (see [27]). Although as E_2 -operads they are all quasi-isomorphic, the individual homotopies are of interest. These homotopies are established by realizing that, up to natural homotopy (e.g. contracting intervals), these spaces are configuration spaces $\{F(\mathbb{R}^2, n)\}_{n \geq 1}$ of n distinct ordered points on \mathbb{R}^2 , whose homotopy type is known to be that of a $K(PBr, 1)$. Renewed interest in E_2 -operads stems from various solutions of Deligne's Hochschild cohomology conjecture [2, 6, 20, 27, 28, 32, 33, 41, 42, 46] and in the development of string topology [10]. In this setting cactus-type operads were invented [18, 47].

On the topological level, as we discuss, these are basically all isomorphic to the E_2 -operad Cact of spineless cacti introduced in [18]. The arity n space $\text{Cact}(n)$ roughly consists of isotopy classes of embeddings of circles with positive radii into the plane such that the images form a planted rooted planar tree picture of lobes modulo incidence parameters. For this operad and its other isomorphic versions, the proof of being an E_2 -operad is rather indirect. It was shown using pure braid group technique of Fiedorowicz [13] and cellular operad technique of Berger [4]. Here we offer a direct topological proof for the part of Fiedorowicz recognition concerning the homotopy type.

Using the different perspective of permutohedral covers, we prove the homotopy equivalence between $F(\mathbb{R}^2, n)$ and $\text{Cact}(n)$ explicitly by constructing a single homotopy equivalence between them. Permutohedra

Ralph M. Kaufmann: Department of Mathematics, Purdue University, West Lafayette, IN 47907, USA; and Max-Planck-Institute für Mathematik, Bonn, Germany, e-mail: rkaufman@math.purdue.edu

Yongheng Zhang: Department of Mathematics and Statistics, Amherst College, Amherst, MA 01002, USA, e-mail: yzhang@amherst.edu

are an essential tool in the detection of iterated loop spaces starting with Milgram [35], see also [11, 39] and [3, 29] for nice reviews. They also appear in various other contexts, see e.g. [17, 43]. The full list would be too long to reproduce. They are still an active topic of research, especially through their connection to configuration spaces of points $F(\mathbb{R}^2, n)$, which is how they appear in the E_2 -operad story, see [3]. From a totally different motivation, it has recently been shown how $F(\mathbb{R}^2, n)$ deformation retracts to Milgram's permutohedral model $\mathcal{F}(n)$ obtained by gluing $n!$ copies of permutohedra P_n along their proper faces [7]. This applies directly to all the E_2 -operads above based on configuration spaces, giving them all a permutohedral structure, i.e. they appear as a quotient of permutohedral space $\coprod_{\sigma \in S_n} P_n$ and are homotopy equivalent to Milgram's model. (Here and below, we write S_n for the symmetric group on n letters.) The exceptions are spineless cacti Cact and the models related to it, which are of a different breed. While the configuration space models are adapted to induce operad actions on iterated loop spaces, the spineless cacti models and its relatives are adapted to induce operad actions on Hochschild cochain complexes or more generally on multiplicative non-symmetric operads.

We will prove that spineless cacti and hence all of its incarnations, see Section 5, have a permutohedral cover. The appearance of permutohedra in this model is very surprising, although the construction with hindsight looks very natural. After passing to normalized spineless cacti, i.e. the spaces $\text{Cact}^1(n)$, we will show that they admit a presentation $\mathcal{C}(n)$ as the quotient of $n!$ copies of P_n . It is important to note that here there is not only gluing along faces, but parts of the interior of the permutohedra are also identified. We give an explicit description. Namely, $\text{Cact}^1(n)$ is a CW complex whose cells are indexed by a certain type of labelled rooted (actually planted) planar trees. Each planar tree has an underlying poset structure which transfers to the set of labels. We can succinctly state that each permutohedron corresponds to a possible total order on $[n] = \{1, \dots, n\}$, viz. a permutation, and it is comprised of the sub-CW complex of cells indexed by partial orders on $[n]$ that are compatible with the given total order. The gluing is then along the cells that are indexed by non-total orders. Going beyond this, there is an explicit relation between the codimension of the cells and a partial order on the partial orders. The highest codimension cells, that is cells of dimension 0 are indexed by the partial order in which no elements are comparable. Since we are dealing with planar trees, see [18], there are again orders on the sets of equal height, which means that there are indeed $n!$ dimension 0 cells, which are the vertices of the permutohedra. These combinatorics are all explained in detail below.

Due to the nature of the quotient, there is a natural map $\mathcal{F}(n) \rightarrow \text{Cact}(n)$, whose description already yields a quasi-isomorphism. We will explicitly construct the homotopy inverse induced from compatible homotopies on the $n!$ permutohedra P_n . In a sense, this map answers the question "where are the centers of the lobes in cacti?". This is not as straightforward as for the little discs, where the centers are given by the projection onto the factor of configuration space. For spineless cacti, Cact^1 corresponds to the centers. The quotient of \mathcal{F} shows how this is related to configuration.

Recall that Cact^1 has a topological operad structure, which is associative up to homotopy. This already induces an operad structure on the cellular level. No such structure is known for \mathcal{F} . This also explains why it was so difficult to find a proof of Deligne's conjecture. One can say that the operad structure only becomes apparent after taking quotients, see Section 5. This is astonishing, since instead of enlarging, we make things smaller by taking quotients.

The methods we use are classical maps and homotopies, but for the combinatorics, we use partial orders, partitions and b/w planar trees. For these, we give a common treatment and introduce several new operators, which link our work to that of Connes and Kreimer [12].

Another upshot of our treatment is a new cellular decomposition of permutohedra, which has a cube at its core and $n - 1$ shells for each P_n . In the tree language, the k th shell is given by trees with initial branching number k . There is also a nice duality between the outer faces in this decomposition of P_{n-1} and the top-dimensional cells of P_n leading to a recursion. This is established via the operators mentioned above.

The decomposition of the P_n also allows us to recognize them as the cells responsible for the Dyer–Lashof operations.

In retrospect, spineless cacti are a natural geometric model for the sequence operad of [33] (respectively the surjection operad of [6]), see [23]. We make this explicit in Section 5.1. This gives a way to show that

the model of formulas [32] and hence sequences have the right homotopy type. Our topological result also implies the result [44] on the quasi-isomorphism between the cellular chains of $\mathcal{F}(n)$ and the cellular chains of $\text{Cact}^1(n)$. See Section 5 for more details on these remarks.

The paper uses the formalism of trees, which is the most natural way to present things here. For instance the poset structures and the $B_{b/w}^\pm$ operators become obvious in this language. Some readers might be more familiar with some other encoding for the type of trees we use, such as sequences of formulas. For these readers, we provide a dictionary between the different encodings of the same structures.

The organization of the paper is as follows. Section 1 fixes frequently used notations and introduces the definition of unshuffles of a sequence. We also recall the definition and basic properties of the permutohedron P_n and the permutohedral structure $\mathcal{F}(n)$ of $F(\mathbb{R}^2, n)$. Section 2 recalls the definition of spineless cacti and makes explicit its polysimplicial structure. The permutohedral structure $\mathcal{C}(n)$ of $\text{Cact}^1(n)$ is given in Section 3 using partial and total orders. This contains one direction of the homotopy equivalence. Here, we also introduce four operators $B_{b/w}^\pm$ acting on trees that are essential in keeping track of the combinatorics. These operators are analogous to those used in [12]. The homotopy equivalence between $\mathcal{F}(n)$ and $\mathcal{C}(n)$ is proven in Section 4, by giving an explicit homotopy inverse. Some of the more tedious details are relegated to Appendix A. We give a more detailed discussion of E_2 -operads and applications in Section 5. Appendix B contains the dictionary needed to translate the different ways to encode things, namely trees, sequences and formulas.

1 Permutations, permutohedra and Milgram's model

In this section, we start by recalling the definition of a permutohedron. We then set up the combinatorial language, which we will use for indexing. This is unavoidably a bit complex, as we will have to deal with lists of lists. Thus we will introduce a short hand notation for these lists and manipulations on them. Besides reducing clutter, an additional benefit is an easy description of a poset structure and a grading. This allows us to encode the poset structure of the faces of permutohedra in this formalism.

1.1 Permutohedra

Before we recall the definition of our main actors, the permutohedra [35], we fix our notations for sequences in general and elements in the symmetric group S_n in particular.

Definition 1.1. Let \mathbb{N}^+ the set of positive integers. For $n \in \mathbb{N}^+$, set $[n] = \{1, 2, \dots, n\}$. A *sequence* of length n is a function $\phi : [n] \rightarrow \mathbb{N}^+$; ϕ is called a *non-repeating sequence* (nr-sequence) if this function is also injective. We say the length $|\phi|$ of ϕ is n . By Seq_n , we mean the set of all sequences of length n and Seq_n^{nr} , the set of all nr-sequences of length n .

Notation 1.2. Any nr-sequence can be identified by a nonempty ordered list of distinct elements in \mathbb{N}^+ given by its images. Denote by $\phi_i := \phi(i)$ the image of i under ϕ . By abuse of notation, to specify ϕ , we will use the following list notation, $\phi_1\phi_2 \cdots \phi_n$, where we do not use commas to separate the terms if no confusion arises. We write $\{\phi\}$ for the image of ϕ , which is the set $\{\phi(1), \phi(2), \dots, \phi(n)\}$.

Example. The symmetric group S_n consists of $n!$ bijective functions $\sigma : [n] \leftrightarrow [n]$, namely nr-sequences of length n whose domain and codomain coincide. Each σ can be identified with the list of its images $\sigma_1\sigma_2 \cdots \sigma_n$. This is a short hand for the traditional notation

$$\begin{pmatrix} 1 & 2 & 3 & \dots & n \\ \sigma(1) & \sigma(2) & \sigma(3) & \dots & \sigma(n) \end{pmatrix}.$$

For example 1234 is $\text{id} \in S_4$ and 2143 is the product of the transpositions switching 1 and 2, and 3 and 4, respectively.

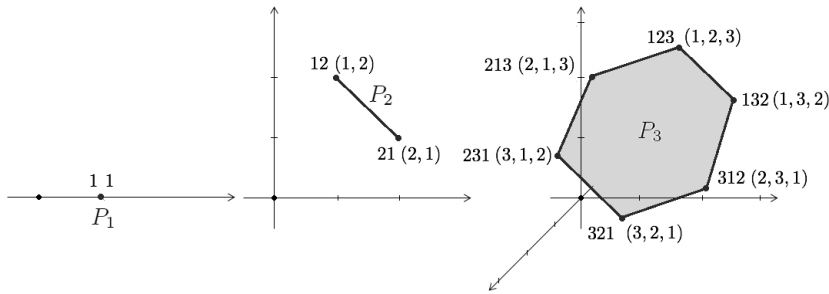


Figure 1. The permutohedra P_1 , P_2 and P_3 . Each vertex is labelled σ on the left and \mathbf{v}_σ on the right.

Definition 1.3. Given $\sigma \in S_n$, we define the vector \mathbf{v}_σ in \mathbb{R}^n as follows:

$$\mathbf{v}_\sigma := (\sigma^{-1}(1), \sigma^{-1}(2), \dots, \sigma^{-1}(n)).$$

Remark 1.4. Here, we follow the convention of labelling the vertices by the inverse permutations, see e.g. [17], which has the effect that the faces of permutohedra will be conveniently labelled by unshuffles (see below). This is the formalism we will work with.

Alternatively, see [37], one can look at the list of coordinates as a surjection and then the faces are also labelled by surjections. The passage from σ to σ^{-1} also has the effect changing the action from a left to a right action and accordingly from the left weak Bruhat order to the right weak Bruhat order.

Example. If $\sigma = 3241$, then $\sigma^{-1} = 4213$ and thus $\mathbf{v}_\sigma = (4, 2, 1, 3) \in \mathbb{R}^4$.

Definition 1.5. The permutohedron P_n is the convex hull of the set of points $\{\mathbf{v}_\sigma \in \mathbb{R}^n : \sigma \in S_n\}$, i.e.

$$P_n = \left\{ \sum_{\sigma \in S_n} t_\sigma \mathbf{v}_\sigma \in \mathbb{R}^n : \sum_{\sigma \in S_n} t_\sigma = 1, t_\sigma \geq 0 \right\}.$$

See Figure 1 for examples.

The permutohedron P_n enjoys the following features which are readily checked:

- (1) P_n is a polytope of dimension $n - 1$.
- (2) The vertex set of P_n is $\{\mathbf{v}_\sigma \in \mathbb{R}^n : \sigma \in S_n\}$.
- (3) P_n is contained in the hyperplane $\{(x_1, \dots, x_n) \in \mathbb{R}^n : x_1 + \dots + x_n = \frac{(n+1)n}{2}\}$.
- (4) Two vertices $\mathbf{v}_\sigma, \mathbf{v}_\tau$ of P_n , $n \geq 2$, are adjacent if and only if \mathbf{v}_τ is obtained from \mathbf{v}_σ by switching two coordinate values differing by 1 (or τ is obtained from σ by switching two adjacent numbers in their image lists). In this case the Euclidean distance from \mathbf{v}_σ to \mathbf{v}_τ is the minimal distance between two vertices, which is $\sqrt{2}$.
- (5) Its dimension $n - k$ faces are affinely isomorphic to $P_{m_1} \times P_{m_2} \times \dots \times P_{m_k}$.

1.2 Notation for subsequences and unshuffles

1.2.1 Subsequences

Definition 1.6. A *subsequence* of length k ($k \leq n$) of the sequence $\phi : [n] \rightarrow \mathbb{N}^+$ is a composite of functions $\phi \circ \psi$, where $\psi : [k] \hookrightarrow [n]$ is strictly increasing. In the short hand notation, $\phi \circ \psi$ is simply written as $\phi_{\psi_1} \phi_{\psi_2} \dots \phi_{\psi_k}$. In particular, for $n \geq 2$ and $\sigma \in S_n$, we define $\sigma \setminus \sigma_1$ to be the subsequence $\sigma \circ \delta_1$, where $\delta_1 : [n - 1] \rightarrow [n]$ is the first face map $\delta_1(i) = i + 1$.

So $\sigma \setminus \sigma_1$ can also be written $\sigma_2 \sigma_3 \dots \sigma_n$. Thus, $\sigma \setminus \sigma_1$ is obtained by removing the first term in the sequence $\sigma_1 \sigma_2 \dots \sigma_n$.

Example. If $\sigma \in S_4$ is the sequence 2341, then $\sigma \setminus \sigma_1$ is 341.

1.2.2 Shuffles and unshuffles

Definition 1.7. An *unshuffle* (or *deshuffle*) of a sequence ϕ into k subsequences of lengths m_1, m_2, \dots, m_k is an ordered list of subsequences $\mathbf{l}_1, \mathbf{l}_2, \dots, \mathbf{l}_k$ of ϕ such that $|\mathbf{l}_i| = m_i$ and the disjoint union $\coprod_{i=1}^k \{\mathbf{l}_i\}$ equals $\{\phi\}$. We also call ϕ a *shuffle* of $\mathbf{l}_1, \mathbf{l}_2, \dots, \mathbf{l}_k$.

We define $\text{dSh}_\phi[m_1, \dots, m_k]$ to be the set of all unshuffles of the sequence ϕ into subsequences of lengths m_1, \dots, m_k , $\text{dSh}_\phi(k) = \coprod_{(m_1, \dots, m_k)} \text{dSh}_\phi[m_1, \dots, m_k]$ to be the set of all unshuffles of ϕ into k subsequences and $\text{dSh}_\phi = \coprod_k \text{dSh}_\phi(k)$ to be the set of all unshuffles of ϕ .

Notation 1.8. We will use the following bar notation to give elements of $\text{dSh}_\phi(k)$. We write $\mathbf{l}_1|\mathbf{l}_2|\dots|\mathbf{l}_k$, $k \geq 1$, for the list $\mathbf{l}_1, \mathbf{l}_2, \dots, \mathbf{l}_k$, i.e. when ϕ is a shuffle of $\mathbf{l}_1, \mathbf{l}_2, \dots, \mathbf{l}_k$.

Example. Let $3214 \in S_4$. Then $\text{dSh}_{3214}[3, 1]$ consists of the four elements $321|4$, $324|1$, $314|2$ and $214|3$, and $\text{dSh}_{3214}[2, 2]$ consists of $32|14$, $31|24$, $34|21$, $21|34$, $24|31$ and $14|32$.

1.2.3 Grading and poset structure

We define the degree (deg) of elements in $\text{dSh}_\phi(k)$ to be $|\phi| - k$. This is the length of ϕ minus 1, minus the number of bars ($k - 1$). It lies between $|\phi| - 1$ and 0.

On lists there is the operation of merging lists. Given two sequences $\mathbf{l}_1, \mathbf{l}_2$ with disjoint images $\{\mathbf{l}_1\}$ and $\{\mathbf{l}_2\}$, we define $\mathbf{l}_1\mathbf{l}_2 : [|\mathbf{l}_1| + |\mathbf{l}_2|] \rightarrow \mathbb{N}^+$ by

$$\mathbf{l}_1\mathbf{l}_2(i) = \begin{cases} (\mathbf{l}_1)_i & \text{if } i = 1, \dots, |\mathbf{l}_1|, \\ (\mathbf{l}_2)_{i-|\mathbf{l}_1|} & \text{if } i = |\mathbf{l}_1| + 1, \dots, |\mathbf{l}_1| + |\mathbf{l}_2|. \end{cases}$$

Note that in our shorthand notation the merging of two lists is exactly the juxtaposition given by removing a bar.

The partial order $<$ on dSh_ϕ is generated by removing bars and shuffling the lists. More precisely, $<$ is the transitive closure of the relation

$$\mathbf{l}_1 \cdots |\mathbf{l}_{i-1}|\mathbf{l}_i|\mathbf{l}_{i+1}|\mathbf{l}_{i+2}| \cdots |\mathbf{l}_k| < \mathbf{l}_1|\cdots|\mathbf{l}_{i-1}|\mathbf{h}|\mathbf{l}_{i+2}| \cdots |\mathbf{l}_k|, \quad (1.1)$$

where $\mathbf{l}_i|\mathbf{l}_{i+1} \in \text{dSh}_\mathbf{h}(2)$ or simply \mathbf{h} is a shuffle of $\mathbf{l}_i, \mathbf{l}_{i+1}$. It follows that the partial order decreases degree; that is if two elements that are in the relation $\mathbf{a} < \mathbf{b}$, then $\text{deg}(\mathbf{a}) < \text{deg}(\mathbf{b})$.

Notation 1.9. Let \mathcal{J}_ϕ denote the poset $(\text{dSh}_\phi, <)$ and let \mathcal{J}_ϕ^i , $i = 0, 1, \dots, |\phi| - 1$, be the subset consisting of elements of degree i in \mathcal{J}_ϕ .

Example. For $\sigma = 145372896 \in S_9$, we have $153|49|76|28 < 153|4796|28$, which are elements in \mathcal{J}_σ^5 and \mathcal{J}_σ^6 , respectively.

Remark 1.10. Notice that any poset \mathcal{J}_ϕ represents a category by setting $\text{Hom}(\mathbf{a}, \mathbf{b}) = \{(\mathbf{a}, \mathbf{b})\}$ if $(\mathbf{a} \leq \mathbf{b})$. The category has a terminal element $\phi_1 \cdots \phi_n$. One can formally add the one element set \mathcal{J}_ϕ^{-1} and obtain an initial object.

Remark 1.11. Another way to understand the poset structure is that for $\phi = 12 \cdots n$, the elements of the set $\text{dSh}_\phi[m_1, \dots, m_k]$ can be seen as the cosets of S_n with respect to the Young subgroups $S_{m_1} \times \cdots \times S_{m_k}$, partially ordered by inclusion. For this identification one should choose the representative in the coset that agrees with the original order given by ϕ .

1.2.4 Geometric realization

We define the geometric realization of \mathcal{J}_ϕ which is formally a functor \mathcal{F} from \mathcal{J}_ϕ to the category of topological spaces and inclusions – in fact, polytopes and face inclusions, which are inclusions of $\mathbb{R}^n \rightarrow \mathbb{R}^m$ and affine

transformations. Although it would be more natural to order using ϕ , to match the conventions of faces given by lists, instead of surjections, we will use the inverse ordering.

Let $\phi \in \text{Seq}_n^{\text{nr}}$. Now ϕ is injective and hence restricting it to its image, we get a map $\phi^{-1} : \text{Im}(\phi) \rightarrow [n]$. We let $\phi_1^{-1}, \dots, \phi_n^{-1}$ be the ordered preimage, that is ϕ_1^{-1} is ϕ^{-1} applied to the smallest image of ϕ . In particular, if $\phi = \sigma$ a permutation, then $\phi^{-1} = \sigma^{-1}$, the inverse permutation and the notation agrees with the previous one.

Define $\mathbf{v}_\phi = (\phi_1^{-1}, \phi_2^{-1}, \dots, \phi_n^{-1}) \in \mathbb{R}^n$. Then \mathcal{F} is defined by

$$\mathcal{F}(\phi_1|\phi_2|\dots|\phi_n) = \mathbf{v}_\phi$$

on degree 0 elements and $\mathcal{F}(\mathbf{a})$ is defined to be the convex hull of $\{\mathcal{F}(\mathbf{b}) \in \mathbb{R}^n : \mathbf{b} \in \mathcal{J}_\phi^0, \mathbf{b} \leq \mathbf{a}\}$ for general $\mathbf{a} \in \mathcal{J}_\phi$. Finally, we define \mathcal{F} on $<$ to be face inclusions.

Proposition 1.12. *If $\phi \in \text{Seq}_n^{\text{nr}}$, then $\mathcal{F}(\phi)$ is a $(|\phi| - 1 = n - 1)$ -dimensional polytope, whose dimension i faces correspond to elements of \mathcal{J}_ϕ^i . In particular, for a permutation $\sigma : [n] \hookrightarrow [n]$, we have*

$$\mathcal{F}(\mathcal{J}_\sigma) = P_n.$$

In the latter equality the data of σ is present in the labellings.

Proof. One can reduce to $\sigma = \text{id}$ and then we refer the reader to [3, 9, 17, 29, 35, 49] for a proof. □

The example of the labelling of P_σ for $\sigma = 1234 \in S_4$ is given in Figure 2.

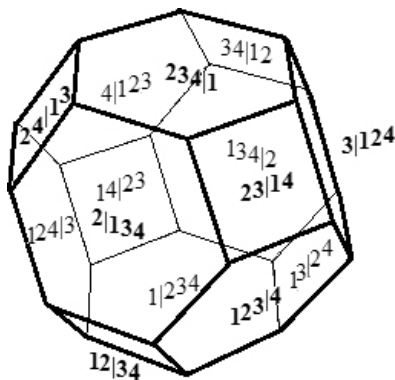


Figure 2. The codimension 1 faces of P_4 and their indexing elements in \mathcal{J}_{1234}^2 . Visible faces are labelled by bold-faced numbers. The faces of the types $abc|d$, $ab|cd$ and $a|bcd$ are affinely isomorphic to $P_3 \times P_1$, $P_2 \times P_2$ and $P_1 \times P_3$, respectively.

Note that $F(\mathbb{R}^2, n)$ deformation retracts to a space which is obtained by gluing $n!$ copies of P_n . We first describe the gluing data through a poset \mathcal{J}_n which contains all the $n!$ posets \mathcal{J}_σ introduced in the previous section.

1.3 Milgram’s model via the poset $\mathcal{J}(n)$

Definition 1.13. As a set, the poset $\mathcal{J}(n)$ equals the union $\bigcup_{\sigma \in S_n} \mathcal{J}_\sigma$. The partial order of $\mathcal{J}(n)$ is defined the same way as that in (1.1).

Notice that we are dealing with the union and not the disjoint union. So elements of \mathcal{J}_σ and $\mathcal{J}_{\sigma'}$ can become identified. The poset structure on the union is still given by removing bars and shuffling the lists, such that resulting partial orderings are compatible with restriction to subsequences.

Example. Note that 1234 is the only element in \mathcal{J}_{1234} that is greater than 13|24. But in $\mathcal{J}(4)$, the elements greater than 13|24 are 1324, 1234, 1243, 2134, 2143 and 2413.

Definition 1.14. We extend \mathcal{F} from $\mathcal{J}_\sigma, \sigma \in S_n$ to $\mathcal{J}(n)$ naturally by setting

$$\mathcal{F}(n) := \operatorname{colim}_{\mathcal{J}(n)} \mathcal{F}.$$

This means that as a topological space $\mathcal{F}(n)$ is obtained by gluing $n!$ copies of P_n along their proper faces according to the partially order set $\mathcal{J}(n)$. Alternatively, we can write

$$\mathcal{F}(n) = \left(\prod_{\sigma \in S_n} P_n \right) / \sim_{\mathcal{F}},$$

where for $x \in P_n$ indexed by σ and $y \in P_n$ indexed by τ , $x \sim_{\mathcal{F}} y$ if there is $\mathbf{a} \in \mathcal{J}_\sigma \cap \mathcal{J}_\tau$ such that x and y have the same coordinates in $\mathcal{F}_{\mathbf{a}}$ (we simply write $x = y \in \mathcal{F}_{\mathbf{a}}$ in the future).

1.4 Permutohedral structure of $F(\mathbb{R}^2, n)$: A theorem of Blagojević and Ziegler

Theorem 1.15 ([7]). *The space $\mathcal{F}(n)$ is homeomorphic to a strong deformation retract of $F(\mathbb{R}^2, n)$.*

Remark. That $\mathcal{F}(n)$ and $F(\mathbb{R}^2, n)$ have the same homotopy type was known before this theorem. For example, Berger [3] showed this by establishing a zig-zag connecting $\mathcal{F}(n)$ and $F(\mathbb{R}^2, n)$. But this theorem is stronger: it shows that one is actually the deformation retract of the other. In fact, [7] described regular CW complex models which are homeomorphic to deformation retracts of the configuration spaces $F(\mathbb{R}^k, n)$ for all $k, n \geq 1$, which were used in their proof when n is a prime power of the conjecture of Nandakumar and Ramana Rao that every polygon can be partitioned into n convex parts of equal area and perimeter. The same CW complex models were also studied in [3] and [16] and they were called the Milgram's permutohedral model in [3].

Historically, the first reference dealing with a combinatorial stratification of $F(\mathbb{R}^2, n)$ is Fox–Neuwirth [14] and the connection to hyperplane arrangements was given by Salvetti [38]. A main contribution of [7] and [38] consists in having well understood that the duals of the Fox–Neuwirth posets can be realized themselves as certain deformation retracts of $F(\mathbb{R}^2, n)$. This dualization process is important because it yields precisely the Milgram posets $\mathcal{J}(n)$.

We briefly review the proof of the above theorem here.

Sketch of proof according to [7]. First, \mathbb{R}^{2n} deformation retracts to the subspace $W_n^{\oplus 2}$ in which the geometric center of each configuration is shifted to the origin. We denote this retraction by r_1 . Then $W_n^{\oplus 2} \setminus 0^n$ is partitioned into relatively open infinite polyhedral cones. These cones give the Fox-Neuwirth stratification of $W_n^{\oplus 2} \setminus 0^n$ and they constitute a partially ordered set. Next, a relative interior point for each cone is chosen. These points yield the vertices of a star-shaped PL cell. Then $W_n^{\oplus 2} \setminus 0^n$ radially deformation retracts to the boundary of this PL cell. We denote this retraction by r_2 . Finally, the Poincaré–Alexander dual complex of $r_2 \circ r_1(F(\mathbb{R}^2, n))$ relative to $r_2(W_n^{\oplus 2} \setminus 0^n \setminus r_1(F(\mathbb{R}^2, n)))$ is constructed, which is a deformation retract of $r_2 \circ r_1(F(\mathbb{R}^2, n))$. Let this third retraction be r_3 . In conclusion, $F(\mathbb{R}^2, n)$ deformation retracts to $r_3 \circ r_2 \circ r_1(F(\mathbb{R}^2, n))$, which has a partially ordered set structure with the partial order the reverse of that of the Fox-Neuwirth stratification. This partially ordered set is precisely $\mathcal{J}(n)$ and $\mathcal{F}(n)$ is homeomorphic to $r_3 \circ r_2 \circ r_1(F(\mathbb{R}^2, n))$. \square

2 The operad of spineless cacti

2.1 The spineless cacti operad \mathbf{Cact} and its normalized version $\mathbf{Cact}^1(n)$

The operad of spineless cacti \mathbf{Cact} was introduced in [18]. We first briefly review $\mathbf{Cact} = \{\mathbf{Cact}(n)\}_{n \geq 1}$ using the intuitive picture of cacti from [47]. Although very intuitive, this description is unexpectedly hard to make precise topologically. A better way to define the spaces is to first define CW complexes \mathbf{Cact}^1 , the spaces of normalized spineless cacti, which correspond to the restriction to lobes of radius 1 and then extend to all positive radii by taking products with \mathbb{R}_+^n (see [18]).

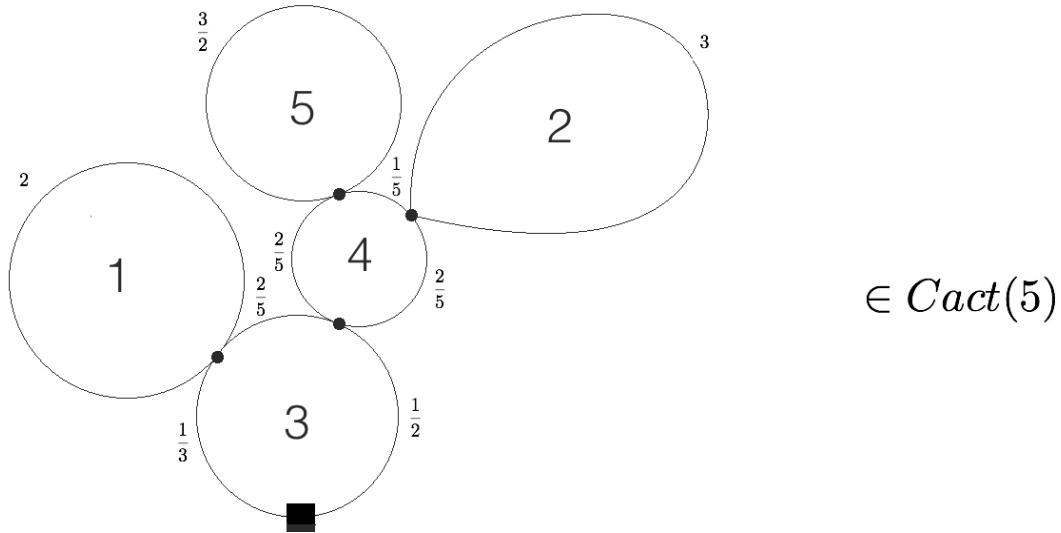


Figure 3. A representative of an element in $Cact(5)$ representing isotopy class of orientation and intersection parameter preserving embeddings of the five standard circles of radii $2, 3, \frac{37}{30}, 1, \frac{3}{2}$ such that the images form a rooted planted tree-like configuration of circles. The local zeros are denoted by black dots. The global zero is denoted by a black square.

2.1.1 Pictorial description

Roughly a cactus [47] is an isotopy class of tree-like configuration of circles in the plane with a given base point. Here a circle is an orientation preserving embedding $S^1_r \rightarrow \mathbb{R}^2$, where $S^1_r = \{x^2 + y^2 = r^2\}$ and the isotopies should preserve the incidence relations. The circles are also called lobes. The images of the base points are called local roots or zeros and the root is called a global zero. To be a spineless cactus means that any local zero is the unique intersection point of the lobe with the lobe closer to the global zero (this exists due to the tree-like structure). An element of $Cact(5)$ is given in Figure 3.

Notice that for any $c \in Cact(n)$, if one starts from the root vertex (the black square) and travel around the perimeter of the configuration, then one will eventually come back to the root vertex. The path travelled gives a map from S^1 to the configuration and is called the outside circle.

2.1.2 CW-complex

First notice that a configuration as described above gives rise to a b/w rooted bipartite graph τ . The white vertices are the lobes and the black vertices are the zeros, with the global zero being the root. A black vertex is joined by an edge to a white vertex if the corresponding point lies on the lobe. Tree-like means that the graph is a tree. This tree is also planar, since the configuration was planar. A cactus is spineless if the local zero is at the unique intersection point nearest the root, and hence can be ignored. We now turn this observation around to make a precise definition.

Each $Cact^1(n)$ is a regular CW complex whose cells are indexed by planted planar black and white bipartite trees with a black root and white leaves and a total of n labelled white vertices. The open cell \dot{C}_τ indexed by the tree τ is defined as the product of open simplices $\prod_{i=1}^n \Delta^{|v_i|-1}$, where $|v_i|$ is the number of incident edges of the white vertex labelled i . The number of incoming edges or the arity is then $|v_i| - 1$. The closure $C(\tau)$ equals $\prod_{i=1}^n \Delta^{|v_i|-1}$ and it is attached by collapsing angles at white vertices, see [18] and Figure 4 for details. This angle collapse corresponds to the contraction of an arc of a lobe, e.g. the arc labelled by $\frac{1}{2}$ or $\frac{2}{5}$ in Figure 3. These arc-labels correspond to the barycentric coordinates of the simplices. The attaching map can then be understood as sending one of these coordinates to zero, removing this coordinate and identifying the result with the barycentric coordinates of the tree obtained by collapsing the angle.

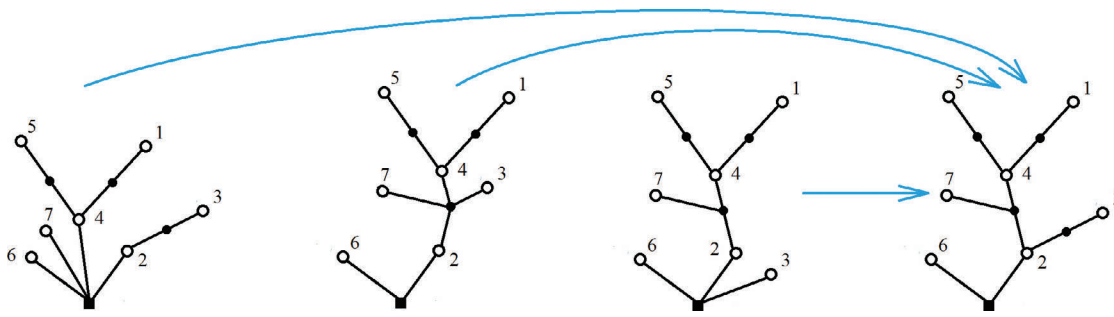


Figure 4. Example of angle collapses having the same target τ .

The space $\text{Cact}(n)$ is the product $\text{Cact}^1(n) \times \mathbb{R}_{>0}^n$ with the product topology. Note that $\text{Cact}(n)$ naturally deformation retracts to $\text{Cact}^1(n)$.

2.1.3 Grading

For a tree τ we define its degree as $i = \dim(C(\tau)) = \sum_i (|v_i| - 1)$. It follows from the fact that τ is a b/w bipartite tree that the maximal dimension of cells in $\text{Cact}^1(n)$ is $n - 1$ and the codimension of a cell $C(\tau)$ is $\text{codim}(C(\tau)) = \sum_{v: \text{black vertex}} (\text{ar}(v) - 1)$, where $\text{ar}(v)$ is the arity of v , that is the number of incoming edges $\text{ar}(v) = |v| - 1$. This is also the number of angle collapses, as each angle collapse reduces the number of black vertices by one and adds the arities. Let \mathcal{T}_n^i be the subset of \mathcal{T}_n of degree i . The set \mathcal{T}_n^0 consists of the minimal degree elements in \mathcal{T}_n and \mathcal{T}_n^{n-1} the maximal degree elements; \mathcal{T}_n^0 is also the set of trees indexing the spineless corolla cacti $\text{SCC}(n)$ [18]. We let $\text{scc}(\sigma)$ be the element in \mathcal{T}_n^0 shown in Figure 5.

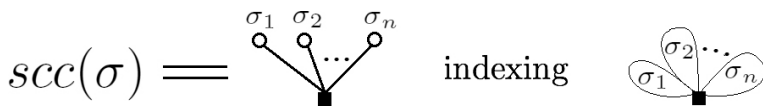


Figure 5. The spineless corolla cactus element $\text{scc}(\sigma)$ for $\sigma \in S_n$.

2.1.4 Operadic structure

Although not strictly needed for the present discussion, we give the operad structure of this E_2 -operad using the intuitive picture. Given $c_1 \in \text{Cact}(m)$ and $c_2 \in \text{Cact}(n)$, $c_1 \circ_i c_2 \in \text{Cact}(m + n - 1)$ is obtained by rescaling the outside circle of c_2 to that of the i th circle of c_1 and then identifying the outside circle of the resultant configuration to the i th lobe of c_1 . Note that S_n acts on $\text{Cact}(n)$ by permuting the labels.

One can check that the above structures make Cact an operad (more precisely, pseudo-operad).

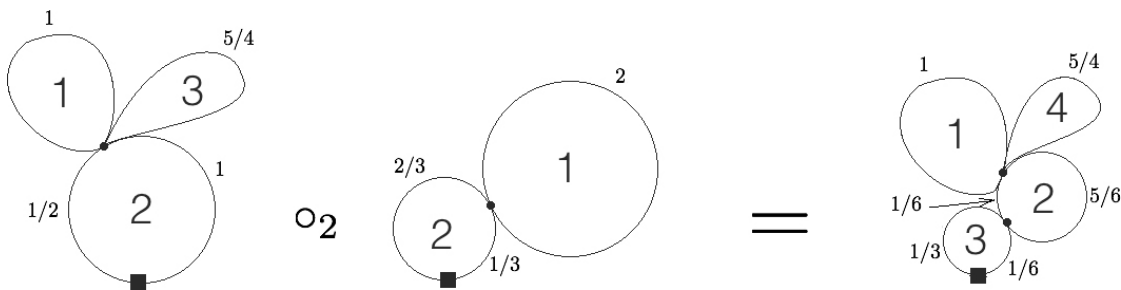


Figure 6. An example of operadic insertion $\circ_2 : \text{Cact}(3) \times \text{Cact}(2) \rightarrow \text{Cact}(4)$.

2.1.5 Summary

Let \mathcal{T}_n denote the partially ordered set of planar planted bipartite (black and white) trees with white leaves, a black root, and n white vertices labelled from 1 to n . Denote by \mathcal{T}_n^i the subset of trees with degree i . Then as a stratified set

$$\text{Cact}^1(n) = \coprod_{\tau \in \mathcal{T}_n} \mathring{C}_\tau \tag{2.1}$$

and as a space

$$\text{Cact}^1(n) = \coprod_{\tau \in \mathcal{T}_n} C(\tau)/\sim = \coprod_{\tau \in \mathcal{T}_n^{n-1}} C(\tau)/\sim, \tag{2.2}$$

where $x \sim y$ is in the closure of the relation induced by the attaching maps. The last equation is true, since all points are included in some top-dimensional cell.

2.2 Reformulation of $\text{Cact}^1(n)$ as the colimit of a poset

The main result in this subsection is that the angle collapse actually gives a poset structure to \mathcal{T}_n . Moreover, since gluing procedures are alternatively described by relative coproducts, we can ultimately describe Cact^1 as the colimit of a realization functor over a poset category.

We say that $\tau \angle \tau'$ if τ can be obtained from τ' by an angle collapse.

Definition 2.1. Let $\prec_{\mathcal{T}}$ be the partial order obtained from the transitive closure of the relation \angle on \mathcal{T}_n induced by angle collapse.

Again, $\tau \prec_{\mathcal{T}} \tau'$ implies $\deg(\tau) < \deg(\tau')$ and the minimal elements form the set $\text{SCC}(n)$ and the maximal elements are those of \mathcal{T}_n^{n-1} .

Let C be the following functor from the poset category $(\mathcal{T}_n, \prec_{\mathcal{T}})$ to the category of topological spaces. That is for each pair $\tau \preceq_{\mathcal{T}} \tau'$ there is a unique arrow $\tau \rightarrow \tau'$.

- (1) For $\tau \in \mathcal{T}_n$, $C(\tau)$ is defined as before: $C(\tau) = \Delta^{w_1} \times \Delta^{w_2} \times \cdots \times \Delta^{w_n}$, where w_i is the number of incoming edges to the white vertex labelled by i .
- (2) If $\tau \angle \tau'$, and τ is obtained from τ' by collapsing the angle between the j th and the $(j + 1)$ th incoming edges of the white vertex i (where we define the 0th and the $(w_i + 1)$ st incoming edges to be the outgoing edge of this white vertex), then

$$C(\tau \angle \tau') = \text{id}_{\Delta^{w_1}} \times \cdots \times \text{id}_{\Delta^{w_{j-1}}} \times s_j \times \text{id}_{\Delta^{w_{j+1}}} \times \cdots \times \text{id}_{\Delta^{w_n}},$$

where s_j is the j th degeneracy map

$$s_j : \Delta^{w_i-1} \rightarrow \Delta^{w_i}, \quad (t_0, t_1, \dots, t_{w_i-1}) \mapsto (t_0, t_1, \dots, t_{j-1}, 0, t_j, \dots, t_{w_i-1}).$$

Then it follows from (2.2) that:

Proposition 2.2. We have $\text{Cact}^1(n) = \text{colim}_{\mathcal{T}_n} C$. □

An example of the gluing is given in Figure 7.

2.3 $\text{Cact}^1(n)$ as a multi-simplicial set

What is actually obvious from this reformulation, but not stated explicitly in [18] is that Cact^1 is not only a regular CW complex, but the realization of a multi-semi-simplicial set. This becomes obvious by the description of the cells as products of simplices: $C(\tau) = \Delta^{w_1} \times \Delta^{w_2} \times \cdots \times \Delta^{w_n}$. The multi-degeneracy maps are given by angle collapses.

Proposition 2.3. The set \mathcal{T}_n is multi-semi-simplicial and $\text{Cact}^1(n) = |\mathcal{T}_n|$. □

In a different language, this has been observed explicitly in [2].

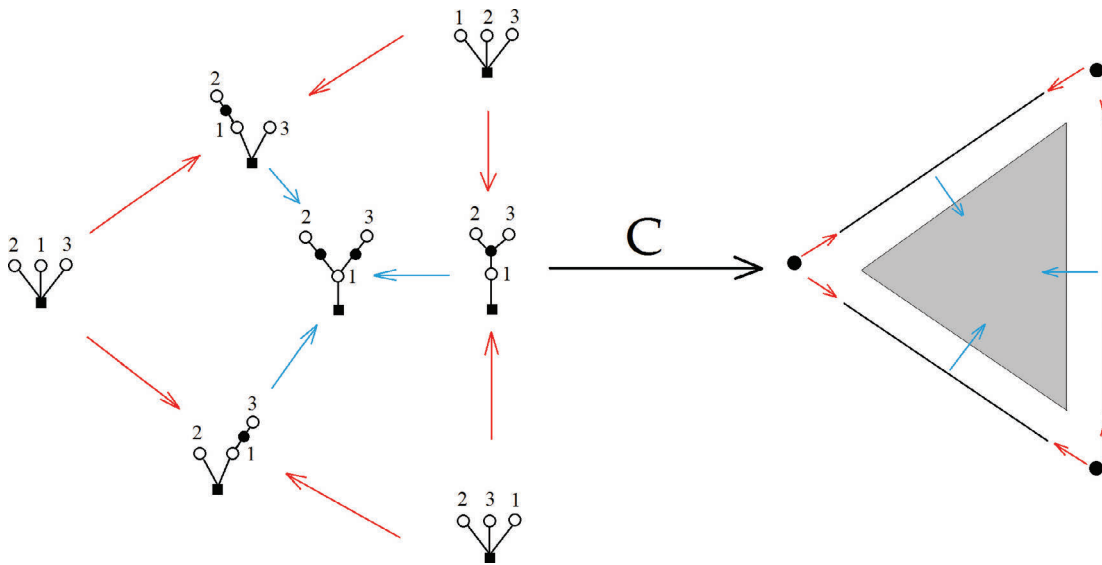


Figure 7. A subset of \mathcal{T}_n and its image under the functor C .

3 A permutohedral cover for $\text{Cact}^1(n)$

3.1 Tools and setup

Here we provide the necessary combinatorial tools for the statements and proofs. We introduce several partial and total orders in order to define $n!$ sub-posets, each of which corresponds to a permutohedron P_n .

3.1.1 Total and partial orders

For a given finite set S with $|S| = n$ the linear orders on S are in bijection with the set of bijective maps $\phi : [n] \rightarrow S$. In particular, the linear orders on $[n]$ are in bijection with permutations $\sigma \in S_n$, the order being explicitly given by $\sigma_1 < \dots < \sigma_n$. We denote this linear order (total order) by $<_\sigma$.

Every rooted tree τ yields a partial order on its vertices by the height where the root is considered to be the lowest vertex. The root is the unique minimal element and the leaves are the maximal elements. For the trees in \mathcal{T}_n , by abuse of notation, we denote by $<_\tau$ the induced partial order on the set of labels $[n]$ of the white vertices. We say $v <_\tau w$ if w is above v . This is especially easy to read off the cactus picture.

Definition 3.1. On a given set S a partial order $<$ is coarser than $<'$, if $a < b$ implies $a <' b$. If $<'$ is a total order $<$, then we also say that $<$ is compatible with $<'$.

Notice that if S is finite to show that $<$ is coarser than $<'$ one can simply check along all maximal intervals $[s_1, s_2]$ with respect to $<$.

3.1.2 The posets for P_n

To describe the permutohedral structure of $\text{Cact}^1(n)$, for any $\sigma \in S_n$, we introduce the sub-poset $(\mathcal{T}_\sigma, <_\mathcal{T})$ of $(\mathcal{T}_n, <_\mathcal{T})$ as follows.

Definition 3.2. The elements of \mathcal{T}_σ are the trees in \mathcal{T}_n such that $<_\tau$ is compatible with $<_\sigma$. The partial order of \mathcal{T}_σ is the restriction of that of \mathcal{T}_n . These sets inherit the degree splitting $\mathcal{T}_\sigma^i, i = 0, 1, \dots, n - 1$, of trees of degree i .



Figure 8. Examples of trees in \mathcal{T}_{53214} and the associated cacti pictures.

Recall that for the trees the set S is the set of white vertices. This means that the trees in \mathcal{T}_σ are those whose white vertices are labelled by S , such that the partial tree order on S , seen as the white vertices, is compatible with the one given by σ .

The maximal intervals of \prec_τ correspond the leaf vertices and are given by the sequence of labels on the white vertices along the shortest path from the root vertex to this leaf vertex. Thus \prec_τ is compatible with \prec_σ if all these sequences are subsequence of $\sigma_1 \cdots \sigma_n$. Some examples of trees in \mathcal{T}_{53214} are given in Figure 8.

Notice that in \mathcal{T}_σ there is a unique element which we call τ_σ such that the partial order $\prec_{\tau_\sigma} = \prec_\sigma$.

Collapsing an angle between the leftmost (or rightmost) incoming edge with the outgoing edge of a white vertex makes the partial order on a tree coarser. Collapsing an angle between two adjacent incoming edges does not change the partial order on a tree. Thus, we have that:

Lemma 3.3. *The sub-posets \mathcal{T}_σ are closed under angle collapses. That is if $\tau \in \mathcal{T}_\sigma$ and $\tau' \prec \tau$, then τ' is also in \mathcal{T}_σ .* □

In our later proofs, we also need trees whose white vertices are labelled with an arbitrary subset S of \mathbb{N}^+ and the corresponding orders, the generalization is intuitively clear from the example in Figure 9.

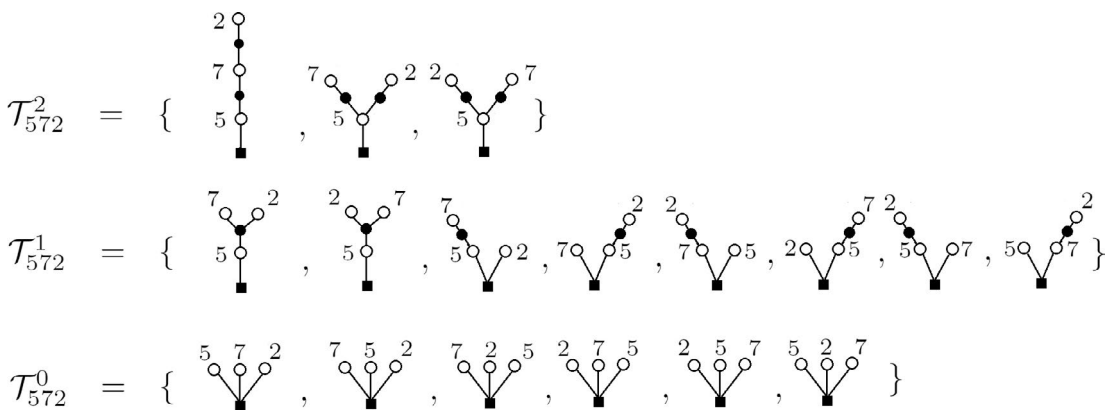


Figure 9. The sets $\mathcal{T}_{572}^2, \mathcal{T}_{572}^1, \mathcal{T}_{572}^0$.

To be precise, we give the technical version. If V_w is the set of white vertices, then a labelling $\text{lab} : S \subset \mathbb{N}^+ \rightarrow V_w$ is a bijection $\phi : S \xrightarrow{\sim} V_w$. We let \mathcal{T}_S be the set of S -labelled planar b/w bipartite trees with a black root and white leaves. If $|V_w| = n$, let $\phi : [n] \rightarrow S$ be a linear order on S .

Definition 3.4. Given S and an order ϕ on it we define the set \mathcal{T}_ϕ to be the subset of \mathcal{T}_S of trees τ whose partial order $<_\tau$ is compatible with the order $<_\phi$.

This directly generalizes Definition 3.2 and Lemma 3.3 holds accordingly.

Example. If $\phi : [3] \rightarrow S = \{2, 5, 7\} \subset \mathbb{N}^+$ maps $1 \mapsto 5$, $2 \mapsto 7$ and $3 \mapsto 2$, then we can consider the S -labelled trees τ such that $<_\tau$ is compatible with $<_\phi$. This is depicted in Figure 9.

3.1.3 Cutting and grafting trees: B^\pm operators

There are two types of trees, those that have a unique lowest (i.e. closest to the root) white vertex, which we will call the white root. The set of these tree will be called the white rooted trees \mathcal{T}_\circ . The other type of tree has several white vertices adjacent to the black root. These are, by slight abuse of notation, called black rooted trees \mathcal{T}_\bullet . We will call *ordered collections* of such trees “forests” in \mathcal{T} , \mathcal{T}_\bullet or \mathcal{T}_\circ . Here, we allow arbitrary labels on the white vertices.

In the proof of Theorem 3.9, the white rooted trees will play the role of indecomposables, and the black rooted trees that of decomposables. Combinatorially, however, the choice of the colours is arbitrary. And there are grafting operators, defined below, for which the role of decomposable and indecomposable becomes interchanged.

Definition 3.5. The *initial branching number* of a tree $\tau \in \mathcal{T}_\circ$ is the number of incoming edges of the unique white root.

We will now define four operators:

- (1) $B_b^+ : \text{ordered forests of } \mathcal{T} \rightarrow \mathcal{T}$. This operation simply identifies all the black roots of the trees in the ordered forest into one black root. The linear order being the one coming from the trees and the order in the forrest. See Figure 10 for an example.
- (2) $B_b^- : \mathcal{T} \rightarrow \text{ordered forests in } \mathcal{T}_\circ$. This operations cuts all edges to the root vertex, takes the ordered collection of branches and puts one new black root on each branch. For an example, see Figure 11.
- (3) $B_w^- : \mathcal{T}_\circ \rightarrow \text{ordered forests in } \mathcal{T}$. Cut off all the edges above the unique *white* root vertex. Collect the branches in the order given by this white vertex, and add a black root to each of them. (NB: If one starts with an $\{\sigma\}$ -labelled $\tau \in \mathcal{T}_\sigma \cap \mathcal{T}_\circ$ and the white root is labelled by σ_1 , then for some elements $\mathbf{l}_1, \dots, \mathbf{l}_k \in \text{dSh}_{\sigma \setminus \sigma_1}[m_1, \dots, m_k]$ we have $B_w^-(\tau) \in \mathcal{T}_{\mathbf{l}_1} \times \dots \times \mathcal{T}_{\mathbf{l}_k}$, where k is the initial branching number of τ and m_i is the number of white vertices on the i th branch.)
- (4) $B_s^+ : \mathcal{T}_{S_1} \times \dots \times \mathcal{T}_{S_k} \rightarrow \mathcal{T}_S \cap \mathcal{T}_\circ$ whenever the S_i are pairwise disjoint and none of them contain the singleton $\{s\}$. Here $S = \coprod_i S_i \amalg \{s\}$.

$$B_s^+(\tau_1, \tau_2, \dots, \tau_k) = \{\tau \text{ obtained by grafting } \tau_1, \dots, \tau_k \text{ to } \text{scc}(s)\} \subset \mathcal{T}_n,$$

where $\text{scc}(s)$ is only element in $\mathcal{T}_{\{s\}}$. Here grafting means that each τ_i is connected to the unique white vertex of $\text{scc}(s)$ by an additional edge in the order starting with τ_1 . This is illustrated in Figure 12. We will use this operator when (S_1, \dots, S_n) is a partition of the set $[n] \setminus \{s\}$.

Notation 3.6. To make contact with the permutohedra, especially the notation of Section 1, we will use a vertical bar notation for the B_b^+ operator. That is, we will denote $B_b^+(\tau_1, \tau_2, \dots, \tau_k)$ by $\tau_1 | \tau_2 | \dots | \tau_k$. See Figure 10.

Remark 3.7. It is clear that B_b^+ and B_b^- are inverses of each other. Since a label is forgotten by B_w^- , B_s^+ is a left inverse for B_w^- on the subset of \mathcal{T}_\circ , whose white roots are labelled by s . Furthermore, B_w^- is a left inverse for B_s^+ on the domain of definition of B_s^+ .

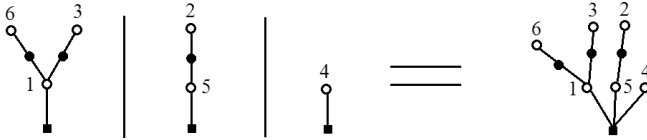


Figure 10. An example of B_b^+ and the bar notation.

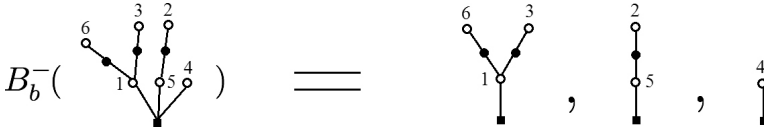


Figure 11. An example of B_b^- .

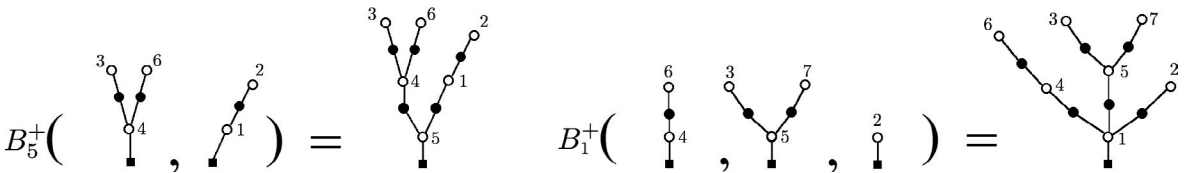


Figure 12. Two examples of B_s^+ .

Lastly if s is not in the labelling set of τ : $B_s^+ B_b^-$ switches the color of the root from black to white, labels it by s and adds a new black root.

3.1.4 Decompositions and filtrations

The set \mathcal{T}_n^{n-1} consists of the maximal elements in \mathcal{T}_n , i.e. exactly those elements that index the top-dimensional cells in $\text{Cact}^1(n)$. By (2.2), these cover Cact^1 . These trees are all in \mathcal{T}_\circ , since otherwise, the tree would not have maximal degree.

To provide the setup for later inductive proofs, for each $\sigma \in S_n$, we will partition and then filter \mathcal{T}_σ^{n-1} according to the initial branching number k . For trees in \mathcal{T}_σ^{n-1} , k can take values from 1 to $n - 1$. Let $\mathcal{T}_\sigma^{n-1}(k) \subset \mathcal{T}_\sigma^{n-1}$ be the subset containing all the trees with initial branching number k . Then we have the following decomposition:

$$\mathcal{T}_\sigma^{n-1} = \coprod_{k=1}^{n-1} \mathcal{T}_\sigma^{n-1}(k). \tag{3.1}$$

This decomposition gives rise to an ascending filtration of \mathcal{T}_σ^{n-1} :

$$\mathcal{T}_\sigma^{n-1}(1) = \mathcal{T}_{\sigma,1}^{n-1} \subset \mathcal{T}_{\sigma,2}^{n-1} \subset \dots \subset \mathcal{T}_{\sigma,n-2}^{n-1} \subset \mathcal{T}_{\sigma,n-1}^{n-1} = \mathcal{T}_\sigma^{n-1}, \tag{3.2}$$

where

$$\mathcal{T}_{\sigma,k}^{n-1} = \coprod_{q \leq k} \mathcal{T}_\sigma^{n-1}(q). \tag{3.3}$$

We can further decompose each $\mathcal{T}_\sigma^{n-1}(k)$ using the B_w^- or the $B_{\sigma_1}^+$ operator. The following observation is the key: since the $B_{\sigma_1}^+$ operator lands in \mathcal{T}_\circ , it is in general not surjective, but it is surjective on the top degree trees.

Definition 3.8. Fix $\sigma \in S_n$, $k \in \mathbb{N}^+$ with $1 \leq k \leq n - 1$, and let m_1, m_2, \dots, m_k be k positive integers such that $m_1 + \dots + m_k = n - 1$. Let $\mathbf{l} = \mathbf{l}_1, \mathbf{l}_2, \dots, \mathbf{l}_k \in \text{dSh}_{\sigma \setminus \sigma_1}[m_1, m_2, \dots, m_k]$.

We define $\mathcal{T}_\sigma^{n-1}[\mathbf{l}]$ to be the set of all trees $B_{\sigma_1}^+(\tau_1, \tau_2, \dots, \tau_k)$ in \mathcal{T}_σ obtained by grafting τ_1, \dots, τ_k , with $\tau_i \in \mathcal{T}_{\mathbf{l}_i}^{m_i-1}$ to $\text{scc}(\sigma_1)$. Since, the order of the branches is recorded, it follows that indeed the image under $B_{\sigma_1}^+$ is in \mathcal{T}_σ^{n-1} and furthermore $\tau \in \mathcal{T}_\sigma^{n-1}[\mathbf{l}]$ if and only if $B_w^-(\tau) \in \mathcal{T}_{\mathbf{l}_1}^{m_1-1} \times \dots \times \mathcal{T}_{\mathbf{l}_k}^{m_k-1}$.

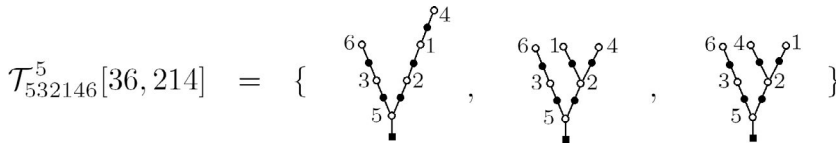


Figure 13. The elements of $\mathcal{T}_{532146}^5[\mathbf{l}]$ where $\mathbf{l} = \mathbf{l}_1, \mathbf{l}_2$ and $\mathbf{l}_1 = 36, \mathbf{l}_2 = 214$.

To extend this decomposition to all degrees, we now define $\mathcal{T}_\sigma[\mathbf{l}]$ to be the subset of \mathcal{T}_σ such that each element in $\mathcal{T}_\sigma[\mathbf{l}]$ is less than or equal to an element in $\mathcal{T}_\sigma^{n-1}[\mathbf{l}]$. Similarly, we define the pieces of the filtration $\mathcal{T}_{\sigma,k}$.

Since angle collapse only potentially decreases the initial branching number, we also have the inherited poset structures on $\mathcal{T}_\sigma[\mathbf{l}]$ and $\mathcal{T}_{\sigma,k}$.

Example. The elements of $\mathcal{T}_{532146}^5[\mathbf{l}_1, \mathbf{l}_2]$ where $\mathbf{l}_1 = 36, \mathbf{l}_2 = 214$ are shown in Figure 13.

Summing up, we have the decomposition

$$\mathcal{T}_\sigma^{n-1}(k) = \coprod_{m_1, \dots, m_k} \coprod_{\mathbf{l} \in \text{dSh}_{\sigma|\sigma_1}[m_1, \dots, m_k]} \mathcal{T}_\sigma^{n-1}[\mathbf{l}] \tag{3.4}$$

and

$$\mathcal{T}_{\sigma,1} \subset \mathcal{T}_{\sigma,2} \subset \dots \subset \mathcal{T}_{\sigma,n-2} \subset \mathcal{T}_{\sigma,n-1}. \tag{3.5}$$

The realization functor C on \mathcal{T}_n restricts to $(\mathcal{T}_\sigma, \prec_{\mathcal{T}})$, $(\mathcal{T}_\sigma[\mathbf{l}], \prec_{\mathcal{T}})$ and $(\mathcal{T}_{\sigma,k}, \prec_{\mathcal{T}})$, respectively.

3.2 Permutohedra in $\text{Cact}^1(n)$

We can now start to prove that indeed $\text{Cact}^1(n)$ is covered by $n!$ permutohedra $P_\sigma := P_n, \sigma \in S_n$, as shown below.

Theorem 3.9. For any $\sigma \in S_n$, $\text{colim}_{\mathcal{T}_\sigma} C$ is a polytope, which is piecewise linearly homeomorphic (\cong) to P_n .

Proof. We proceed by nested induction. When $n = 1, 2$, $\text{colim}_{\mathcal{T}_\sigma} C$ is a point and a closed line segment, respectively. So the statement is true in these two cases.

Suppose the statement is true for all m and all $\sigma \in S_m$, where $m < n$. Let $\sigma \in S_n$. We will first show that $\text{colim}_{\mathcal{T}_\sigma} C$ is a PL (piecewise linear) cell of dimension $n - 1$. We will simply say that $\text{colim}_{\mathcal{T}_\sigma} C$ is a PL D^{n-1} .

We will iteratively use the following observation. The connected sum of two PL D^{n-1} 's along a sub PL D^{n-2} is a PL D^{n-1} . More precisely: if X and Y are both PL D^{n-1} 's and $i : D^{n-2} \hookrightarrow X$ and $j : D^{n-2} \hookrightarrow Y$ are injective PL maps such that $i(D^{n-2})$ is the connected union of some facets of X and $j(D^{n-2})$ is the connected union of some facets of Y (so both $i(D^{n-2})$ and $j(D^{n-2})$ are PL D^{n-2}), then the glued object (pushout of $X \hookrightarrow D^{n-2} \hookrightarrow Y$) is again a PL D^{n-1} .

Also, notice that by the induction hypothesis and the definition of the realization functor C , for an element $\mathbf{l} \in \text{dSh}_{\sigma|\sigma_1}[m_1, \dots, m_k]$,

$$\text{colim}_{\mathcal{T}_\sigma[\mathbf{l}]} C \cong P_{m_1} \times P_{m_2} \times \dots \times P_{m_k} \times \Delta^k. \tag{3.6}$$

So $\text{colim}_{\mathcal{T}_\sigma[\mathbf{l}]} C$ is a PL D^{n-1} .

We now use a second induction on k , to show that

$$\text{colim}_{\mathcal{T}_{\sigma,k}} C \text{ is a PL } D^{n-1}. \tag{3.7}$$

When $k = 1$ we know that $\mathcal{T}_{\sigma,1}^{n-1} = \mathcal{T}_\sigma^{n-1}(1) = \mathcal{T}_\sigma^{n-1}[\mathbf{l}]$, with $\mathbf{l} = \sigma_2 \dots \sigma_n$, (see Section 3.1.4), and hence $\text{colim}_{\mathcal{T}_{\sigma,1}} C = \text{colim}_{\mathcal{T}_\sigma[\mathbf{l}]} C \cong P_{n-2} \times \Delta^1$ is a PL D^{n-1} .

Now suppose for $2 \leq k \leq n - 1$, $\text{colim}_{\mathcal{T}_{\sigma,k-1}} C$ is a PL D^{n-1} .

For each $\mathbf{l} \in \text{dSh}_{\sigma|\sigma_1}[m_1, \dots, m_k]$, $\text{colim}_{\mathcal{T}_\sigma[\mathbf{l}]} C$, which is a PL D^{n-1} , is glued to the PL D^{n-1} given by $\text{colim}_{\mathcal{T}_{\sigma,k-1}} C$ along $P_{m_1} \times \dots \times P_{m_k} \times \bigcup_{i=2}^k \partial_i \Delta^k$. Here ∂_i is the i th face map which on the simplex in the vertex notation $\Delta^k = v_1 \dots v_{k+1}$ can be written as $v_1 \dots \widehat{v}_i \dots v_{k+1}$. In the cactus picture, this corresponds to

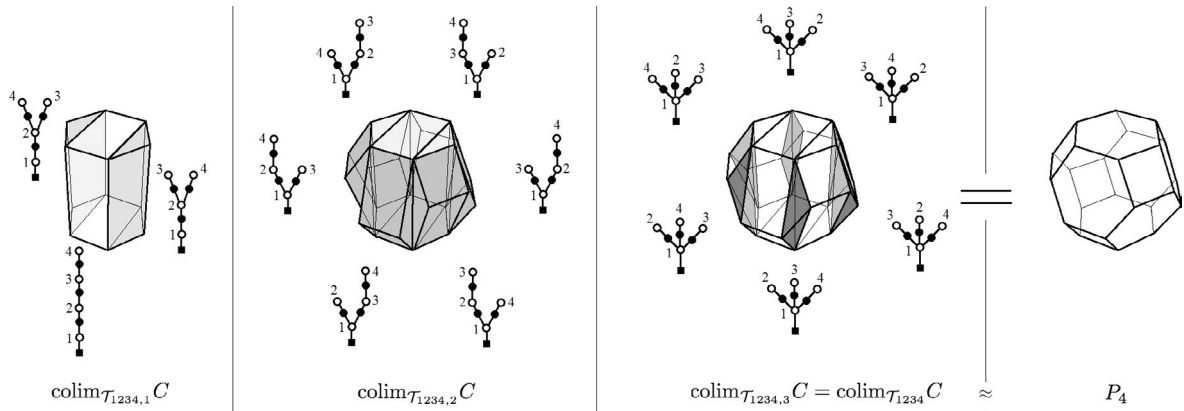


Figure 14. The colimits $\text{colim}_{\mathcal{T}_{1234,i}} C$, $i = 1, 2, 3$.

the contraction of the i th arc on the root lobe. Notice that since $\partial\Delta^k = \bigcup_{i=1}^{k+1} v_1 \cdots \widehat{v}_i \cdots v_{k+1}$ is a PL S^{k-1} , it follows that $(v_2 v_3 \cdots v_{k+1}) \cup (v_1 v_2 \cdots v_k)$ is a PL D^{k-1} and $\bigcup_{i=2}^k v_1 \cdots \widehat{v}_i \cdots v_{k+1}$ is also a PL D^{k-1} . Thus, $P_{m_1} \times \cdots \times P_{m_k} \times (\bigcup_{i=2}^k v_1 \cdots \widehat{v}_i \cdots v_{k+1})$ is a PL D^{n-2} . And hence we are gluing two PL D^{n-1} 's along a common PL D^{n-2} and the result is a PL D^{n-1} . This is true for each $\mathbf{l} \in S_\sigma[m_1, \dots, m_k]$ in (3.4) individually, so we can glue in these $\text{colim}_{\mathcal{T}_\sigma[\mathbf{l}]} C$ one by one and end up with a PL D^{n-1} and obtain (3.7).

From this it follows that: $\text{colim}_{\mathcal{T}_\sigma} C = \text{colim}_{\mathcal{T}_{\sigma,n-1}} C$ is a PL D^{n-1} , by applying C to the filtration (3.5). Indeed, we have the following filtration of the PL cell $\text{colim}_{\mathcal{T}_{\sigma,n-1}} C$ by PL cells:

$$\text{colim}_{\mathcal{T}_{\sigma,1}} C \subset \text{colim}_{\mathcal{T}_{\sigma,2}} C \subset \cdots \subset \text{colim}_{\mathcal{T}_{\sigma,n-2}} C \subset \text{colim}_{\mathcal{T}_{\sigma,n-1}} C.$$

An example is illustrated in Figure 14.

Next, we show that the PL cell $\text{colim}_{\mathcal{T}_\sigma} C$ is indeed piecewise linearly isomorphic to P_n . Let us define a new functor. For any $\sigma \in S_n$, let \mathcal{C} be the realization functor from \mathcal{T}_σ to the category of PL topological spaces defined by

$$\mathcal{C}_{\text{scc}(\sigma)} = \mathbf{v}_\sigma \in \mathbb{R}^n$$

on degree 0 elements and let \mathcal{C}_τ be the convex hull of $\{\mathcal{C}_{\tau'} : \tau' \in \mathcal{T}_\sigma^0, \tau' <_{\mathcal{T}} \tau\}$ for general $\tau \in \mathcal{T}_\sigma^i$, where $i > 0$. Again, the image of $<_{\mathcal{T}}$ under \mathcal{C} are defined to be face inclusions.

There is hence a piecewise linear homeomorphism from $\text{colim}_{\mathcal{T}_{\mathbf{i}}} C$ to $\text{colim}_{\mathcal{T}_{\mathbf{i}}} \mathcal{C}$ by extending the vertex correspondences $\mathcal{C}_{\text{scc}(\sigma)} \mapsto \mathcal{C}_{\text{scc}(\sigma)}$.

It remains to identify the face structure. For this, we characterize the codim 1 cells as “interior” or “exterior”, where the exterior cells form the boundary of the ball and hence of the polytope. Using the formula for the codimension from Section 2.1.3 this means that there is precisely one black vertex of arity 2 for the tree τ indexing the cell, which we called the collapsed vertex. If this vertex is the root, the cell is exterior and if it is not it is interior. The reason for this is as follows. If the collapsed vertex is not the root, then there are two possible angle collapses that can be obtained from the involved trees that fit the order given by σ . Namely, let the white vertex directly above the collapsed black vertex be labelled by i and j and the label of the white vertex directly below the collapsed black vertex be labelled by k . Since σ gives the order, we either have $i <_\sigma j$ or $j <_\sigma i$. Assume without loss of generality that $j <_\sigma i$. Then τ can be obtained by angle collapse from τ' where in τ' both i and j are directly above k or from the tree τ'' in which $k <_{\tau''} j <_{\tau''} i$ and hence on both sides of this codim 1 cell there are top-dimensional cells and hence it is inside. In the other case, there is no white vertex k below the collapsed vertex and hence there is only one top-dimensional cell whose boundary contains $C(\tau)$ and $C(\tau)$ is exterior. Since we already showed that the CW complex realized a ball, we can iteratively characterize cells of any codimension as “interior” or “exterior” as follows. A cell $C(\tau)$ is exterior if it is on the boundary of an exterior cell of lower codimension. Another way of stating this is that the inductive procedure glues along all “interior” cells. See Figure 15 and Figure 16.

We now show that the exterior cells consolidate into products of permutohedra. Form the above, it follows each cell on the boundary of $\text{colim}_{\mathcal{T}_\sigma} C$ is indexed by a tree obtained as $B_b^+(\tau_1, \tau_2, \dots, \tau_k)$,

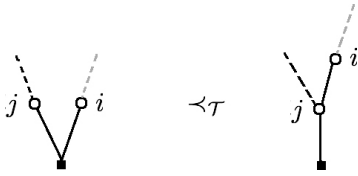


Figure 15. The only codim 0 element having the codim 1 element $B_j^+(\dots)|B_i^+(-)$ as a face is $B_j^+(\dots, B_i^+(-))$.

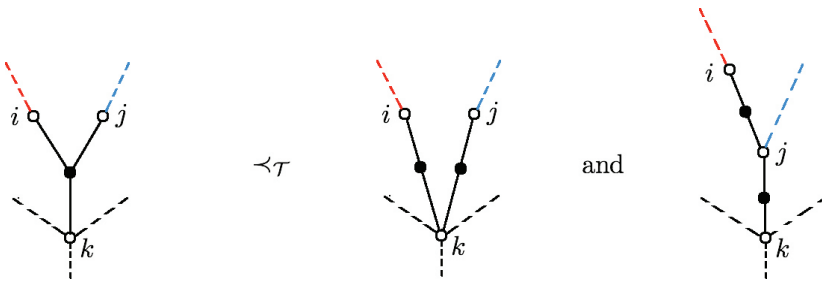


Figure 16. The only two codim 0 elements having the codim 1 element $\dots B_k^+(\dots, B_i^+(-1)|B_j^+(-2), \dots) \dots$ as a face are $\dots B_k^+(\dots, B_i^+(-1), B_j^+(-2), \dots) \dots$ and $\dots B_k^+(\dots, B_j^+(B_i^+(-1), -2), \dots) \dots$.

where $\tau_i \in \mathcal{T}_{\mathbf{l}_i}^{m_i-1}$ such that $\mathbf{l}_1, \mathbf{l}_2, \dots, \mathbf{l}_k \in \text{dSh}_\sigma[m_1, m_2, \dots, m_k]$. As mentioned previously, we denote such a tree by $\tau_1|\dots|\tau_k$.

Let

$$\mathcal{T}_{\mathbf{l}_1}|\mathcal{T}_{\mathbf{l}_2}|\dots|\mathcal{T}_{\mathbf{l}_k} = B_b^+(\mathcal{T}_{\mathbf{l}_1} \times \dots \times \mathcal{T}_{\mathbf{l}_k}) = \{\tau_1|\tau_2|\dots|\tau_k : \tau_i \in \mathcal{T}_{\mathbf{l}_i}\}.$$

We shall consolidate the cells indexed by all $\tau_1|\tau_2|\dots|\tau_k \in \mathcal{T}_{\mathbf{l}_1}^{m_1-1}|\mathcal{T}_{\mathbf{l}_2}^{m_2-1}|\dots|\mathcal{T}_{\mathbf{l}_k}^{m_k-1}$ together to form the faces. We can then again use induction on n as previously. Namely, by the induction hypothesis and the way that B_b^+ is defined, we know for each $\mathbf{l}_1|\mathbf{l}_2|\dots|\mathbf{l}_k$,

$$\text{colim}_{\mathcal{T}_{\mathbf{l}_1}|\mathcal{T}_{\mathbf{l}_2}|\dots|\mathcal{T}_{\mathbf{l}_k}} \mathcal{C} = P_{m_1} \times P_{m_2} \times \dots \times P_{m_k}.$$

But this is the characterization of the cells of P_n . Therefore, $\text{colim}_{\mathcal{T}_\sigma} \mathcal{C} = P_n$ and thus $\text{colim}_{\mathcal{T}_\sigma} C \cong P_n$.

Notice that the colimits can be taken before realization, and all the combinatorics can also be taken on the level of polytopes. This gives the strengthening of the statement. □

Remark 3.10. Let $\sigma \in S_n$, since $\text{colim}_{\mathcal{T}_\sigma} C \cong P_n$, we say that P_n has the decomposition into cactus cells (products of simplices) associated to σ .

For $n \geq 2$, we have $\frac{n!}{2}$ different decompositions of P_n . The number is $\frac{n!}{2}$ instead of $n!$ because σ and $\sigma \circ s$ give the same decomposition, where $s : [n] \rightarrow [n]$ is defined by $s|_{[n-2]} = \text{id}_{[n-2]}$, $s_{n-1} = n$ and $s_n = n - 1$.

3.3 Further consequences. Recursion and Dyer–Lashof operations

3.3.1 Operadic generation and Dyer–Lashof operations

The indexing set $\mathcal{T}_{12\dots n}^{n-1}$ of the top-dimensional cells of the decomposition of P_n associated to $12\dots n$ can be generated from the single tree $B_1^+(\text{scc}(2))$ with two white vertices using the operadic composition \circ_1 for the cellular chain operad $\text{CC}_*(\text{Cact}^1)$. This observation allows us to link permutohedra to Dyer–Lashof operations.

Let $c = \sum_{i \in I} n_i c_i$, where $n_i \in \mathbb{Z}$, be a chain in $\text{CC}_{n-1}(\text{Cact}^1(n))$ for some n . Let $\{c\}$ be the set of support of c , i.e. $\{c\} = \{c_i : n_i \neq 0\}$. Let $\tau = B_1^+(\text{scc}(2))$. Define $\{\tau \circ_1 \mathcal{T}_{12\dots i}^{i-1}\}$ to be the (disjoint) union of the sets $\{\tau \circ_1 \tau'\}$, where $\tau' \in \mathcal{T}_{12\dots i}^{i-1}$. It can be readily checked that the following holds.

Lemma 3.11. We have $\{\tau \circ_1 \mathcal{T}_{12\dots i}^{i-1}\} = \mathcal{T}_{12\dots(i+1)}^i$. □

Theorem 3.12. *Let*

$$\tau^{n-1} = \underbrace{\{\tau \circ_1 \{\dots \{\tau \circ_1 \{\tau \circ_1 \{\tau\}\}\}\dots\}\}}_{\text{there are } n-1 \tau \text{ and thus } n-2 \circ_1}.$$

Then $\tau^{n-1} = \mathcal{T}_{12\dots n}^{n-1}$ and moreover, the multiplicity of each summand in $\tau \circ_1 (\dots (\tau \circ_1 (\tau \circ_1 (\tau))) \dots)$ is 1. So τ^{n-1} indexes the top-dimensional cells of the decomposition of P_n associated to $12 \dots n$. This is the cell for the Dyer–Lashof operation.

Proof. By iterating $i = 2, 3, \dots, n - 1$, where $n \geq 3$, we see that indeed, we get all the cells indexing $P_{\text{id}} = P_n$. By [24, Proposition 2.13] this iteration also has coefficients 1 and yields the cell for the Dyer–Lashof operation. \square

Remark 3.13. This also allows us to give a concrete homotopy between the right iteration above and the left iteration

$$\underbrace{(\tau \circ_2 (\dots (\tau \circ_2 (\tau \circ_2 (\tau))) \dots))}_{\text{there are } n-1 \tau \text{ and thus } n-2 \circ_2} = \tau_{\text{id}} = B_{\sigma_1}^+ (B_{\sigma_2}^+ (\dots B_{\sigma_{n-1}}^+ (\text{scc}(\sigma_n)) \dots)).$$

Here the support is the single tree τ_{id} in \mathcal{T}_{id} , whose cell is the hypercube I^{n-1} that sits at the center of the permutohedron P_σ .

3.3.2 Iterative decomposition into cactus cells

There is an interesting duality in the cactus decomposition. On one hand, recall from the proof of Theorem 3.9, that each codim $k - 1$ face of P_n is labelled by $\mathcal{T}_{\mathbf{l}_1}^{m_1-1} |\mathcal{T}_{\mathbf{l}_2}^{m_2-1}| \dots |\mathcal{T}_{\mathbf{l}_k}^{m_k-1}$ and the subdivision is given by the elements of this set. More precisely: for $n \geq 2$, $1 \leq k \leq n - 1$, fix m_1, m_2, \dots, m_k satisfying $m_i \geq 1$ and $m_1 + m_2 + \dots + m_k = n - 1$ and let $\mathbf{l} = \mathbf{l}_1, \mathbf{l}_2, \dots, \mathbf{l}_k \in \text{dSh}_\sigma[m_1, m_2, \dots, m_k]$. Then the elements in $\mathcal{T}_{\mathbf{l}_1}^{m_1-1} |\mathcal{T}_{\mathbf{l}_2}^{m_2-1}| \dots |\mathcal{T}_{\mathbf{l}_k}^{m_k-1}$ are $\tau_1 | \tau_2 | \dots | \tau_k$, where each $\tau_i \in \mathcal{T}_{\mathbf{l}_i}^{m_i-1}$ is a tree with the maximal number ($m_i - 1$) of white edges and its partial order is compatible with the total order \mathbf{l}_i . On the other hand, recall from (3.4), the top cells of P_σ are naturally indexed by the fibers of $B_{\sigma_1}^-$

$$\mathcal{T}_\sigma^{n-1}(k) = \coprod_{m_1, \dots, m_k} \coprod_{\mathbf{l} \in \text{dSh}_{\sigma \setminus \sigma_1}[m_1, \dots, m_k]} \mathcal{T}_\sigma^{n-1}[\mathbf{l}].$$

To sum this up, for fixed k , we define $\mathcal{T}_{\sigma \setminus \sigma_1}^{\text{face}}(k)$ as follows:

$$\mathcal{T}_{\sigma \setminus \sigma_1}^{\text{face}}(k) = \coprod_{m_1 + \dots + m_k = n-1} \coprod_{\mathbf{l}_1, \dots, \mathbf{l}_k \in \text{dSh}_{\sigma \setminus \sigma_1}[m_1, \dots, m_k]} \mathcal{T}_{\mathbf{l}_1}^{m_1-1} |\mathcal{T}_{\mathbf{l}_2}^{m_2-1}| \dots |\mathcal{T}_{\mathbf{l}_k}^{m_k-1} \subset T_{\sigma \setminus \sigma_1}^{n-1-k}.$$

This is the set of trees indexing all the cells making up the codim $k - 1$ -faces of $P_{\sigma \setminus \sigma_1}$. Then we have the diagram:

$$\begin{array}{ccc} \mathcal{T}_{\mathbf{l}_1}^{m_1-1} |\mathcal{T}_{\mathbf{l}_2}^{m_2-1}| \dots |\mathcal{T}_{\mathbf{l}_k}^{m_k-1} & \begin{array}{c} \xleftarrow{B_b^+} \\ \xrightarrow{B_b^-} \end{array} & \mathcal{T}_{\mathbf{l}_1}^{m_1-1} \times \mathcal{T}_{\mathbf{l}_2}^{m_2-1} \times \dots \times \mathcal{T}_{\mathbf{l}_k}^{m_k-1} & \begin{array}{c} \xleftarrow{B_{\sigma_1}^+} \\ \xrightarrow{B_{\sigma_1}^-} \end{array} & \mathcal{T}_\sigma^{n-1}[\mathbf{l}] \\ \downarrow & & & & \downarrow \\ \mathcal{T}_{\sigma \setminus \sigma_1}^{\text{face}}(k) & \xrightarrow{B_{\sigma_1}^+ \circ B_b^-} & \mathcal{T}_\sigma^{n-1}(k). \end{array} \tag{3.8}$$

We set

$$\mathcal{T}_{\sigma \setminus \sigma_1}^{\text{face}} = \coprod_{k=1}^{n-1} \mathcal{T}_{\sigma \setminus \sigma_1}^{\text{face}}(k),$$

which is the set indexing all the cells making up all faces of $P_{\sigma \setminus \sigma_1}$

Proposition 3.14. *The map obtained by taking the disjoint union over k of the lower arrows*

$$B_{\sigma_1}^+ \circ B_b^- : \mathcal{T}_{\sigma \setminus \sigma_1}^{\text{face}}(k) \rightarrow \mathcal{T}_\sigma^{n-1}(k),$$

is a bijection:

$$B_{\sigma_1}^+ \circ B_b^- : \mathcal{T}_{\sigma \setminus \sigma_1}^{\text{face}} \rightarrow \mathcal{T}_\sigma^{n-1}.$$

Proof. From Remark 3.7, we see that in the upper row all the arrows are bijections and this proves the claim of the proposition. \square

The elements in the codomain \mathcal{T}_σ^{n-1} of $B_{\sigma_1}^+ \circ B_b^-$ label the top-dimensional cells of the decomposition of P_n into cactus cells. The above proposition means the top-dimensional cells of P_n can instead be labelled by the top-dimensional cells of the decomposition of each face of P_{n-1} . Figure 17 below uses color to illustrate this from P_{n-1} to P_n for $n = 2, 3, 4$.

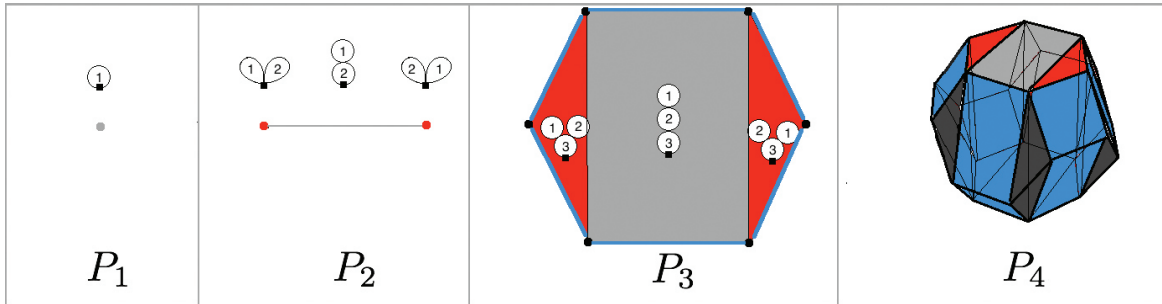


Figure 17. The subdivisions of P_1 by 1, P_2 by 21, P_3 by 321 and P_4 by 4321, see also Figure 28 for a more detailed marking of P_3 including a marking by sequences.

Even though we are not able to draw the subdivision of P_5 , we can at least compute the number of top-dimensional cells of it $|\mathcal{T}_{54321}^4|$ using the above bijection, where $|X|$ denote the number of elements of the set X . We have

- $|\mathcal{T}_{4321}^{\text{face}}(1)| = |\mathcal{T}_{4321}^3| = 15.$
 - $|\mathcal{T}_{4321}^{\text{face}}(2)| = 30.$
 - $|\mathcal{T}_{4321}^{\text{face}}(3)| = 36.$
 - $|\mathcal{T}_{4321}^{\text{face}}(4)| = 4!.$
- So $|\mathcal{T}_{54321}^4| = \sum_{k=1}^4 |\mathcal{T}_{4321}^{\text{face}}(k)| = 105.$

3.3.3 Remark

Our construction is related to a statement [4, Remark 1.10].

“Jim McClure and Jeff Smith construct an E_2 -operad which acts on topological Hochschild cohomology... Its multiplication uses prismatic decomposition of the permutohedra P_k (labelled by “formulae”) which can be described as follows: The image of $P_2 \times P_1 \times P_{k-1} \rightarrow P_k$ is a prism $\Delta^1 \times P_{k-1}$, thus by induction endowed with a prismatic decomposition; it turns out that the (closure of the) complement of the image also admits a prismatic decomposition labelled by the set of proper faces of P_{k-1} ...”

Namely, the above comment is almost true. It is true that P_n can first be decomposed into two parts: $P_{n-1} \times I$, where I is a closed interval of length $\sqrt{n(n-1)}$, and the closure of the complement of $P_{n-1} \times I$ in P_n , then $P_{n-1} \times I$ has the decomposition induced from that of P_{n-1} . But the closure of the complement of $P_{n-1} \times I$ in P_n has the decomposition into pieces not labelled by the proper faces of P_{n-1} , but by the top-dimensional cells from subdivisions of each proper face of P_{n-1} .

3.4 The Permutoheral cover of $\text{Cact}^1(n)$

Definition 3.15. We extend \mathcal{C} from \mathcal{T}_σ to \mathcal{T}_n and then let

$$\mathcal{C}(n) := \text{colim}_{\mathcal{T}_n} \mathcal{C}.$$

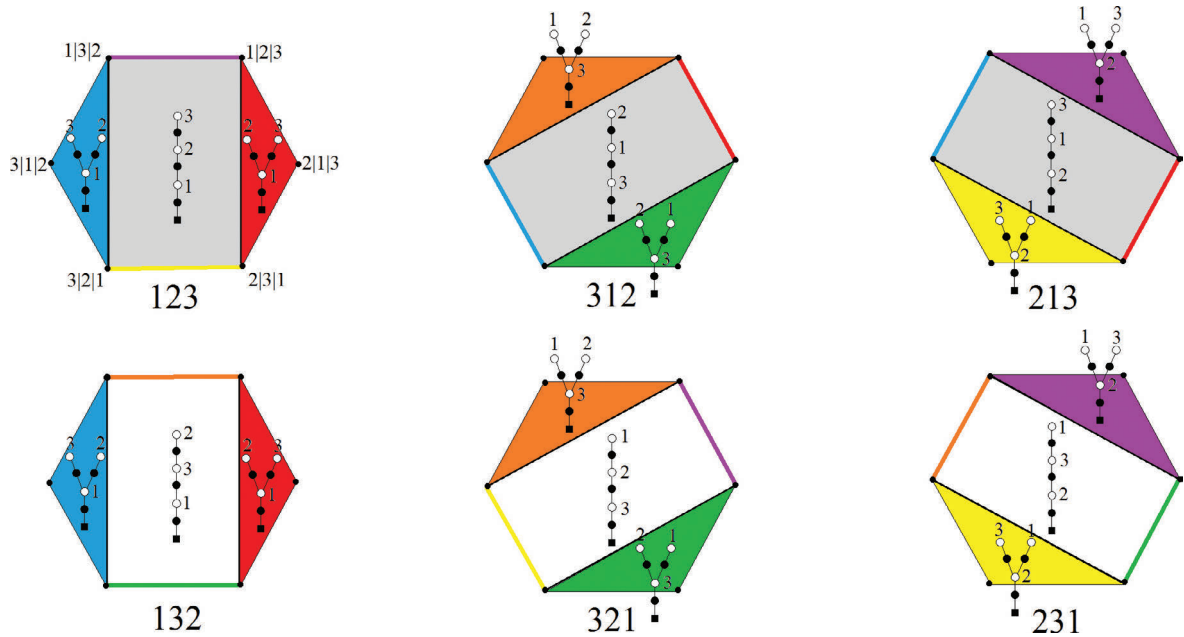


Figure 18. The space $\mathcal{C}(3)$ is obtained by gluing six copies of P_3 , one for each $\sigma \in P_3$. For simplicity, the indexing elements from \mathcal{J}_σ^0 for the vertices are only shown for the first P_3 ($\sigma = 123$). The points that are to be glued are labelled by the same color and put in the same position.

By construction, the resulting space is homeomorphic to $\text{Cact}^1(n)$, that is there is a homeomorphism $L_n : \mathcal{C}(n) \approx \text{Cact}^1(n)$. This homeomorphism is actually almost the identity. It is just two different realizations of the same complex, which is why we will write

$$\mathcal{C}(n) = \text{Cact}^1(n).$$

Proposition 3.16. Then space Cact^1 is a quotient of a coproduct of permutohedra $\coprod_{\sigma \in S_n} P_n$.

Proof. By taking the colimit iteratively that is first over each T_σ and then gluing the resulting spaces further and using Theorem 3.9, we can write

$$\text{Cact}^1(n) = \mathcal{C}(n) = \left(\coprod_{\sigma \in S_n} P_n \right) / \sim_{\mathcal{C}}. \tag{3.9}$$

Here explicitly, for P_n indexed by σ , the subdivision is indexed by elements in \mathcal{T}_σ and for $x \in P_n$ indexed by σ and $y \in P_n$ indexed by ν , $x \sim_{\mathcal{C}} y$ if there is $\tau \in \mathcal{T}_\sigma \cap \mathcal{T}_\nu$ such that $x = y$ in \mathcal{C}_τ . \square

Examples when $n = 3$ and $n = 4$ are shown in Figure 18 and Figure 19, respectively.

4 Homotopy equivalence between the permutohedral spaces $\text{Cact}^1(n)$ and $\mathcal{F}(n)$

The two spaces $\mathcal{F}(n)$ and $\mathcal{C}(n)$ are closely related insofar as they both are quotients of coproducts of permutohedra:

$$\begin{array}{ccc} & \coprod_{\sigma \in S_n} P_n & \\ p_{\mathcal{F}} \swarrow & & \searrow p_{\mathcal{C}} \\ \mathcal{F}(n) & & \mathcal{C}(n). \end{array}$$

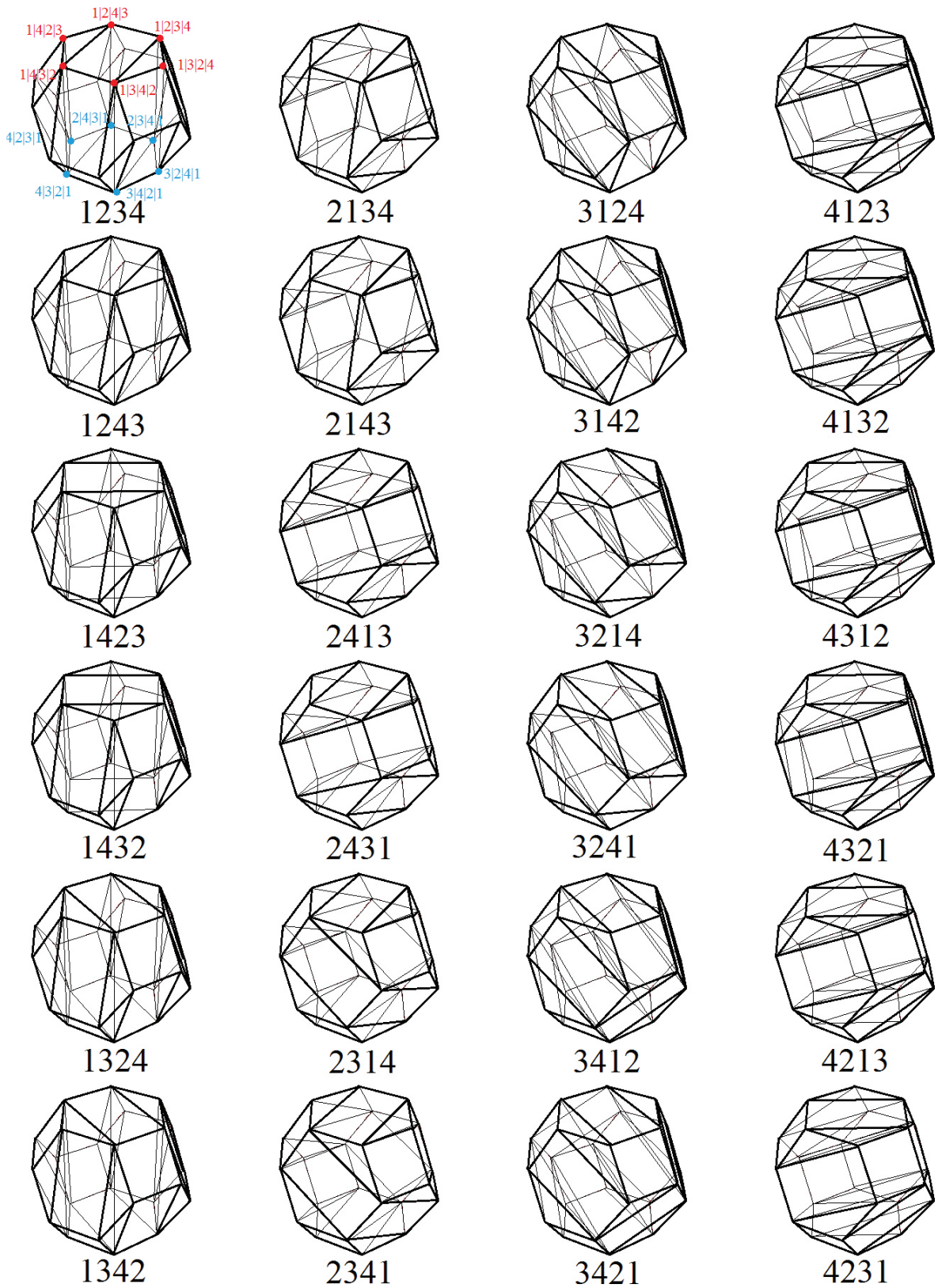


Figure 19. The space $\mathcal{C}(4)$ is obtained by gluing 24 copies of P_4 , one for each $\sigma \in P_4$. For simplicity, only twelve of the indexing elements from \mathcal{P}_σ^0 for the vertices are shown for the first P_4 ($\sigma = 1234$). One can find out which cells are glued.

But the gluings for $\mathcal{F}(n)$ only occur on the proper faces of P_n while those for $\mathcal{C}(n)$ also happen in the interior of P_n . In fact, only the interiors of the hyper-cubes $\mathcal{C}_{B_{\sigma_1}^+(B_{\sigma_2}^+(\dots B_{\sigma_{n-1}}^+(\text{scc}(\sigma_n))\dots))}$ in each of the $n!$ copies of P_n are not glued. The gluings for $\mathcal{C}(n)$ are cell-wise and we identify the cells $C(\tau)$ in the decomposition of P_σ and P_ν if the order \prec_τ is compatible with both \prec_σ and \prec_ν .

Lemma 4.1. *The map p_c is constant on fibers of $p_{\mathcal{F}}$ and hence there is an induced map $\bar{1}_n$:*

$$\begin{array}{ccc} & \coprod_{\sigma \in S_n} P_n & \\ p_{\mathcal{F}} \swarrow & & \searrow p_c \\ \mathcal{F}(n) & \xrightarrow{\bar{1}_n} & \mathcal{C}(n). \end{array} \tag{4.1}$$

Proof. If $x \sim_{\mathcal{F}} y$, where $x \in P_n$ indexed by σ and $y \in P_n$ indexed by ν , let $\mathbf{l} = \mathbf{l}_1 | \dots | \mathbf{l}_k$ be an element in \mathcal{J}_n such that $\mathbf{l} \in \mathcal{J}_\sigma \cap \mathcal{J}_\nu$ and $x = y$ in the interior of $\mathcal{F}(\mathbf{l})$. Then we can find $\tau = \tau_1 | \dots | \tau_k \in \mathcal{T}_\sigma \cap \mathcal{T}_\nu$, where $\tau_i \in \mathcal{T}_{\mathbf{l}_i}$, $i = 1, \dots, k$, by using cactus decomposition of each $P_{|\mathbf{l}_i|}$ associated to \mathbf{l}_i such that $x = y$ in \mathcal{C}_τ . So $x \sim_c y$. \square

It is easily seen that this map is again a quotient map and induces a map

$$CC_*(\bar{1}_n) : CC_*(\mathcal{F}(n)) \rightarrow CC_*(\mathcal{C}(n)) = CC_*(\text{Cact}^1(n)),$$

where $CC_*(P_\sigma) \rightarrow \sum_{\prec_\tau \text{ compatible with } \prec_\sigma} C(\tau)$. It is well known that $\mathcal{F}(n)$ has the homotopy type of $K(PB_n, 1)$ and it is proved in [18] that the same holds for $\text{Cact}^1(n)$, with this one can directly prove that the map above induces a quasi-isomorphism.

We will prove a little more, namely we will prove that $\bar{1}_n$ is a homotopy equivalence by constructing an explicit homotopy inverse \bar{h}_n . The quasi-isomorphism part of the above then follows without resorting to abstract recognition principles.

Theorem 4.2. *The map $\bar{1}_n : \mathcal{F}(n) \rightarrow \mathcal{C}(n)$ is a homotopy equivalence with explicit homotopy inverse \bar{h}_n constructed in Section 4.2.*

Proof. This follows from Proposition 4.9 below. \square

Corollary 4.3. *The map $\bar{1}_n$ is a quasi-isomorphism and furthermore, it induces a map on the level of cellular chains $CC_*(\bar{1}_n) : CC_*(\mathcal{F}(n)) \rightarrow CC_*(\mathcal{C}(n)) = CC_*(\text{Cact}^1(n))$, where $CC_*(P_\sigma) \rightarrow \sum_{\prec_\tau \text{ compatible with } \prec_\sigma} C(\tau)$.*

The way the maps are constructed is by considering lifts along one projection, then a map

$$f : \coprod_{\sigma \in S_n} P_n \rightarrow \coprod_{\sigma \in S_n} P_n$$

followed by the other projection. We will call the resulting map the map induced by f . For the induced map to exist, of course f should be suitably constant along fibers. In particular, the map $\bar{1}_n$ is defined by lifting along $p_{\mathcal{F}}$ and then simply projecting along p_c . Thus it is induced by the identity map 1_n which is the identity on all of the P_σ .

Remark 4.4. We will describe the homotopy inverse $\bar{h}_n : \mathcal{C}(n) \rightarrow \mathcal{F}(n)$ as a map induced from

$$h_n := \coprod_{\sigma \in S_n} h_\sigma : \coprod_{\sigma \in S_n} P_n \rightarrow \coprod_{\sigma \in S_n} P_n.$$

That is, we consider the diagram

$$\begin{array}{ccc} \coprod_{\sigma \in S_n} P_n & \xleftarrow{h_n = \coprod h_\sigma} & \coprod_{\sigma \in S_n} P_n \\ p_{\mathcal{F}} \downarrow & & \downarrow p_c \\ \mathcal{F}(n) & \xleftarrow{\bar{h}_n} & \mathcal{C}(n) \end{array}$$

with the condition that $h_n(x) \sim_{\mathcal{F}} h_n(y)$ if $x \sim_c y$.

This will be achieved by having each h_σ map all points in P_n other than those in the interior of the hyper-cube $\mathcal{C}_{B_{\sigma_1}^+(B_{\sigma_2}^+(\dots B_{\sigma_{n-1}}^+(\text{scc}(\sigma_n))\dots))}$ to the proper faces of P_n and then analogous conditions on the proper faces of P_n are inductively satisfied.

We will define h_σ and the homotopy showing it is a homotopy inverse at the same time. That is, we will define $H_\sigma : P_n \times I \rightarrow P_n$ and then set $h_\sigma = H_\sigma(\cdot, 1)$ for each σ .

To prove the homotopy equivalence, we notice that the two maps

$$\bar{h}_n \circ \bar{1}_n : \mathcal{F}(n) \rightarrow \mathcal{F}(n) \quad \text{and} \quad \bar{1}_n \circ \bar{h}_n : \mathcal{C}(n) \rightarrow \mathcal{C}(n)$$

are both induced from $h_n : \coprod_{\sigma \in \mathcal{S}_n} P_n \rightarrow \coprod_{\sigma \in \mathcal{S}_n} P_n$, in the sense that we have the diagrams

$$\begin{array}{ccc} \coprod_{\sigma \in \mathcal{S}_n} P_n & \xrightarrow{h_n \circ 1_n = h_n} & \coprod_{\sigma \in \mathcal{S}_n} P_n & \xleftarrow{1_n \circ h_n = h_n} & \coprod_{\sigma \in \mathcal{S}_n} P_n \\ p_{\mathcal{F}} \downarrow & & \downarrow p_{\mathcal{F}} & & \downarrow p_{\mathcal{C}} \\ \mathcal{F}(n) & \xrightarrow{\bar{h}_n \circ \bar{1}_n} & \mathcal{F}(n), & & \mathcal{C}(n) \xleftarrow{\bar{1}_n \circ \bar{h}_n} \mathcal{C}(n). \end{array}$$

This means that if the homotopies proving the homotopy equivalence are $H_{\mathcal{F}}$ and $H_{\mathcal{C}}$, i.e. $1_{\mathcal{F}(n)} \simeq_{H_{\mathcal{F}}} \bar{h}_n \circ \bar{1}_n$ and $1_{\mathcal{C}(n)} \simeq_{H_{\mathcal{C}}} \bar{1}_n \circ \bar{h}_n$, we can look for a common homotopy $\coprod_{\sigma \in \mathcal{S}_n} H_\sigma$ inducing both $H_{\mathcal{F}}$ and $H_{\mathcal{C}}$.

This homotopy has to and will satisfy the following conditions:

- (*1) $H_\sigma(\cdot, 0) = 1_\sigma : P_n \rightarrow P_n$.
- (*2) If $x \sim_{\mathcal{F}} y$, where x is in P_n indexed by σ and y is in P_n indexed by ν , then $H_\sigma(x, t) \sim_{\mathcal{F}} H_\nu(y, t)$ for all $t \in I$.
- (*3) If $x \sim_{\mathcal{C}} y$, where x is in P_n indexed by σ and y is in P_n indexed by ν , then
 - (*3a) $H_\sigma(x, t) \sim_{\mathcal{C}} H_\nu(y, t)$ for all $t \in I$,
 - (*3b) $H_\sigma(x, 1) \sim_{\mathcal{F}} H_\nu(y, 1)$.

4.1 Rough sketch of a proof of Theorem 4.2

Before delving into the intricate details of fully constructing the homotopy, we will present a short argument. First, we know that the individual permutohedra P_n are homotopic to their core I^{n-1} , abstractly. More concretely, by Theorem 3.9, we know that the cells are glued iteratively in $n - 1$ steps, parameterized by the initial branching number. We obtain a retract $r : P_n \rightarrow I_n$, by collapsing the cells in reverse order to the piece of the boundary that is attached to the lower shell. That is, first we look at

$$I_n \begin{array}{c} \xleftarrow{i} \\ \xrightarrow{r} \end{array} P_n.$$

It is not hard to show that this is a deformation retract. When the gluing maps are added, however it will be more convenient to realize that there is actually a map going the other way around. Although it is constructed a bit differently, the idea is that if V is the vertex set of P_n , then $W = r(V)$ contains the vertex set of I_n and additional points in the boundary. Mapping back W to V using the PL-structure, gives a map the other way around. This map can be extended to the whole of P_n , which is the sought after map h_n . It maps I_n homeomorphically onto P_n and is homotopic to the identity:

$$P_n \begin{array}{c} \xrightarrow{\simeq h_n} \\ \xleftarrow{\text{id}} \end{array} P_n.$$

On the cellular level, we contract all the cells that are not of the type I^n and then obtain a complex which is isomorphic to $\mathcal{F}(n)$.

4.2 Explicit construction of the homotopy

For the actual homotopy, the idea is that one retracts the cells building up the P_σ to the part of their boundary that is *not glued*. These cells are given by (3.6) as $P_{m_1} \times P_{m_2} \times \cdots \times P_{m_k} \times \Delta^k$ which, for concreteness, can be viewed as in $\mathbb{R}^{m_1-1} \times \mathbb{R}^{m_2-1} \times \cdots \times \mathbb{R}^{m_k-1} \times \mathbb{R}^k$. They are attached to cells of lower initial branching numbers along $P_{m_1} \times P_{m_2} \times \cdots \times P_{m_k} \times (\bigcup_{i=2}^k v_1 \cdots \widehat{v}_i \cdots v_{k+1}) \subset P_{m_1} \times P_{m_2} \times \cdots \times P_{m_k} \times \partial \Delta^k \subset \partial(P_{m_1} \times P_{m_2} \times \cdots \times P_{m_k} \times \Delta^k)$.

The basic homotopy is the following.

Proposition 4.5. *Let $n \geq 3$. For $m_1, \dots, m_k \geq 1$, where $k \geq 2$ and $m_1 + \dots + m_k = n - 1$,*

$$\partial(P_{m_1} \times P_{m_2} \times \dots \times P_{m_k} \times \Delta^k) \setminus \text{Int}\left(P_{m_1} \times P_{m_2} \times \dots \times P_{m_k} \times \left(\bigcup_{i=2}^k v_1 \cdots \widehat{v}_i \cdots v_{k+1}\right)\right)$$

is a deformation retract of $P_{m_1} \times P_{m_2} \times \dots \times P_{m_k} \times \Delta^k$.

Proof. A short argument is as follows. Consider $P_{m_1} \times P_{m_2} \times \dots \times P_{m_k} \times \Delta^k$ as fibered over $P_{m_1} \times P_{m_2} \times \dots \times P_{m_k} \times (\bigcup_{i=2}^k v_1 \cdots \widehat{v}_i \cdots v_{k+1})$. The fibers are singletons along $\partial(P_{m_1} \times P_{m_2} \times \dots \times P_{m_k} \times (\bigcup_{i=2}^k v_1 \cdots \widehat{v}_i \cdots v_{k+1}))$ and the fibers over the points not in the previous set are closed intervals. Then we can contract $P_{m_1} \times P_{m_2} \times \dots \times P_{m_k} \times \Delta^k$ onto the space $\partial(P_{m_1} \times P_{m_2} \times \dots \times P_{m_k} \times \Delta^k) \setminus \text{Int}(P_{m_1} \times P_{m_2} \times \dots \times P_{m_k} \times (\bigcup_{i=2}^k v_1 \cdots \widehat{v}_i \cdots v_{k+1}))$. The full proof is in the Appendix. \square

4.2.1 Extended products and extended homotopies

These homotopies cannot be used directly, since we have to take care of the attaching maps. For this, we have to slightly thicken the cell and while retracting the interior of the cell to the boundary, “pull” the thickening into the interior.

Let I_ϵ be a closed line segment with small length ϵ . Consider $(P_{m_1} \times \dots \times P_{m_k} \times (\bigcup_{i=2}^k v_1 \cdots \widehat{v}_i \cdots v_k)) \times I_\epsilon$ to be embedded into \mathbb{R}^{n-1} . Define $\text{Ext}_\epsilon(P_{m_1} \times \dots \times P_{m_k} \times \Delta^k)$ to be the union of $P_{m_1} \times \dots \times P_{m_k} \times \Delta^k$, which we call the *basic cell*, and $(P_{m_1} \times \dots \times P_{m_k} \times (\bigcup_{i=2}^k v_1 \cdots \widehat{v}_i \cdots v_{k+1})) \times I_\epsilon$, which we call the *tab*, along the subspace $P_{m_1} \times \dots \times P_{m_k} \times (\bigcup_{i=2}^k v_1 \cdots \widehat{v}_i \cdots v_{k+1})$.

Proposition 4.6. *There is a homotopy*

$$H_{\text{Ext}_\epsilon(P_{m_1} \times \dots \times P_{m_k} \times \Delta^k)} : \text{Ext}_\epsilon(P_{m_1} \times \dots \times P_{m_k} \times \Delta^k) \times I \rightarrow \text{Ext}_\epsilon(P_{m_1} \times \dots \times P_{m_k} \times \Delta^k),$$

satisfying the following conditions:

- (1) *It contracts $P_{m_1} \times P_{m_2} \times \dots \times P_{m_k} \times \Delta^k$ onto $\partial(P_{m_1} \times P_{m_2} \times \dots \times P_{m_k} \times \Delta^k) \setminus \text{Int}(P_{m_1} \times P_{m_2} \times \dots \times P_{m_k} \times (\bigcup_{i=2}^k v_1 \cdots \widehat{v}_i \cdots v_{k+1}))$.*
- (2) *It maps $(P_{m_1} \times \dots \times P_{m_k} \times (\bigcup_{i=2}^k v_1 \cdots \widehat{v}_i \cdots v_{k+1})) \times I_\epsilon$ homeomorphically to $\text{Ext}_\epsilon(P_{m_1} \times \dots \times P_{m_k} \times \Delta^k)$.*
- (3) *Let X be space and I' a closed subinterval of I , then we call a map $G : X \times I' \rightarrow X$ the identity homotopy on X if $G(\cdot, t) = 1_X$ for all $t \in I'$. Then $H_{\text{Ext}_\epsilon(P_{m_1} \times \dots \times P_{m_k} \times \Delta^k)}$ is the identity homotopy on $\partial\text{Ext}_\epsilon(P_{m_1} \times \dots \times P_{m_k} \times \Delta^k)$.*

Proof. See Appendix A. \square

4.2.2 Embedding the extensions

Now we describe how to embed the extended products inside each P_n .

Let $n \geq 3$. We will do the construction for the P_n corresponding the identity element $1_n = 12 \cdots n \in S_n$. Once we have this, we can push it forward by σ to obtain the construction for P_n corresponding to σ .

Let $2 \leq k \leq n - 1$. For any $m_1, \dots, m_k \geq 1$ with $m_1 + \dots + m_k = n - 1$, we again first consider the standard partition $\mathbf{j} = \mathbf{j}_1, \dots, \mathbf{j}_k \in \text{dSh}_{23 \cdots n}[m_1, \dots, m_k]$, where $\mathbf{l}_1 = 23 \cdots (m_1 + 1)$ and

$$\mathbf{l}_i = (m_1 + \dots + m_{i-1} + 2) \cdots (m_1 + \dots + m_i + 1)$$

for $i = 2, \dots, k$. Notice that the sequence $1\mathbf{j}_1 \cdots \mathbf{j}_k$ is the sequence $12 \cdots n$ for 1_n . We know that

$$\text{colim}_{\mathcal{T}_{1_n}[\mathbf{j}]} \mathcal{C} \cong P_{m_1} \times \dots \times P_{m_k} \times \Delta^k.$$

Let $\text{Ext}_{\phi_{m_1, \dots, m_k}}(\text{colim}_{\mathcal{T}_{1_n}[\mathbf{j}]} \mathcal{C})$ be the image in P_n of $\text{Ext}_\epsilon(P_{m_1} \times \dots \times P_{m_k} \times \Delta^k)$ under an homeomorphism ϕ_{m_1, \dots, m_k} first satisfying the following conditions.

- (1) It is a homeomorphism onto its image.
- (2) It maps the basic cell to the corresponding cell in P_n .
- (3) It maps the tab into the cells that the corresponding cell is attached to in the iteration.

Maps like this exist in abundance, which is easily seen by regarding a neighborhood of the common boundary.

Now for general permutation $\sigma \in S_n$, and $\mathbf{l} = \mathbf{l}_1, \dots, \mathbf{l}_k \in \text{dSh}_{\sigma \setminus \sigma_1}[m_1, \dots, m_k]$, let $\omega = \sigma_1 \mathbf{l}_1 \cdots \mathbf{l}_k \in S_n$. We let $\text{Ext}_{\phi_{m_1, \dots, m_k}}(\text{colim}_{\mathcal{T}_\sigma[\mathbf{l}]} \mathcal{C})$ be the image of $\text{Ext}_{\phi_{m_1, \dots, m_k}}(\text{colim}_{\mathcal{T}_{1_n}[\mathbf{j}]} \mathcal{C})$ under the linear map, which permutes it into the right position,

$$\sum_{v \in S_n} t_v \mathcal{C}_{\text{scc}(v_1, \dots, v_n)} \mapsto \sum_{v \in S_n} t_v \mathcal{C}_{\text{scc}((\omega v)_1, \dots, (\omega v)_n)}.$$

Since for fixed σ and k , any two from the collection of $\text{colim}_{\mathcal{T}_\sigma[\mathbf{l}]} \mathcal{C}$ for all m_1, \dots, m_k and all elements $\mathbf{l} \in \text{dSh}_{\sigma \setminus \sigma_1}[m_1, \dots, m_k]$ either are disjoint or share a subspace homeomorphic to D^i , where i is at most $n - 3$, after possibly shrinking and perturbing the image of the tabs, we can choose the homeomorphisms ϕ_{m_1, \dots, m_k} such that:

- (4) The interiors of $\text{Ext}_{\phi_{m_1, \dots, m_k}}(\text{colim}_{\mathcal{T}_\sigma[\mathbf{l}]} \mathcal{C})$ are pairwise disjoint for fixed σ and k .
- (5) The same top-dimensional cells in P_n for different σ have the same extended products.

Notation 4.7. Since for fixed n and the homeomorphisms ϕ_{m_1, \dots, m_k} , $\text{Ext}_{\phi_{m_1, \dots, m_k}}(\text{colim}_{\mathcal{T}_\sigma[\mathbf{l}]} \mathcal{C})$ only depends on \mathbf{l} , for simplicity, we denote it by $E_{\mathbf{l}}$. For the example $n = 3$, see Figure 20. Under the homeomorphisms ϕ_{m_1, \dots, m_k} and the linear maps, we transfer the homotopies $H_{\text{Ext}_e(P_{m_1} \times \cdots \times P_{m_k} \times \Delta^k)}$ from $\text{Ext}_e(P_{m_1} \times \cdots \times P_{m_k} \times \Delta^k)$ to each $E_{\mathbf{l}}$. We call this homotopy $H_{\mathbf{l}} : E_{\mathbf{l}} \times I \rightarrow E_{\mathbf{l}}$.

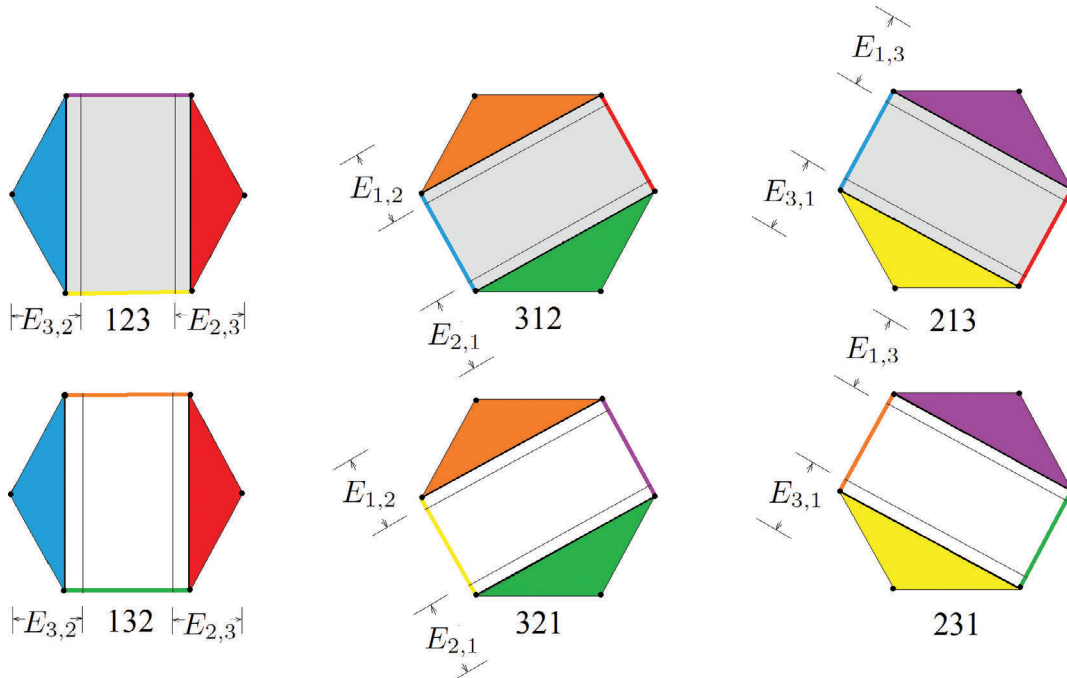


Figure 20. The subsets $E_{\mathbf{l}}$ when $n = 3$.

It is clear that these homotopies have the three properties transferred from those in Proposition 4.6.

Corollary 4.8. *The homotopies $H_{\mathbf{l}} : E_{\mathbf{l}} \times I \rightarrow E_{\mathbf{l}}$ satisfy the following conditions:*

- (1) Choose $\sigma \in S_n$ such that $\mathbf{l} = \mathbf{l}_1, \dots, \mathbf{l}_k \in \text{dSh}_{\sigma \setminus \sigma_1}[m_1, \dots, m_k]$. For each $i = 1, 2, \dots, k - 1$, let

$$d_i \mathcal{T}_\sigma^{n-2}[\mathbf{l}] = \{B_{\sigma_1}^+(\tau_1, \dots, \tau_i | \tau_{i+1}, \dots, \tau_k) : \tau_j \in \mathcal{T}_{\mathbf{l}_j}^{m_j-1}\} \quad \text{and} \quad d \mathcal{T}_\sigma^{n-2}[\mathbf{l}] = \bigcup_{i=1}^{k-1} d_i \mathcal{T}_\sigma^{n-2}[\mathbf{l}].$$

Let $d \mathcal{T}_\sigma[\mathbf{l}]$ be the set of trees in \mathcal{T}_σ such that each tree is smaller than or equal to an element in $d \mathcal{T}_\sigma^{n-2}[\mathbf{l}]$.

Then $H_{\mathbf{l}}$ contracts $\text{colim}_{\mathcal{T}_\sigma[\mathbf{l}]} \mathcal{C}$ onto $(\partial \text{colim}_{\mathcal{T}_\sigma[\mathbf{l}]} \mathcal{C}) \setminus \text{Int}(\text{colim}_{d \mathcal{T}_\sigma[\mathbf{l}]} \mathcal{C})$.

- (2) It maps the closure of $E_{\mathbf{l}} \setminus \text{colim}_{\mathcal{T}_\sigma[\mathbf{l}]} \mathcal{C}$ homeomorphically to $E_{\mathbf{l}}$.
- (3) $H_{\mathbf{l}}$ is the identity homotopy on $\partial E_{\mathbf{l}}$. □

4.2.3 Iterated cone construction

Starting from $n = 4$, we have to take care of the boundaries. For this we will use the so-called iterated cones, which we now define.

Let $n \geq 4$ and $1_n = 12 \cdots n \in S_n$. Notice that $\text{colim}_{\mathcal{F}_{1_n,1}} \mathcal{C}$, as a subspace of $\mathcal{F}_{1_n} = \text{colim}_{\mathcal{F}_{1_n}} \mathcal{C} = P_n$, is the cartesian product of P_{n-1} with $I_{\sqrt{n(n-1)}}$, where $I_{\sqrt{n(n-1)}}$ is the interval $[0, \sqrt{n(n-1)}]$. We construct the iterated cones of the faces of P_n of dimension i ($2 \leq i \leq n-2$), where P_n is seen as the realization of 1_n under \mathcal{F} , as follows. We then transfer the cones to all the P_σ symmetrically by using the S_n action. The cones are specified, by giving their cone vertex which will be a point inside P_n .

There is a choice for such cone vertices. We will choose these vertices “as close to the base as needed” and the cones at each step are mutually disjoint. This is technically done by requiring that the line determined by the vertex v and the geometric center of the base is perpendicular to the face and the distance from v to the geometric center is small. Since there are only finitely many cones in each cactus cell it follows that this is possible. The distance and perpendicularity do not fix v uniquely starting at codimension 2. In that case, we will choose v such that the entire cone lies *inside* a union of top-dimensional cactus cells with maximal possible initial branching number k .

Step 1. For any dimension 2 face $\mathcal{F}_{\mathbf{1}_1|\cdots|\mathbf{1}_{n-2}}$ of P_n , let v be a point in the interior of P_n with distance ϵ_2 to the geometric center of $\mathcal{F}_{\mathbf{1}_1|\cdots|\mathbf{1}_{n-2}}$. We choose this v as explained above and such that v is not in $\text{colim}_{\mathcal{F}_{1_n,1}} \mathcal{C}$. Then we form the join $\mathcal{F}_{\mathbf{1}_1|\cdots|\mathbf{1}_{n-2}} * v$, which is a cone with base $\mathcal{F}_{\mathbf{1}_1|\cdots|\mathbf{1}_{n-2}}$. We call such a cone $\mathcal{C}^1(\mathcal{F}_{\mathbf{1}_1|\cdots|\mathbf{1}_{n-2}})$. These cones are 3-dimensional.

Step $i - 1$, $3 \leq i \leq n - 3$. For any dimension i face $\mathcal{F}_{\mathbf{1}_1|\cdots|\mathbf{1}_{n-i}}$ of P_n , we consider its union with the $(i - 2)$ -cones of its codimension 1 faces:

$$\mathcal{F}_{\mathbf{1}_1|\cdots|\mathbf{1}_{n-i}} \cup \bigcup_{\mathbf{k} \in \mathcal{J}_{1_n}^{i-1}, \mathbf{k} < \mathbf{1}_1|\cdots|\mathbf{1}_{n-i}} \mathcal{C}^{i-2}(\mathcal{F}_{\mathbf{k}}).$$

Let v be a point in the interior of P_n with distance ϵ_i below the face $\mathcal{F}_{\mathbf{1}_1|\cdots|\mathbf{1}_{n-i}}$ as explained above. If necessary, we move the previous cone vertices, so that the line segments from v to any point in the union do not contain any other point. Again this is possible, since there are only finitely many cones and we can vary the distance and the position of the cone points for lower dimensions. Then we form the join of v with this union and denote it by $\mathcal{C}^{i-1}(\mathcal{F}_{\mathbf{1}_1|\cdots|\mathbf{1}_{n-i}})$ and call it the $(i - 1)$ -cone of $\mathcal{F}_{\mathbf{1}_1|\cdots|\mathbf{1}_{n-i}}$. Its dimension is $(i + 1)$.

Step $n - 3$. For any dimension $n - 2$ (codimension 1) face $\mathcal{F}_{\mathbf{1}_1|\mathbf{l}_2}$ of P_n , we form the union

$$B(\mathbf{l}_1|\mathbf{l}_2) := \mathcal{F}_{\mathbf{1}_1|\mathbf{l}_2} \cup \bigcup_{\mathbf{k} \in \mathcal{J}_{1_n}^{n-3}, \mathbf{k} < \mathbf{1}_1|\mathbf{l}_2} \mathcal{C}^{n-4}(\mathcal{F}_{\mathbf{k}}).$$

For the special elements $1|2 \cdots n$ and $2 \cdots n|1$, we let $\text{Cyl}(\mathcal{F}_{1|2 \cdots n}) = \text{Cyl}(\mathcal{F}_{2 \cdots n|1})$ be the space as the union of line segments such that each line segment joins a point in $B(1|2 \cdots n)$ to the corresponding point in $B(2 \cdots n|1)$. We call it the cylinder of $\mathcal{F}_{1|2 \cdots n}$ (or of $\mathcal{F}_{2 \cdots n|1}$).

For general $\mathbf{l}_1|\mathbf{l}_2$ (including $1|2 \cdots n$ and $2 \cdots n|1$), let v be a point in the interior of P_n with distance ϵ_{n-2} directly below the geometric center of $\mathcal{F}_{\mathbf{l}_1|\mathbf{l}_2}$ such that if $\mathbf{l}_1|\mathbf{l}_2$ is neither $1|2 \cdots n$ nor $2 \cdots n|1$, v is not in the interior of $\text{Cyl}(\mathcal{F}_{1|2 \cdots n})$. We form the join $B(\mathbf{l}_1|\mathbf{l}_2) * v$ and denote it by $\mathcal{C}^{n-3}(\mathcal{F}_{\mathbf{l}_1|\mathbf{l}_2})$. We call it the $(n - 3)$ -cone of $\mathcal{F}_{\mathbf{l}_1|\mathbf{l}_2}$.

We choose the values of $\epsilon_2, \dots, \epsilon_{n-2}$ small enough and the orientation of each v such that

- (1) all the previous conditions are satisfied,
- (2) each iterated cone is contained in the union of the elements of a collection $\{\mathcal{C}_{\mathbf{l}_i}\}$ such that each $\mathbf{l}_i \in \mathcal{J}_{1_n}^{n-1}$ has the largest possible arity number,
- (3) the union of all $(n - 3)$ -cones exhibits maximal symmetry.

To construct the iterated cones for P_n as \mathcal{F}_σ for any $\sigma \in S_n$, we take as images of the iterated cones of \mathcal{F}_{1_n} under the linear map

$$\sum_{v \in S_n} t_v \mathcal{F}_{v_1|\cdots|v_n} \mapsto \sum_{v \in S_n} t_v \mathcal{F}_{(\sigma v)_1|\cdots|(\sigma v)_n}.$$

4.2.4 Transferring homotopies from faces to cones

We will use the following observation to transfer the previously defined homotopies as homotopies on faces into the ambient P_n by inducing a homotopy on a cone over the face with vertex v which lies inside P_n .

Let P be a polytope and $H_P : P \times I \rightarrow P$ a homotopy with $H_P(\cdot, t)|_{\partial P} = 1_{\partial P}$ for all $t \in I$. We define $H_{P \times I} : (P \times I) \times I \rightarrow P \times I$ by $((x, s), t) \mapsto (H_P(x, t), s)$. So $H_{P \times I}(\cdot, \cdot, t)|_{(\partial P) \times I} = 1_{(\partial P) \times I}$ for all $t \in I$. Thus, if we identify $P \times I/P \times \{1\}$ with a cone $P * v$, the homotopy $H_{P \times I}$ induces a homotopy on $P \times I/P \times \{1\} \approx P * v$, which we call it $H_{P * v}$. This homotopy then satisfies

$$H_{P * v}(\cdot, t)|_{(\partial P) * v} = 1_{(\partial P) * v}. \tag{4.2}$$

4.2.5 The homotopy

Now we describe the homotopies H_σ where $\sigma \in S_n$ for some $n \geq 1$.

For $n = 1, 2$, we let H_σ be the identity homotopies. In fact, $\mathcal{C}(n) \approx \mathcal{F}(n)$ in these two cases. For $n = 3$, we let $H_\sigma(\cdot, t)$ be $H_{\sigma_2, \sigma_3}(\cdot, t)$ on E_{σ_2, σ_3} and $H_{\sigma_3, \sigma_2}(\cdot, t)$ on E_{σ_3, σ_2} ; we let H_σ be the identity homotopy on $P_3 \setminus \text{Int}(E_{\sigma_2, \sigma_3} \cup E_{\sigma_3, \sigma_2})$. By Corollary 4.8, H_σ is a well-defined homotopy on P_3 . See Figure 21.

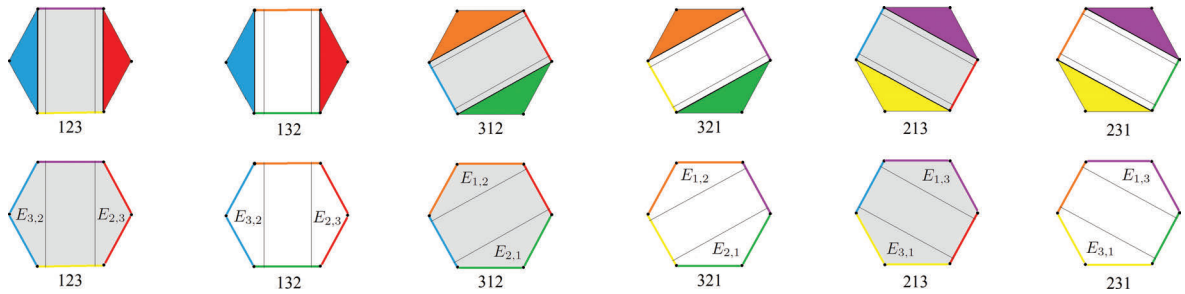


Figure 21. Top row: the domains of $h_\sigma = H_\sigma(\cdot, 1)$. Bottom row: the images of $h_\sigma = H_\sigma(\cdot, 1)$.

For each $n \geq 4$, we describe H_σ in n steps, assuming we know the homotopies for all $m < n$.

In the first $n - 1$ steps the homotopy is applied according to the initial branching number starting with $k = 1$ and ending with $k = n - 1$. After that, in the last step (Step n), the homotopy is done on the faces. The homotopy on the faces uses the iterated cones of degree $\leq n - 3$ while in Steps $2, \dots, n - 1$, we use the extensions. The first step is more complicated since part of the boundary of the cells that we are moving is connected to other cells of other P_σ . So in this step, there is an additional use of iterated cones.

In the steps with iterated cones, the homotopy is done in several substeps. For this we need the following technical details: For $\mathbf{l} = \mathbf{l}_1 | \dots | \mathbf{l}_k \in \mathcal{J}_\sigma$, let l_i be the length of the string \mathbf{l}_i and l the maximum of $\{l_i : i = 1, \dots, k\}$. The homotopies over the cones of the faces will be performed inductively over l .

Correspondingly, we subdivide the interval I in such a way that the homotopy can take place at different times in I . Let $f_0^m : I \rightarrow I$ be defined by $t \mapsto \frac{1}{m}t$ and $f_1^m : I \rightarrow I$ by $t \mapsto \frac{1}{m}(t + m - 1)$, where $m \geq 4$. Let $f_0^m : I \rightarrow I$ and $f_1^m : I \rightarrow I$ be the identity maps if $m = 3, 2, 1$. Then we let

$$f_{i_1 i_2 \dots i_k} = f_{i_1}^n \circ f_{i_2}^{n-1} \circ \dots \circ f_{i_k}^{n-k+1}$$

for $1 \leq k \leq n$, where $i_j = 0, 1, j = 1, \dots, k$. We also let $I_{i_1 i_2 \dots i_k} = f_{i_1 i_2 \dots i_k}(I)$. For an example, see Figure 22. From now on, $i_1 = 0$ corresponds to step 1 while $i_1 = 1$ corresponds to step n .

Step 1: $t \in [0, \frac{1}{n}]$, $\mathbf{i}_0 = \mathbf{0}$. For $\mathbf{l} = \mathbf{l}_1 | \dots | \mathbf{l}_{n-2} \in \mathcal{J}_\sigma$, if $l = 2$, then all but two of $\mathbf{l}_1, \dots, \mathbf{l}_{n-2}$ are of length 1 and we let $H_{C^1(\mathcal{F}_1)} : C^1(\mathcal{F}_1) \times [0, \frac{1}{n}] \rightarrow C^1(\mathcal{F}_1)$ be the identity homotopy. If $l = 3$, then $\mathbf{l} = \dots | \mathbf{l}_l | \dots$, where $\mathbf{l}_l = ijk$ and all the other \mathbf{l}_m s are of length 1. We define $H_{\mathcal{F}_1} : \mathcal{F}_1 \times [0, \frac{1}{n}] \rightarrow \mathcal{F}_1$ by

$$(x, t) \mapsto \psi_1^{-1}(* \times \dots \times * \times H_{\mathcal{F}_{123}}(\psi_{\mathbf{l}_l}(x), f_{i_1 \dots i_{n-3}}^{-1}(t)) \times * \times \dots \times *)$$



Figure 22. The subspaces $I_{i_1 \dots i_k}$ when $n = 6$. Notice that $I_{i_1 i_2 i_3 i_4 i_5 i_6} = I_{i_1 i_2 i_3}$.

if $t \in I_{i_1 i_2 \dots i_{n-3}}$ for some i_1, \dots, i_{n-3} and $(x, t) \mapsto x$ otherwise, where

$$\psi_{\mathbf{1}} = (*, \dots, *, \psi_{\mathbf{1}}, *, \dots, *) : \mathcal{F}_{\mathbf{1}} \rightarrow * \times \dots \times * \times \mathcal{F}_{123} \times * \times \dots \times *$$

is the homeomorphism defined under $i \mapsto 1, j \mapsto 2$ and $k \mapsto 3$. Then we get the induced homotopy

$$H_{C^1(\mathcal{F}_{\mathbf{1}})} : C^1(\mathcal{F}_{\mathbf{1}}) \times [0, \frac{1}{n}] \rightarrow C^1(\mathcal{F}_{\mathbf{1}}).$$

Let $3 \leq i \leq n - 3$. Suppose we have described the homotopies for $t \in [0, \frac{1}{n}]$ on the $(i - 2)$ -cones. For $\mathbf{l} = \mathbf{l}_1 | \dots | \mathbf{l}_{n-i}$, define $H_{\mathcal{F}_{\mathbf{l}}} : \mathcal{F}_{\mathbf{l}} \times [0, \frac{1}{n}] \rightarrow \mathcal{F}_{\mathbf{l}}$ by

$$(x, t) \mapsto \psi_{\mathbf{1}}^{-1}(H_{\mathcal{F}_{12 \dots i-1}}(\psi_{\mathbf{1}}(x), f_{i_1 i_2 \dots i_{n-1}}^{-1}(t)), \dots, H_{\mathcal{F}_{12 \dots n-i}}(\psi_{\mathbf{l}_{n-i}}(x), f_{i_1 i_2 \dots i_{n-i}}^{-1}(t))),$$

where

$$\psi_{\mathbf{l}} = (\psi_{\mathbf{l}_1}, \dots, \psi_{\mathbf{l}_{n-i}}) : \mathcal{F}_{\mathbf{l}} \rightarrow \mathcal{F}_{12 \dots i-1} \times \dots \times \mathcal{F}_{12 \dots n-i}$$

is the homeomorphism under the assignments $(\mathbf{l}_j)_k \mapsto k$, for $k = 1, 2, \dots, l_j$ and $j = 1, 2, \dots, n - i$, and we define $H_{\mathcal{F}_{12 \dots l_j}}(\psi_{\mathbf{l}_j}(x), f_{i_1 i_2 \dots i_{n-l_j}}^{-1}(t))$ to be $\psi_{\mathbf{l}_j}(x)$ if $f_{i_1 i_2 \dots i_{n-l_j}}^{-1}(t) = \emptyset$. The homotopies $H_{\mathcal{F}_{\mathbf{l}}}$ and $H_{C^{i-1}(\mathcal{F}_{\mathbf{k}})}$, where $\mathbf{k} \in \mathcal{J}_{\sigma}^{i-1}$ and $\mathbf{k} < \mathbf{l}$, agree on their overlaps.

Thus, we get a well-defined homotopy on $\mathcal{F}_{\mathbf{l}_1 | \dots | \mathbf{l}_{n-i}} \cup \bigcup_{\mathbf{k} \in \mathcal{J}_{\sigma}^{i-1}, \mathbf{k} < \mathbf{l}_1 | \dots | \mathbf{l}_{n-i}} C^{i-2}(\mathcal{F}_{\mathbf{k}})$, which induces the homotopy

$$H_{C^{i-1}(\mathcal{F}_{\mathbf{l}})} : C^{i-1}(\mathcal{F}_{\mathbf{l}}) \times [0, \frac{1}{n}] \rightarrow C^{i-1}(\mathcal{F}_{\mathbf{l}}).$$

Lastly, for $\mathbf{l} = \mathbf{l}_1 | \mathbf{l}_2$, define

$$H_{\mathcal{F}_{\mathbf{l}}} : \mathcal{F}_{\mathbf{l}} \times [0, \frac{1}{n}] \rightarrow \mathcal{F}_{\mathbf{l}}$$

by

$$(x, t) \mapsto \psi_{\mathbf{l}}^{-1}(H_{\mathcal{F}_{12 \dots i-1}}(\psi_{\mathbf{l}_1}(x), f_{i_1 i_2 \dots i_{n-1}}^{-1}(t)), H_{\mathcal{F}_{12 \dots l_2}}(\psi_{\mathbf{l}_2}(x), f_{i_1 i_2 \dots i_{n-l_2}}^{-1}(t)))$$

as above. Again, we get a well-defined homotopy on

$$B(\mathbf{l}_1 | \mathbf{l}_2) = \mathcal{F}_{\mathbf{l}_1 | \mathbf{l}_2} \cup \bigcup_{\mathbf{k} \in \mathcal{J}_{\sigma}^{n-3}, \mathbf{k} < \mathbf{l}_1 | \mathbf{l}_2} C^{n-4}(\mathcal{F}_{\mathbf{k}}).$$

Then we get induced homotopies $H_{C^{n-3}(\mathcal{F}_{\mathbf{l}})} : C^{n-3}(\mathcal{F}_{\mathbf{l}}) \times [0, \frac{1}{n}] \rightarrow C^{n-3}(\mathcal{F}_{\mathbf{l}})$, where \mathbf{l} is neither $1|2 \dots n$ nor $2 \dots n|1$. Let θ be the homeomorphism $\theta = (\theta_1, \theta_2) : \text{Cyl}(\mathcal{F}_{1|2 \dots n}) \rightarrow B(1|2 \dots n) \times I$. Then we also have the homotopy

$$H_{\text{Cyl}(\mathcal{F}_{1|2 \dots n})} : \text{Cyl}(\mathcal{F}_{1|2 \dots n}) \times [0, \frac{1}{n}] \rightarrow \text{Cyl}(\mathcal{F}_{1|2 \dots n})$$

defined by $(x, t) \mapsto \theta^{-1}(H_{B(1|2 \dots n)}(\theta_1(x), t), \theta_2(x))$. The homotopies $H_{\text{Cyl}(\mathcal{F}_{1|2 \dots n})}$ and the $H_{C^{n-3}(\mathcal{F}_{\mathbf{l}})}$ s agree on their overlaps. On the other hand, we let $H_{\sigma} : P_n \times [0, \frac{1}{n}] \rightarrow P_n$ be the identity homotopy on the complement of the interior of the subspace $\text{Cyl}(\mathcal{F}_{1|2 \dots n}) \cup \bigcup_{\mathbf{l} \in \mathcal{J}_{\sigma}^{n-2} \setminus \{1|2 \dots n, 2 \dots n|1\}} C^{n-3}(\mathcal{F}_{\mathbf{l}})$. By (4.2), $H_{\sigma} : P_n \times [0, \frac{1}{n}] \rightarrow P_n$ is a well-defined homotopy.

Step $j, j = 2, \dots, n - 1$: $t \in [\frac{j-1}{n}, \frac{j}{n}]$. Let $H_{\sigma}(\cdot, t)$ be $H_1(\cdot, nt - j + 1)$ on $E_{\mathbf{l}}$, where $\mathbf{l} = \mathbf{l}_1, \dots, \mathbf{l}_j$ is compatible with σ (recall this means each \mathbf{l}_i is a subsequence of $\sigma_2 \dots \sigma_n$), and let $H_{\sigma}(\cdot, t)$ be the identity homotopy on the complement of the interior of the union of these $E_{\mathbf{l}}$ s in P_n . By Corollary 4.8, each $H_{\sigma} : P_n \times [\frac{j-1}{n}, \frac{j}{n}] \rightarrow P_n$ is a well-defined homotopy.

Step n : $t \in [\frac{n-1}{n}, 1]$. We get the induced homotopies $H_{C^{n-3}(\mathcal{F}_1)} : C^{n-3}(\mathcal{F}_1) \times [\frac{n-1}{n}, 1] \rightarrow C^{n-3}(\mathcal{F}_1)$ for all $\mathbf{l} \in \mathcal{J}_\sigma^{n-2}$ as those in Step 1 except that we let $i_1 = 1$ and we do not consider the cylinders. On the other hand, we let $H_\sigma : P_n \times [\frac{n-1}{n}, 1] \rightarrow P_n$ be the identity homotopy on the complement of the interior of $\bigcup_{\mathbf{l} \in \mathcal{J}_\sigma^{n-2}} C^{n-3}(\mathcal{F}_1)$. By (4.2), $H_\sigma : P_n \times [\frac{n-1}{n}, 1] \rightarrow P_n$ is a well-defined homotopy.

The above n homotopies agree on their overlaps, thus we get a well-defined homotopy $H_\sigma : P_n \times I \rightarrow P_n$.

Proposition 4.9. *For any $n \geq 1$, the homotopies H_σ satisfy conditions (*1), (*2) and (*3) of Remark 4.4 and hence induce the homotopies $1_{\mathcal{F}(n)} \simeq_{H_\mathcal{F}} \bar{h}_n \circ \bar{1}_n$ and $1_{\mathcal{C}(n)} \simeq_{H_\mathcal{C}} \bar{1}_n \circ \bar{h}_n$ detailed in Remark 4.4.*

Proof. There is nothing to check for $n = 1, 2$. By our previous discussion, it suffices to prove that the homotopies H_σ , $\sigma \in S_n$ satisfy (*1), (*2) and (*3).

As a warm-up, let us consider the case for $n = 3$ in detail first. Condition (*1) holds by Corollary 4.8. Let $x \sim_{\mathcal{F}} y$, where $x \in P_n$ indexed by σ and $y \in P_n$ indexed by ν . Then $x = y$ in $\text{Int}(\mathcal{F}_1)$ for some $\mathbf{l} \in \mathcal{J}_\sigma \cap \mathcal{J}_\nu$. If the order of \mathbf{l} is 2, then $\sigma = \nu$. So $H_\sigma(x, t) = H_\nu(x, t) = H_\nu(y, t)$ in \mathcal{F}_1 . Otherwise (the order of \mathbf{l} is smaller than 2), $H_\sigma(x, t) = x = y = H_\nu(y, t)$ in \mathcal{F}_α because we have the identity homotopy on the 1-skeleton. So $H_\sigma(x, t) \sim_{\mathcal{F}} H_\nu(y, t)$ for any t , verifying (*2). Let $x \sim_{\mathcal{C}} y$, where $x \in P_n$ indexed by σ and $y \in P_n$ indexed by ν . Then there is $\mathbf{l} \in \mathcal{J}_\sigma^2 \cap \mathcal{J}_\nu^2$ with the lowest arity number such that $x = y$ in \mathcal{C}_1 . Then for any t , either $H_\sigma(x, t) = H_\nu(y, t)$ in \mathcal{C}_1 or $H_\sigma(x, t) = H_\nu(y, t)$ in \mathcal{C}_k , where $\mathbf{k} \in \mathcal{J}_\sigma^2 \cap \mathcal{J}_\nu^2$ and \mathbf{k} has arity number one greater than or equal to that of \mathbf{l} . Thus, (*3a) holds. Lastly, if $x = y$ in $\text{Int}(\mathcal{C}_1)$, where \mathbf{l} has arity number 1, then $\sigma = \nu$ and so $H_\sigma(x, 1) = H_\sigma(y, 1) = H_\nu(y, 1)$ in $\mathcal{F}_\sigma = \mathcal{F}_\nu$; otherwise, $H_\sigma(x, 1) = H_\nu(y, 1)$ in \mathcal{F}_k for some $\mathbf{k} \in \mathcal{J}_\sigma^1 \cap \mathcal{J}_\nu^1$. Hence, (*3b) holds.

For $n \geq 4$, from the description of H_σ when $t \in [0, \frac{1}{n}]$, we see that (*1) holds. Now let $x \sim_{\mathcal{F}} y$, where $x \in P_n$ indexed by σ and $y \in P_n$ indexed by ν . Then $x = y$ in $\text{Int}(\mathcal{F}_1)$ for some $\mathbf{l} \in \mathcal{J}_\sigma \cap \mathcal{J}_\nu$. Then $H_\sigma(x, t) = H_\nu(y, t)$ in \mathcal{F}_1 (but not necessarily in $\text{Int}(\mathcal{F}_1)$). Thus, (*2) holds. Now let $x \sim_{\mathcal{C}} y$, where $x \in P_n$ indexed by σ and $y \in P_n$ indexed by ν . Then there is $\mathbf{l} \in \mathcal{J}_\sigma^{n-1} \cap \mathcal{J}_\nu^{n-1}$ with the lowest arity number such that $x = y$ in \mathcal{C}_1 . Then for any t , either $H_\sigma(x, t) = H_\nu(y, t)$ in \mathcal{C}_1 or $H_\sigma(x, t) = H_\nu(y, t)$ in \mathcal{C}_k , where $\mathbf{k} \in \mathcal{J}_\sigma^{n-1} \cap \mathcal{J}_\nu^{n-1}$ and \mathbf{k} has arity number greater than or equal to that of \mathbf{l} . Therefore, (*3a) holds. Finally, let $x \sim_{\mathcal{C}} y$, where $x \in P_n$ indexed by σ and $y \in P_n$ indexed by ν , so there is $\mathbf{l} \in \mathcal{J}_\sigma \cap \mathcal{J}_\nu$ such that $x = y$ in \mathcal{C}_1 . Then there is $\mathbf{k} = \mathbf{k}_1 | \dots | \mathbf{k}_k \in \mathcal{F}_\sigma \cap \mathcal{F}_\nu$ such that $H_\sigma(\mathcal{C}_1, \frac{n-1}{n}) = H_\nu(\mathcal{C}_1, \frac{n-1}{n}) \subset \mathcal{F}_k$. By the definition of the homotopy, there is a $\mathbf{k}' < \mathbf{k}$ such that $H_\sigma(x, 1) = H_\nu(y, 1)$ in $\mathcal{F}_{k'}$, establishing (*3b). \square

5 Discussion: Relations to other E_2 operads, application and outlook

There seem to be two breeds of E_2 operads. The first, and older ones, are useful for the recognition of iterated loop spaces, like the little discs, the little cubes and the Steiner operad. The other, and the newer generation, are good for solving Deligne's conjecture. Of course there are the cofibrant models, which are by definition a hybrid. These have the drawback that they are usually a bit too abstract to handle to give actual operadic operations, by which we mean they act only through a factorization via a more concrete operad.

The first type usually has configuration spaces as deformation retracts, namely, as we have discussed, they have the Milgram model $\{\mathcal{F}(n)\}$ as retract, which is classically used in the iterated loop space program (see [3, 35]). See [29, Section 2.4] as a good survey. One feature of \mathcal{F} , however, is that it is not an operad in any known way. There are some remnants [3, 29] using convex hulls, but there is not even a closed cellular operad structure.

On the other hand, the other models have an algebraic aspect, which allows one to define operations on the Hochschild cochain complex. Their diversity is actually not as big as one would think.

On the cell/chain level they are variations of the Gerstenhaber–Voronov's GV-brace operations [15]. On the topological level, they all retract to Cact , which deformation retracts to $\mathcal{C} = \text{Cact}^1$. The difference to the above is that \mathcal{C} is actually a chain level operad, while \mathcal{F} is not. Moreover, \mathcal{C} has the b/w tree structure, making it ready to give operations, such as in Deligne's conjecture.

Let us briefly go through the list and history. Most of the operads were actually constructed first on the combinatorial level and then realized as topological spaces, using totalizations, realizations or condensations. For the operad Cact the story was the inverse. It existed first as a topological operad [25], and then it was realized that it is E_2 and it has an operadic cellular chain model $\text{CC}_*(\text{Cact}^1)$ (see [18]) corresponding to GV .

The first operad is the Kontsevich–Soibelman minimal operad M [28], which is the generalization of the GV -operad to the A_∞ case. It gave the first solution to Deligne’s conjecture and works over \mathbb{Z} . The procedure here is a little different as the Fulton–MacPherson compactification and a W -construction were used. The fact that it can be realized as a version of cacti is contained in [26]. If the A_∞ algebra is strict, it contacts to $\text{CC}_*(\text{Cact})$, see [24]. The next operad was by McClure and Smith [32] and it gives a cosimplicial description of the GV -operad and hence can realize a topological operad using totalization. The current paper also fixes the homotopy type of formulas in [32] directly.

In their second paper, McClure and Smith [33] introduced sequence notation for the GV -operad, which has been one of the most influential constructions in the theory. The sequence operad S_2 is with hindsight actually isomorphic to the description by b/w bipartite trees [18, 20] as we recall below. The totalization of [32] then reconstructs spineless cacti on the topological level. Alternatively, McClure and Smith [33] used Berger’s machine. The operad structure of this comparison was further clarified in [6].

The third paper [34] contains the very fruitful functor operad approach, which has been reformulated in [2] by means of the lattice path operad. This gives back the usual operations if certain degeneracy maps are applied. That this procedure is also operadic follows from a more general theorem proved in [22, Theorem 4.4]. The degeneracies are given as angle markings. An intermediate step to the full realization is given by partitioning, see [22]. This provides a colored set operad structure. This was cast into a cosimplicial/simplicial picture in [2] as the lattice path operad. Here the map from Δ^n specifies the partitioning in the sense of [22] and is equivalent to using the foliation operator of [20]. After doing the condensation, one again obtains spineless cacti on the topological level.

The quotient map we discuss is probably related to the second filtration of the Barratt–Eccles operad as discussed in [6], but this is unclear at the moment, cf. Section 5.3 below. What is clear is that the quotient makes the non-operad \mathcal{F} into an operad on the cell level and even a topological quasi-operad, i.e. associative up to homotopy.

For the cyclic Deligne conjecture, which is an application of the E_2 identification, the story is similar. The first proof is in [21] using cacti. The first full proof that cacti are indeed equivalent to fD_2 is in [18]. Here one uses the E_2 structure of spineless cacti and the fact that cacti is a bi-crossed product. The paper [2] adds the simplicial structure on the chain level explaining the usual operations as action of a colored operad. Another version of this partitioning is contained in [22]. Condensation then reconstructs cacti. Another chain level action was given slightly later than [21] in [45]. They did not, however, show that the relevant chain level operads are models for the framed little discs. So, on the topological level the operads adapted to prove the cyclic version are basically all cacti. The added difficulty, is that for cacti one is dealing with a bi-crossed product and not just a semi-direct product. The cyclic A_∞ version again based on cacti is contained in [48].

5.1 Bijection of $\text{CC}_*(\text{Cact}^1)$ and S_2

The isomorphism is clear from the isomorphisms

$$S_2 \xleftarrow{\cong} \text{formulas} \xleftarrow{\cong} \text{GV} \xleftarrow{\cong} \text{CC}_*(\text{Cact}^1) \xleftarrow{\cong} \mathcal{F}_{bp}^{pp,nt}$$

contained in [18, 32, 33], see also [2].

This isomorphism between $\text{CC}_*(\text{Cact}^1)$ and S_2 is actually explicitly given in [23], which also contains the idea of cacti with stops, i.e. monotone parameterizations as explained in [19], used by Salvatore in the cyclic case, to rewrite the existing proofs in the language of McClure–Smith. Given a cactus or equivalently a b/w tree, one obtains a sequence as follows. Go around the outside circle and record the lobe number you see. Equivalently, for a planar planted b/w tree all the white angles (i.e. pairs of subsequent flags to a white vertex)

come in a natural order by embedding in the plane. Reading off the labels give the direct morphism, which is easily seen to be an isomorphism.

In fact, [23, Proposition 4.11] actually contains a generalization to the full E_∞ structures. Here one obtains an obviously surjective map. The injectivity is clear on the E_2 level.

5.2 Lifting of a cellular quasi-isomorphism

Let $CC_*(\mathcal{F}(n))$ be the cellular chains of $\mathcal{F}(n)$. In [44], Turchine constructed a homomorphism

$$I_* : CC_*(\mathcal{F}(n)) \rightarrow CC_*(\text{Cact}^1(n))$$

of complexes and showed that I_* is a quasi-isomorphism using homological algebra. By checking the definition of I_* in [44, p. 882], one immediately has the following.

Proposition 5.1. *The homomorphism $I_* : CC_*(\mathcal{F}(n)) \rightarrow CC_*(\text{Cact}^1(n))$ is induced from the homotopy equivalence $\bar{1}_n : \mathcal{F}(n) \rightarrow \text{Cact}^1(n)$. Thus, I_* is a quasi-isomorphism.*

5.3 Further connections

Since both $\mathcal{F}(n)$ and $\mathcal{C}(n)$ are obtained by gluing $n!$ contractible polytopes, our work also has connections to Batanin's theory of the symmetrization of contractible 2-operads (and n -operads in general) [1]. It is worth pointing out that instead of making the spaces bigger by compactifying the various deformation retract models of the configuration spaces $F(\mathbb{R}^2, n)$ to get operadic structures, one can subdivide the constituent contractible pieces (P_n) and then do further gluing to get the quasi-operad $\{\text{Cact}^1(n)\}_{n \geq 1}$, which become a bona-fide operad $\{\text{Cact}(n)\}_{n \geq 1}$ after taking the semi-direct product with the scaling operad [18].

Another E_2 -operad which is quite different from \mathcal{C}_2 or \mathcal{D}_2 is $\{|C_2S_n|\}_{n \geq 1}$, the realization of the second term of the Smith filtration of the simplicial universal bundle WS_n , which is also known as the Barratt–Eccles operad. A reformulation of C_2S_n resembles the presentation of $\mathcal{F}(n)$: C_2S_2 is built up out of $n!$ copies of the nerve $\mathcal{N}(S_n, <)$, where $<$ is the weak Bruhat order on the set S_n (see [5]). It can be readily checked that for $n = 1, 2, 3$, $|\mathcal{N}(S_n, <)|$ deformation retracts to P_n and C_2S_n deformation retracts to $\mathcal{F}(n)$. The retraction can be explicitly described. The same is hoped for $n \geq 4$, even though the dimension of $|C_2S_n|$ grows quadratically as $\frac{n(n-1)}{2}$ and difficulty already arises when $n = 4$.

One could also try to find an explicit combinatorial retraction from $|C_2S_n|$ to $\mathcal{F}(n)$ for each n , as it is known that the two are weakly equivalent as topological preoperads. As it follows from [6] that surjections of complexity ≤ 2 can be faithfully realized inside C_2S_n one would have to prove that this injection is a homotopy equivalence.

A next step would be to relate the higher-dimensional little discs (cubes etc.) operad to higher-dimensional cacti operad through products of permutohedra. We refer the reader to [23] for a higher-dimensional version of the cacti operad.

A Proof of Proposition 4.5 and Proposition 4.6

A.1 Proof of Proposition 4.5

Proposition 4.5 follows from two lemmas.

Lemma A.1. *Let S_\pm^{n-2} be the upper(lower)-hemisphere*

$$S_\pm^{n-2} = \{(x_1, \dots, x_{n-1}) \in \mathbb{R}^{n-1} : x_1^2 + \dots + x_{n-1}^2 = 1, x_{n-1} \geq 0 \text{ (} x_{n-1} \leq 0 \text{)}\}$$

in \mathbb{R}^{n-1} . Then S_\pm^{n-2} is a deformation retract of the unit cell D^{n-1} .

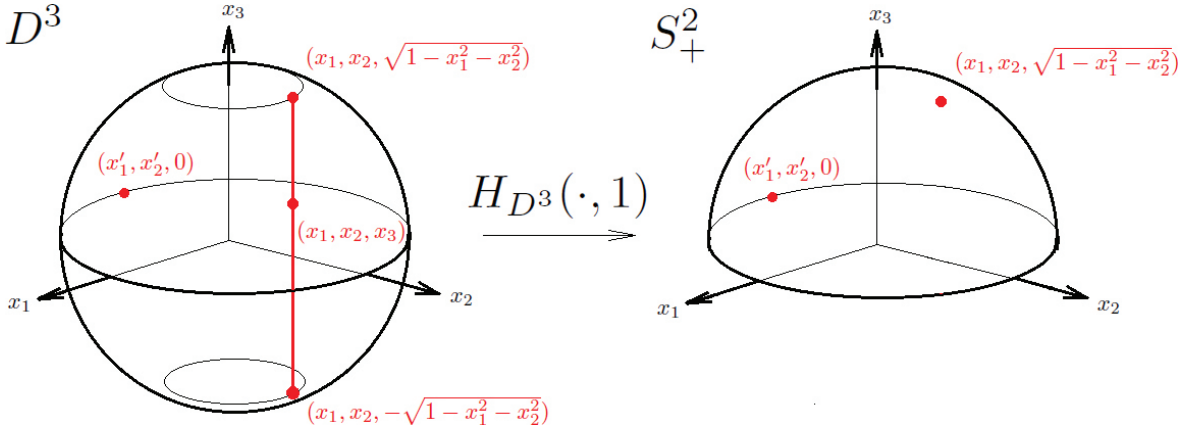


Figure 23. Deformation retraction from D^3 to S_+^2 .

Proof. Define $H_{D^{n-1}} : D^{n-1} \times I \rightarrow D^{n-1}$ by

$$H_{D^{n-1}}((x_1, x_2, \dots, x_{n-1}), t) = (x_1, x_2, \dots, x_{n-2}, (1-t)x_{n-1} + t\sqrt{1-x_1^2-\dots-x_{n-2}^2}).$$

It can be readily checked that $H_{D^{n-1}}$ is a well-defined homotopy. Geometrically, $H_{D^{n-1}}$ contracts each fiber over a point $(x_1, \dots, -\sqrt{1-x_1^2-\dots-x_{n-2}^2})$ on S_+^{n-2} to the point $(x_1, \dots, \sqrt{1-x_1^2-\dots-x_{n-2}^2})$ on S_+^{n-2} . In addition, $H_{D^{n-1}}(\cdot, t)$ is the identity map on S_+^{n-2} for all $t \in I$. So $H_{D^{n-1}}$ is a deformation retraction from D^{n-1} onto S_+^{n-2} (S_+^{n-2} is a deformation retract of D^{n-1}), see Figure 23 for an illustration of the case $n = 4$. \square

Lemma A.2. *There is a homeomorphism from $P_{m_1} \times P_{m_2} \times \dots \times P_{m_k} \times \Delta^k$ to D^{n-1} mapping $P_{m_1} \times P_{m_2} \times \dots \times P_{m_k} \times (\bigcup_{i=1}^k v_1 \cdots \widehat{v}_i \cdots v_{k+1})$ homeomorphically onto S_+^{n-2} .*

Proof. Let \mathcal{C}_{m_l} be the geometric center of P_{m_l} , where $l = 1, \dots, k$, and let F_{j_l} , where $j_l \in I_l$, be the facets of P_{m_l} . Let $\mathcal{C}_k = \frac{1}{k+1}(v_1 + \dots + v_{k+1})$. So \mathcal{C}_k is the barycenter of Δ^k . Then $P_{m_l} = \bigcup_{j_l \in I_l} F_{j_l} * \mathcal{C}_{m_l}$, where $*$ is the join operation, and $\Delta^k = \bigcup_{i=1}^{k+1} v_1 \cdots \widehat{v}_i \cdots v_{k+1} \mathcal{C}_k$. So

$$P_{m_1} \times \dots \times P_{m_k} \times \Delta^k = \bigcup_{l=1}^k \bigcup_{j_l \in I_l} \bigcup_{i=1}^{k+1} (F_{j_l} * \mathcal{C}_{m_l}) \times \dots \times (F_{j_l} * \mathcal{C}_{m_l}) \times \dots \times (F_{j_k} * \mathcal{C}_{m_k}) \times (v_1 \cdots \widehat{v}_i \cdots v_{k+1} \mathcal{C}_k).$$

Notice that each product on the right above has $\mathcal{C} = (\mathcal{C}_{m_1}, \dots, \mathcal{C}_{m_k}, \mathcal{C}_k)$ as one of its vertices and is the union of line segments from \mathcal{C} to a point of the union $\bigcup_{l=1}^k (F_{j_l} * \mathcal{C}_{m_l}) \times \dots \times F_{j_l} \times \dots \times (F_{j_k} * \mathcal{C}_{m_k}) \times (v_1 \cdots \widehat{v}_i \cdots v_{k+1} \mathcal{C}_k) \cup (F_{j_l} * \mathcal{C}_{m_l}) \times \dots \times (F_{j_k} * \mathcal{C}_{m_k}) \times (v_1 \cdots \widehat{v}_i \cdots v_{k+1})$ and the lines intersect only at \mathcal{C} .

The line segments of different products having \mathcal{C} as a vertex above agree on the intersections. So $P_{m_1} \times \dots \times P_{m_k} \times \Delta^k$ is the union of line segments emanating from \mathcal{C} and the union of the end points different from \mathcal{C} of the line segments is $\partial(P_{m_1} \times \dots \times P_{m_k} \times \Delta^k)$. (See Figure 24.)

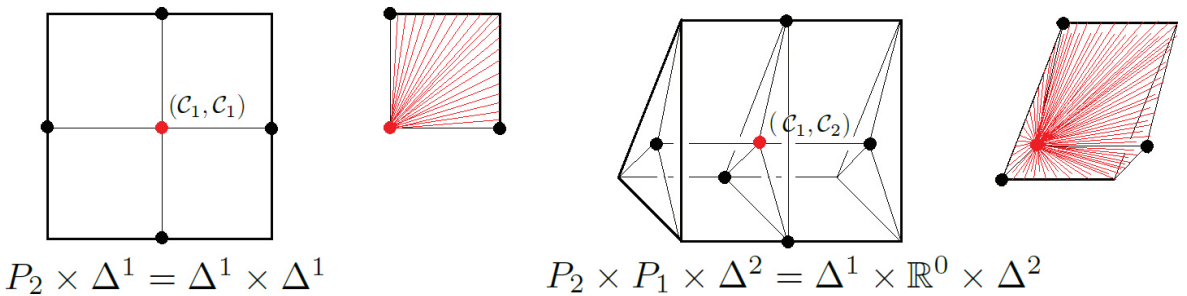


Figure 24. Decompositions of $P_2 \times \Delta^1$ and $P_2 \times P_1 \times \Delta^2$ into line segments joined at their \mathcal{C} .

We will use a similar proof of that of [36, Lemma 1.1] four times from now on. Here is the first time.

Let $T : P_{m_1} \times \cdots \times P_{m_k} \times \Delta^k \rightarrow \mathbb{R}^{n-1}$ be the translation defined by

$$T(x) = x - \mathcal{C}.$$

Let $r' : \mathbb{R}^{n-1} \setminus \{(0, \dots, 0)\} \rightarrow S^{n-2}$ be the radial contraction given as

$$r'(x) = \frac{x}{|x|},$$

where $|x|$ is the Euclidean norm of x . Since each half open ray emanating from $(0, \dots, 0)$ intersects with $T(\partial(P_{m_1} \times \cdots \times P_{m_k} \times \Delta^k))$ at one and only one point, r' restricts to a continuous bijection

$$r : T(\partial(P_{m_1} \times \cdots \times P_{m_k} \times \Delta^k)) \rightarrow S^{n-2}.$$

Being the continuous image of a compact space, $T(\partial(P_{m_1} \times \cdots \times P_{m_k} \times \Delta^k))$ is compact, and S^{n-2} is Hausdorff, so r is indeed a homeomorphism.

Now we extend $r : T(\partial(P_{m_1} \times \cdots \times P_{m_k} \times \Delta^k)) \rightarrow S^{n-2}$ to $R : T(P_{m_1} \times \cdots \times P_{m_k} \times \Delta^k) \rightarrow D^{n-1}$. Define

$$R(x) = \begin{cases} \frac{x}{|r^{-1}(\frac{x}{|x|})|} & \text{if } x \neq (0, \dots, 0), \\ (0, \dots, 0) & \text{if } x = (0, \dots, 0). \end{cases}$$

Except for at $x \neq (0, \dots, 0)$, R is also continuous at $x = (0, \dots, 0)$. To see this, let L be a lower bound of the Euclidean norm on $\partial(P_{m_1} \times \cdots \times P_{m_k} \times \Delta^k)$. Then for any $\epsilon > 0$, if $|x| < L\epsilon$, then

$$|R(x) - R(0)| = \frac{|x|}{|r^{-1}(\frac{x}{|x|})|} \leq \frac{L\epsilon}{L} = \epsilon.$$

Since R is a continuous bijection from compact $T(P_{m_1} \times \cdots \times P_{m_k} \times \Delta^k)$ to Hausdorff D^{n-1} , R is indeed a homeomorphism. Furthermore, T is also a homeomorphism onto its image. So $R \circ T$ is a homeomorphism from $P_{m_1} \times \cdots \times P_{m_k} \times \Delta^k$ to D^{n-1} mapping $\partial(P_{m_1} \times \cdots \times P_{m_k} \times \Delta^k)$ homeomorphically onto S^{n-2} .

So far, $P_{m_1} \times \cdots \times P_{m_k} \times (\bigcup_{i=2}^k v_1 \cdots \widehat{v}_i \cdots v_{k+1})$ has not been mapped to the lower-hemisphere S_-^{n-2} . We will use stereographic projection to achieve this.

Recall $\Delta^k = v_1 v_2 \cdots v_{k+1}$ and $\partial\Delta^k = (\bigcup_{i=2}^k v_1 \cdots \widehat{v}_i \cdots v_{k+1}) \cup (v_1 v_2 \cdots v_k \cup v_2 \cdots v_k v_{k+1})$. Then:

- (1) $\mathcal{N}_k = \frac{1}{k-1}(v_2 + \cdots + v_k)$ is in $\text{Int}(v_1 v_2 \cdots v_k \cup v_2 \cdots v_k v_{k+1})$.
 - (2) $\mathcal{S}_k = \frac{1}{2}(v_1 + v_{k+1})$ is in $\text{Int}(\bigcup_{i=2}^k v_1 \cdots \widehat{v}_i \cdots v_{k+1})$.
 - (3) $\mathcal{N}_k, \mathcal{C}_k$ and \mathcal{S}_k lie on the same line and $|\mathcal{N}_k \mathcal{C}_k| : |\mathcal{N}_k \mathcal{S}_k| = 2 : (k + 1)$.
- (See Figure 25.)

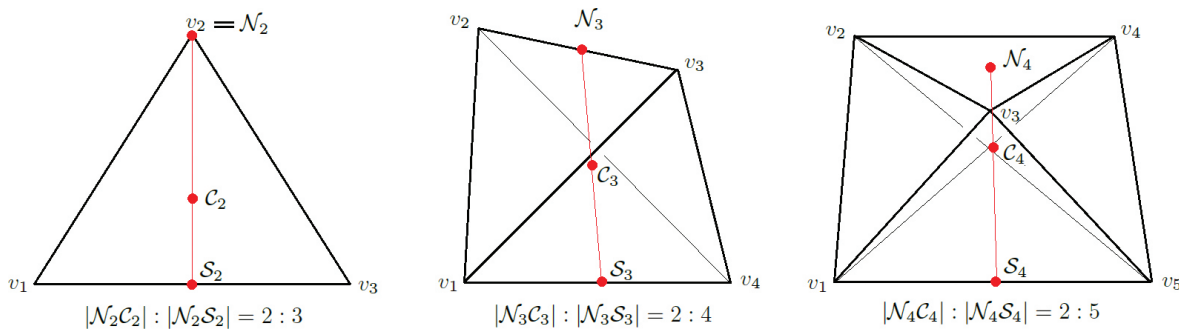


Figure 25. The points $\mathcal{N}_i, \mathcal{C}_i$ and $\mathcal{S}_i, i = 2, 3, 5$.

Now we let $\mathcal{N} = (\mathcal{C}_{m_1}, \dots, \mathcal{C}_{m_k}, \mathcal{N}_k)$ and $\mathcal{S} = (\mathcal{C}_{m_1}, \dots, \mathcal{C}_{m_k}, \mathcal{S}_k)$. So:

- (1) \mathcal{N} is in the relative interior of $\partial(P_{m_1} \times \cdots \times P_{m_k} \times \Delta^k) \setminus \text{Int}(P_{m_1} \times \cdots \times P_{m_k} \times (\bigcup_{i=2}^k v_1 \cdots \widehat{v}_i \cdots v_{k+1}))$.
- (2) \mathcal{S} is in the relative interior of $P_{m_1} \times \cdots \times P_{m_k} \times (\bigcup_{i=2}^k v_1 \cdots \widehat{v}_i \cdots v_{k+1})$.
- (3) \mathcal{C} is in $\text{Int}(P_{m_1} \times \cdots \times P_{m_k} \times \Delta^k)$.
- (4) \mathcal{N}, \mathcal{C} and \mathcal{S} lie on the same line and $|\mathcal{N}\mathcal{C}| : |\mathcal{N}\mathcal{S}| = 2 : (k + 1)$.

Let ϕ be an element in $SO(n - 1)$ rotating the vector $\mathcal{N} - \mathcal{C}$ so that it is aligned with the positive x_{n-1} -axis. Notice that $\phi : D^{n-1} \rightarrow D^{n-1}$ is a homeomorphism. So $b := \phi \circ R \circ T$ is a homeomorphism.

Let $N = (0, \dots, 0, 1) \in \mathbb{R}^{n-1}$ and $S = (0, \dots, 0, -1) \in \mathbb{R}^{n-1}$. The stereographic projections

$$p'_N : S^{n-2} \setminus N \rightarrow \mathbb{R}^{n-2}, \quad (x_1, \dots, x_{n-1}) \mapsto \left(\frac{x_1}{1 - x_{n-1}}, \frac{x_2}{1 - x_{n-1}}, \dots, \frac{x_{n-2}}{1 - x_{n-1}} \right),$$

and

$$p'_S : S^{n-2} \setminus S \rightarrow \mathbb{R}^{n-2}, \quad (x_1, \dots, x_{n-1}) \mapsto \left(\frac{x_1}{1 + x_{n-1}}, \frac{x_2}{1 + x_{n-1}}, \dots, \frac{x_{n-2}}{1 + x_{n-1}} \right),$$

are homeomorphisms with inverses

$$p'^{-1}_N(y_1, \dots, y_{n-2}) = \left(\frac{2y_1}{1 + y_1^2 + \dots + y_{n-2}^2}, \dots, \frac{2y_{n-2}}{1 + y_1^2 + \dots + y_{n-2}^2}, \frac{-1 + y_1^2 + \dots + y_{n-2}^2}{1 + y_1^2 + \dots + y_{n-2}^2} \right),$$

$$p'^{-1}_S(y_1, \dots, y_{n-2}) = \left(\frac{2y_1}{1 + y_1^2 + \dots + y_{n-2}^2}, \dots, \frac{2y_{n-2}}{1 + y_1^2 + \dots + y_{n-2}^2}, \frac{1 - y_1^2 - \dots - y_{n-2}^2}{1 + y_1^2 + \dots + y_{n-2}^2} \right).$$

Since

$$D_S^{n-2} := b \left(P_{m_1} \times \dots \times P_{m_k} \times \left(\bigcup_{i=2}^k v_1 \cdots \widehat{v}_i \cdots v_{k+1} \right) \right) \subset S^{n-2} \setminus N$$

and

$$D_N^{n-2} := b \left(\partial(P_{m_1} \times \dots \times P_{m_k} \times \Delta^k) \setminus \text{Int}(P_{m_1} \times \dots \times P_{m_k} \times \left(\bigcup_{i=2}^k v_1 \cdots \widehat{v}_i \cdots v_{k+1} \right)) \right) \subset S^{n-2} \setminus S,$$

p'_N and p'_S restrict to homeomorphisms p_N and p_S from D_S^{n-2} and D_N^{n-2} respectively to their images.

Notice that $P_{m_1} \times \dots \times P_{m_k} \times (\bigcup_{i=2}^k v_1 \cdots \widehat{v}_i \cdots v_{k+1})$ admits a presentation of the following form

$$\bigcup_{l=1}^k \bigcup_{j_l \in I_l} \bigcup_{i=2}^k \bigcup_{j=1, k+1} (F_{j_l} * \mathcal{C}_{m_1}) \times \dots \times (F_{j_l} * \mathcal{C}_{m_l}) \times \dots \times (F_{j_k} * \mathcal{C}_{m_k}) \times (v_1 \cdots \widehat{v}_i \widehat{v}_j \cdots v_{k+1} \mathcal{S}_k).$$

Each product on the right has $\mathcal{S} = (\mathcal{C}_{m_1}, \dots, \mathcal{C}_{m_k}, \mathcal{S}_k)$ as one of its vertices and it is a union of line segments from \mathcal{S} to a point on $\bigcup_{l=1}^k (F_{j_l} * \mathcal{C}_{m_1}) \times \dots \times F_{j_l} \times \dots \times (F_{j_k} * \mathcal{C}_{m_k}) \times (v_1 \cdots \widehat{v}_i \widehat{v}_j \cdots v_{k+1} \mathcal{C}_k) \cup (F_{j_1} * \mathcal{C}_{m_1}) \times \dots \times (F_{j_k} * \mathcal{C}_{m_k}) \times (v_1 \cdots \widehat{v}_i \widehat{v}_j \cdots v_{k+1})$ and the lines intersect only at \mathcal{S} . The line segments of different products above agree on the intersections. So $P_{m_1} \times \dots \times P_{m_k} \times (\bigcup_{i=2}^k v_1 \cdots \widehat{v}_i \cdots v_{k+1})$ is the union of line segments emanating from \mathcal{S} and the union of the end points different from \mathcal{S} of the line segments is $\partial(P_{m_1} \times \dots \times P_{m_k} \times (\bigcup_{i=2}^k v_1 \cdots \widehat{v}_i \cdots v_{k+1}))$. Thus, $p_N(D_S^{n-2})$ is the closure of an open set in \mathbb{R}^{n-2} containing the origin and $p_N(D_S^{n-2})$ is a union of line segments emanating from the origin such that each segment intersects $\partial(p_N(D_S^{n-2}))$ at only one point. Therefore, we have a homeomorphism $G_S : p_N(D_S^{n-2}) \rightarrow D^{n-2} \subset \mathbb{R}^{n-2}$ obtained similar to that of R .

Every line segment $x\mathcal{S}$ above and the point \mathcal{C} determine a half plane. This half plane intersects the subspace $\partial(P_{m_1} \times \dots \times P_{m_k} \times \Delta^k)$ at a piecewise linear path $\mathcal{N}y_1 \cdots y_mx\mathcal{S}$ such that $\mathcal{N}y_1 \cdots y_mx$ is mapped to a line segment emanating from the origin in $p_S(D_N^{n-2})$. Thus, $p_S(D_N^{n-2})$ is the closure of an open set in \mathbb{R}^{n-2} containing the origin and $p_S(D_N^{n-2})$ is a union of line segments emanating from the origin such that each segment intersects $\partial(p_S(D_N^{n-2}))$ at only one point. Therefore, we have a homeomorphism $G_N : p_S(D_N^{n-2}) \rightarrow D^{n-2} \subset \mathbb{R}^{n-2}$ obtained similar to that of R .

Now we define $f : S^{n-2} \rightarrow S^{n-2}$ by

$$f(x) = \begin{cases} p_N^{-1} \circ G_S \circ p_N(x), & x \in D_S^{n-2}, \\ p_S^{-1} \circ G_N \circ p_S(x), & x \in D_N^{n-2}. \end{cases}$$

Notice that each branch of f is continuous and they agree on the overlap. (See Figure 26.) So f is continuous. Being a continuous bijection from compact Hausdorff S^{n-2} onto itself, f is thus a homeomorphism.

Now we extend $f : S^{n-2} \rightarrow S^{n-2}$ to $F : D^{n-1} \rightarrow D^{n-1}$ by

$$F(x) = \begin{cases} f\left(\frac{x}{|x|}\right)|x|, & x \neq (0, \dots, 0), \\ (0, \dots, 0), & x = (0, \dots, 0). \end{cases}$$

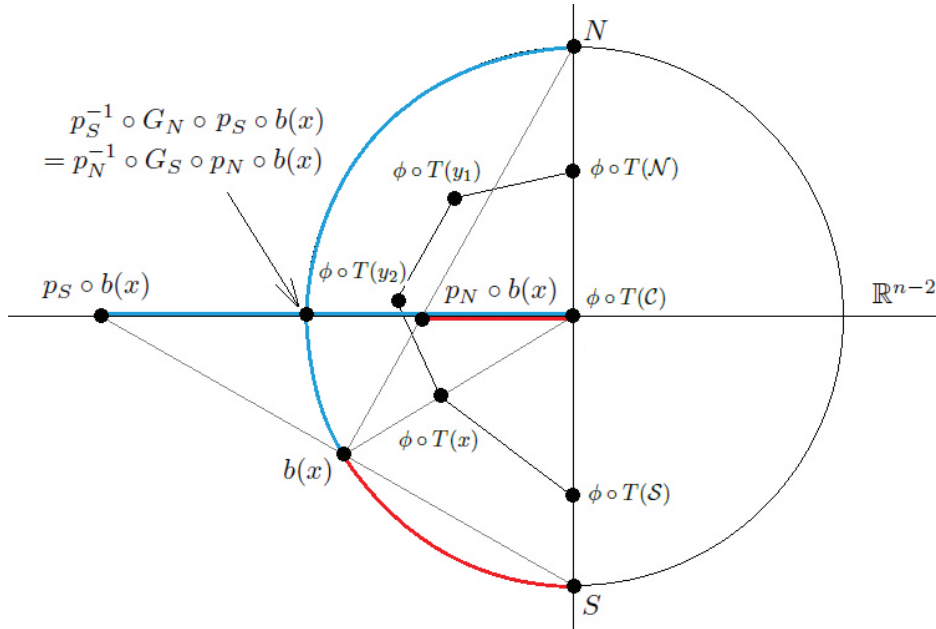


Figure 26. Two stereographic projections.

Similar to R , F is continuous at $x = (0, \dots, 0)$ because for any $\epsilon > 0$, if $|x| < \epsilon$, then

$$|F(x) - F(0)| = \left| f\left(\frac{x}{|x|}\right) \right| |x| = |x| < \epsilon.$$

Being a continuous bijection from compact Hausdorff D^{n-1} onto itself, F is thus a homeomorphism.

Therefore, the composition $F \circ b$ is a homeomorphism from $P_{m_1} \times P_{m_2} \times \dots \times P_{m_k} \times \Delta^k$ to D^{n-1} mapping $P_{m_1} \times P_{m_2} \times \dots \times P_{m_k} \times (\bigcup_{i=2}^k v_1 \dots \widehat{v}_i \dots v_{k+1})$ homeomorphically onto S_-^{n-2} . It follows that $F \circ b$ also maps the subspace $\partial(P_{m_1} \times P_{m_2} \times \dots \times P_{m_k} \times \Delta^k) \setminus \text{Int}(P_{m_1} \times P_{m_2} \times \dots \times P_{m_k} \times (\bigcup_{i=2}^k v_1 \dots \widehat{v}_i \dots v_{k+1}))$ homeomorphically onto S_+^{n-2} . □

Proof of Proposition 4.5. Define $H_{P_{m_1} \times \dots \times P_{m_k} \times \Delta^k} : (P_{m_1} \times \dots \times P_{m_k} \times \Delta^k) \times I \rightarrow P_{m_1} \times \dots \times P_{m_k} \times \Delta^k$ by

$$H_{P_{m_1} \times \dots \times P_{m_k} \times \Delta^k}(x, t) = b^{-1} \circ F^{-1} \circ H_{D^{n-1}}(F \circ b(x), t). \quad \square$$

A.2 Proof of Proposition 4.6

Now we prove Proposition 4.6.

Proof of Proposition 4.6. Let

$$S_-^{n-2} \times I_\epsilon := \{(x_1, \dots, x_{n-2}, x_{n-1} - \delta) \in \mathbb{R}^{n-1} : (x_1, \dots, x_{n-1}) \in S_-^{n-2}, 0 \leq \delta \leq \epsilon\},$$

and let the extended closed $(n - 1)$ -cell be

$$\text{Ext}_\epsilon(D^{n-1}) := D^{n-1} \cup (S_-^{n-2} \times I_\epsilon).$$

(See Figure 27.) Define

$$H_{S_-^{n-2} \times I_\epsilon} : (S_-^{n-2} \times I_\epsilon) \times I \rightarrow \text{Ext}_\epsilon(D^{n-1})$$

by

$$H_{S_-^{n-2} \times I_\epsilon}((x_1, \dots, x_{n-1}), t) = \left(x_1, \dots, x_{n-2}, x_{n-1} + t(x_{n-1} + \sqrt{1 - x_1^2 - \dots - x_{n-2}^2} + \epsilon) \frac{2\sqrt{1 - x_1^2 - \dots - x_{n-2}^2}}{\epsilon} \right).$$

Then $H_{S_-^{n-2} \times I_\epsilon}$ is a well-defined homotopy. It linearly extends each fiber over $(x_1, \dots, x_{n-2}, x_{n-1} - \epsilon)$ in $S_-^{n-2} \times I_\epsilon$ to the fiber in $\text{Ext}_\epsilon(D^{n-1})$. For each $t \in I$, $H_{S_-^{n-2} \times I_\epsilon}(\cdot, t)$ is a homeomorphism onto its image.

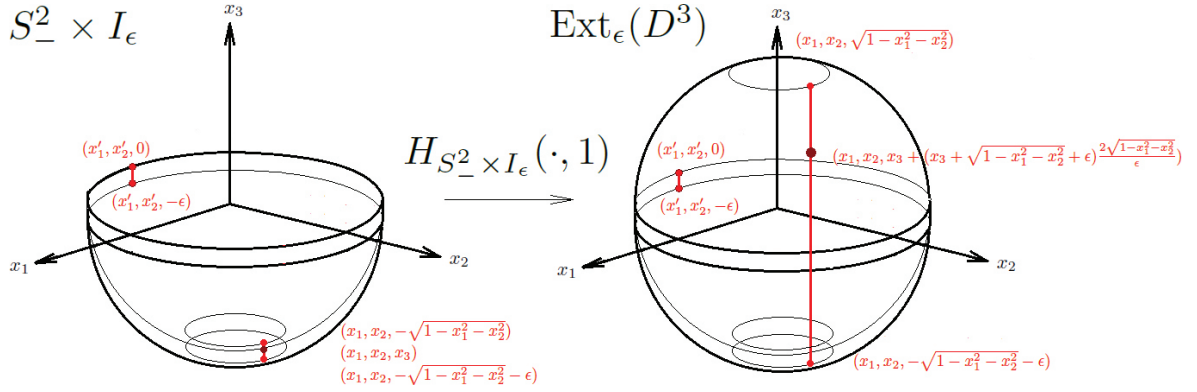


Figure 27. The extended closed 3-cell $\text{Ext}_\epsilon(D^3)$.

By extending R and possibly perturbing F , we get \tilde{R} and \tilde{F} such that

$$\tilde{F} \circ \phi \circ \tilde{R} \circ T : \left(P_{m_1} \times \cdots \times P_{m_k} \times \left(\bigcup_{i=2}^k v_1 \cdots \widehat{v}_i \cdots v_{k+1} \right) \right) \times I_\epsilon \rightarrow S_-^{n-2} \times I_\epsilon$$

is a homeomorphism whose images of $P_{m_1} \times \cdots \times P_{m_k} \times \left(\bigcup_{i=2}^k v_1 \cdots \widehat{v}_i \cdots v_{k+1} \right) \times \{0\}$ and $P_{m_1} \times \cdots \times P_{m_k} \times \left(\bigcup_{i=2}^k v_1 \cdots \widehat{v}_i \cdots v_{k+1} \right) \times \{\epsilon\}$ are S_-^{n-2} and $S_-^{n-2} - \{(0, \dots, 0, \epsilon)\}$, respectively. Furthermore, $F \circ b (= F \circ \phi \circ R \circ T)$ and $\tilde{F} \circ \phi \circ \tilde{R} \circ T$ agree on $P_{m_1} \times \cdots \times P_{m_k} \times \left(\bigcup_{i=2}^k v_1 \cdots \widehat{v}_i \cdots v_{k+1} \right)$.

We define

$$H_{(P_{m_1} \times \cdots \times P_{m_k} \times \left(\bigcup_{i=2}^k v_1 \cdots \widehat{v}_i \cdots v_{k+1} \right)) \times I_\epsilon} : \left(\left(P_{m_1} \times \cdots \times P_{m_k} \times \left(\bigcup_{i=2}^k v_1 \cdots \widehat{v}_i \cdots v_{k+1} \right) \right) \times I_\epsilon \right) \times I \rightarrow \text{Ext}_\epsilon(P_{m_1} \times \cdots \times P_{m_k} \times \Delta^k)$$

by

$$H_{(P_{m_1} \times \cdots \times P_{m_k} \times \left(\bigcup_{i=2}^k v_1 \cdots \widehat{v}_i \cdots v_{k+1} \right)) \times I_\epsilon}(x, t) = T^{-1} \circ \tilde{R}^{-1} \circ \phi^{-1} \circ \tilde{F}^{-1} \circ H_{S_-^{n-2} \times I_\epsilon}(\tilde{F} \circ \phi \circ \tilde{R} \circ T(x), t).$$

Notice that

$$H_{P_{m_1} \times \cdots \times P_{m_k} \times \Delta^k}(\cdot, t) = H_{(P_{m_1} \times \cdots \times P_{m_k} \times \left(\bigcup_{i=2}^k v_1 \cdots \widehat{v}_i \cdots v_{k+1} \right)) \times I_\epsilon}(\cdot, t)$$

on $P_{m_1} \times \cdots \times P_{m_k} \times \left(\bigcup_{i=2}^k v_1 \cdots \widehat{v}_i \cdots v_{k+1} \right)$ for each $t \in I$. Then we can define

$$H_{\text{Ext}_\epsilon(P_{m_1} \times \cdots \times P_{m_k} \times \Delta^k)} : \text{Ext}_\epsilon(P_{m_1} \times \cdots \times P_{m_k} \times \Delta^k) \times I \rightarrow \text{Ext}_\epsilon(P_{m_1} \times \cdots \times P_{m_k} \times \Delta^k)$$

by

$$H_{\text{Ext}_\epsilon(P_{m_1} \times \cdots \times P_{m_k} \times \Delta^k)}(x, t) = H_{P_{m_1} \times \cdots \times P_{m_k} \times \Delta^k}(x, t)$$

if $x \in P_{m_1} \times \cdots \times P_{m_k} \times \Delta^k$ and

$$H_{\text{Ext}_\epsilon(P_{m_1} \times \cdots \times P_{m_k} \times \Delta^k)}(x, t) = H_{(P_{m_1} \times \cdots \times P_{m_k} \times \left(\bigcup_{i=2}^k v_1 \cdots \widehat{v}_i \cdots v_{k+1} \right)) \times I_\epsilon}(x, t)$$

if $x \in (P_{m_1} \times \cdots \times P_{m_k} \times \left(\bigcup_{i=2}^k v_1 \cdots \widehat{v}_i \cdots v_{k+1} \right)) \times I_\epsilon$. It can be readily checked that the three conditions are satisfied. \square

B Different representations for planar planted labelled black and white bipartite trees

In this section, we review the following bijections.

The bijection between formulas and trees was given in [20]. The bijection between sequences of complexity ≤ 2 and formulas was given in [33] and the map from the planar planted labelled black and white bipartite

trees to sequences is contained in [23, Section 4.4] after converting the tree to an arc picture, see below. This is enough to establish the following bijections:

$$\begin{array}{ccc}
 & S \text{ planted planar bipartite trees} & \\
 \swarrow & & \searrow \\
 S \text{ sequences of complexity } \leq 2 & \longleftrightarrow & S \text{ formulas.}
 \end{array}
 \tag{B.1}$$

We will briefly review these constructions and explicitly add a new map back from sequences of complexity ≤ 2 . The interesting feature is that we establish that these sequences explicitly yield a poset structure on the set S , thus exhibiting the tree-like structure explicitly.

In Figure 28, we show the labelings in both cacti (trees) and sequences for the case of P_3 as a kind of Rosetta Stone.

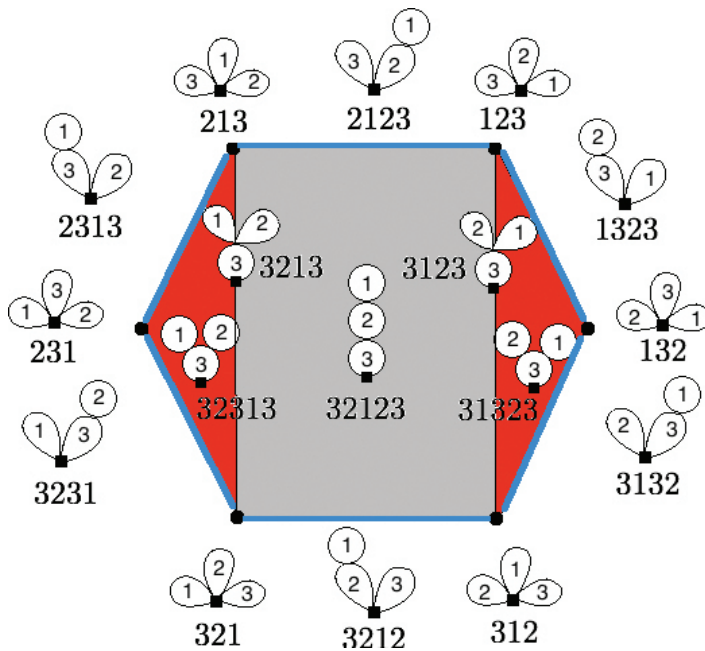


Figure 28. Part of Figure 17 marked with sequences as well.

B.1 Trees/cacti and sequences

B.1.1 From trees to sequences

Given a planar planted b/w labelled tree, whose vertices are labelled by a set S , we get a sequence as follows. Embed the tree in the plane. Start at the root and go counterclockwise around the tree. If you hit a white vertex, record its label.

B.1.2 From sequences of complexity ≤ 2 to trees

Recall from [33] that a non-repeating sequence in S has complexity ≤ 2 if each non-repeating subsequence of i, j has one of the following four forms: ij, ji, iji, jij . This allows us to give a partial relation on S as follows: $i < j$ if the subsequence is of the form iji . The partial relation is actually a partial order, since it is transitive. Indeed, assume that $i < j$ and $j < k$; then the subsequence of i, j, k must be of the form $ijkji$, since deleting k

must yield iji and deleting i must yield jkj . We can represent this partial order by an ordered rooted forests (of planar planted trees with only white vertices), the roots being the initial elements. There might be more than one minimal element, but all of them are linearly ordered by their first appearance in the sequence. We can then add a black root to these using the B_b^+ operator. In order to obtain the a b/w bipartite tree, we notice that if two vertices labelled by i and j , with i coming before j in the sequence, have the same predecessor k , their subsequence can be either $kijk$ or $kijik$. In the first instance, we collapse the angle between i and j . Continuing this with all pairs, we arrive at a b/w tree. It is clear that these maps are inverses to each other.

This also gives a nice interpretation of the exterior cells. These are the cells whose sequences yield a partial order with more that one minimal element. Compare Figure 28.

B.1.3 Cacti/arcs/sequenes

A more general setting is given as follows. Every tree of the above kind corresponds to a cactus which in turn corresponds dually to a family of arcs on a genus 0 surface, see [18, 25] summarized in Figure 29. The morphism from arc families on surface of any genus to sequences is given in [23, Section 4.4]. This coincides with the sequence read off from the tree. Indeed in a cactus, if one deletes all the intersection points and the root, one is left with disjoint union of labelled arcs. The labelling is by the label of the lobe they belong to. Each such arc is actually dual to an arc in the arc picture and the counter-clock wise order of them coincides with the one on the arcs. This is directly seen from the chord diagram (see Figure 29 and [18] as well).

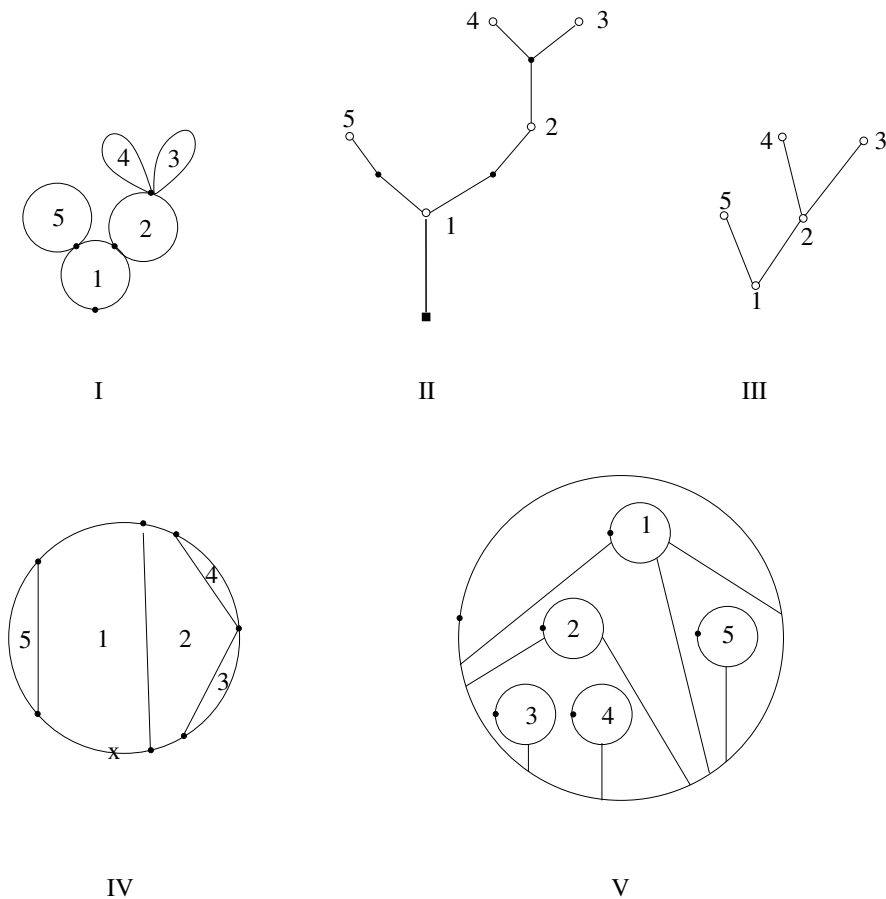


Figure 29. I: a cactus without spines; II: its black and white tree; III: its dual tree giving the poset structure; IV: its chord diagram; V: its image as an arc family, see [18, 20, 25] for details. The corresponding sequence is 12342151.

B.2 From planar planted bipartite trees to formulas

This is contained in [20] simply by using flow charts. It is obvious that the following two procedures are bijective. We will briefly recall them.

B.2.1 From a formula to a tree

A formula is a combination of nested operations of two possible kinds: iterated \cup and higher braces. Given such a formula, write down a flow chart. There is a black vertex of arity l for each iterated cup product multiplying l elements. Put a white vertex of arity l if there is a higher brace operation of the type $f\{g_1, \dots, g_l\}$. Put the edges corresponding to the nesting, that is feed the result of inner operations into the next outer operation. Including the empty iteration of \cup as the identity, one obtains a bipartite tree.

B.2.2 From a tree to a formula

This is simply the reverse procedure, think of every black vertex as the operation “iterated cup” and every white vertex “higher brace” of the natural arity, then read off the sequence of operations defined by this flow chart.

B.3 Surjections and sequences

The relationship between surjections and sequences is given explicitly in [6]. As mentioned previously, it would be very interesting to learn more about the relationship between the current work and the Barrat–Eccles operad.

B.4 Lattice paths and homotopy diagonals

The equivalence of sequences and elements of the lattice path operad is given in [2]. In the case of complexity ≤ 2 this is exactly the sequence given by the homotopy diagonal in [18] (see [18, Figure 9]).

Acknowledgment: We would like thank Clemens Berger for discussions. Ralph M. Kaufmann would like to thank the Max-Planck-Institute for Mathematics in Bonn for the hospitality and the Program of Higher Structures. We also thank the referee for his comments and careful reading of the paper.

Funding: Ralph M. Kaufmann thankfully acknowledges support from the Simons foundation under collaboration grant #317149. Yongheng Zhang acknowledges support from Amherst College.

References

- [1] M. A. Batanin, Symmetrisation of n -operads and compactification of real configuration spaces, *Adv. Math.* **211** (2007), no. 2, 685–725.
- [2] M. A. Batanin and C. Berger, The lattice path operad and Hochschild cochains, in: *Alpine Perspectives on Algebraic Topology. Third Arolla Conference on Algebraic Topology* (Arolla 2008), *Contemp. Math.* 504, American Mathematical Society, Providence (2009), 23–52.
- [3] C. Berger, Combinatorial models of real configuration spaces and E_n -operads, in: *Operads. Proceedings of Renaissance Conferences* (Hartford/Luminy 1995), *Contemp. Math.* 202, American Mathematical Society, Providence (1997), 37–52.
- [4] C. Berger, Cellular structures for E_n -operads, preprint (1998), <http://math.unice.fr/~cberger/cell.pdf>.

- [5] C. Berger, Double loop spaces, braided monoidal categories and algebraic 3-type of space, in: *Higher Homotopy Structures in Topology and Mathematical Physics* (Poughkeepsie 1996), Contemp. Math. 227, American Mathematical Society, Providence (1999), 49–66.
- [6] C. Berger and B. Fresse, Combinatorial operad actions on cochains, *Math. Proc. Cambridge Philos. Soc.* **137** (2004), 135–174.
- [7] P. V. M. Blagojević and G. M. Ziegler, Convex equipartitions via equivariant obstruction theory, *Israel J. Math* **200** (2014), 49–77.
- [8] J. M. Boardman and R. M. Vogt, *Homotopy Invariant Algebraic Structures on Topological Spaces*, Lecture Notes in Math. 347, Springer, Berlin, 1973.
- [9] G. Carlsson and J. Milgram, Stable homotopy and iterated loop spaces, in: *Handbook of Algebraic Topology*, North-Holland, Amsterdam (1995), 505–583.
- [10] M. Chas and D. Sullivan, String topology, preprint (1998), <https://arxiv.org/abs/math/9911159>.
- [11] F. R. Cohen, The homology of C_{n+1} -spaces, $n \geq 0$, in: *Homology of Iterated Loop Spaces*, Lecture Notes in Math. 533, Springer, Berlin (1976), 207–351.
- [12] A. Connes and D. Kreimer, Hopf algebras, renormalization and noncommutative geometry, *Comm. Math. Phys.* **199** (1998), no. 1, 203–242.
- [13] Z. Fiedorowicz, Construction of E_n operads, preprint (1999), <https://arxiv.org/abs/math/9808089>.
- [14] R. Fox and L. Neuwirth, The braid groups, *Math. Scand.* **10** (1962), 119–126.
- [15] M. Gerstenhaber and A. A. Voronov, Higher-order operations on the Hochschild complex (in Russian), *Funktsional. Anal. i Prilozhen.* **29** (1995), no. 1, 1–6, 96; translation in *Funct. Anal. Appl.* **29** (1995), no. 1, 1–5.
- [16] E. Getzler and J. Jones, Operads, homotopy algebras and iterated integrals for double loop spaces, preprint (1994), <https://arxiv.org/abs/hep-th/9403055>.
- [17] M. M. Kapranov, Permuto-associahedron, MacLane coherence theorem and asymptotic zones for the KZ equation, *J. Pure App. Algebra* **85** (1993), 119–142.
- [18] R. M. Kaufmann, On several varieties of cacti and their relations, *Algebr. Geom. Topol.* **5** (2005), 237–300.
- [19] R. M. Kaufmann, Letter to P. Salvatore, Mar 31, (2006), <http://www.math.purdue.edu/~rkaufman/talks.html>.
- [20] R. M. Kaufmann, On spineless cacti, Deligne’s conjecture and Connes–Kreimer’s Hopf algebra, *Topology* **46** (2007), 39–88.
- [21] R. M. Kaufmann, A proof of a cyclic version of Deligne’s conjecture via Cacti, *Math. Res. Lett.* **15** (2008), no. 5, 901–921.
- [22] R. M. Kaufmann, Moduli space actions on the Hochschild cochain complex II: Correlators, *J. Noncommut. Geom.* **2** (2008), no. 3, 283–332.
- [23] R. M. Kaufmann, Dimension vs. genus: A surface realization of the little k -cubes and an E_∞ -operad, in: *Algebraic Topology – Old and New. M. M. Postnikov Memorial Conference*, Banach Center Publ. 85, Polish Academy of Sciences, Warsaw (2009), 241–274.
- [24] R. M. Kaufmann, Graphs, strings and actions, in: *Algebra, Arithmetic and Geometry Vol II: In Honor of Yu. I. Manin*, Progr. Math. 270, Birkhäuser, Boston (2010), 127–178.
- [25] R. M. Kaufmann, M. Livernet and R. C. Penner, Arc operads and arc algebras, *Geom. Topol.* **7** (2003), 511–568.
- [26] R. M. Kaufmann and R. Schwell, Associahedra, cyclohedra and a topological solution to the A_∞ -Deligne conjecture, *Adv. Math.* **223** (2010), no. 6, 2166–2199.
- [27] M. Kontsevich, Operads and motives in deformation quantization, *Lett. Math. Phys.* **48** (1999), no. 1, 35–72.
- [28] M. Kontsevich and Y. Soibelman, Deformations of algebras over operads and the Deligne conjecture, in: *Conférence Moshé Flato 1999: Quantization, Deformation, and Symmetries. Vol. I* (Dijon 1999), Math. Phys. Stud. 21, Kluwer Academic Publishers, Dordrecht (2000), 255–307.
- [29] M. Markl, S. Shnider and J. Stasheff, *Operads in Algebra, Topology and Physics*, Math. Surveys Monogr. 96, American Mathematical Society, Providence, 2002.
- [30] J. P. May, *The Geometry of Iterated Loop Spaces*, Lectures Notes in Math. 271, Springer, Berlin, 1972.
- [31] J. P. May, Definitions: Operads, algebras and modules, in: *Operads. Proceedings of Renaissance Conferences* (Hartford/Luminy 1995), Contemp. Math. 202, American Mathematical Society, Providence (1997), 1–7.
- [32] J. E. McClure and J. H. Smith, A solution of Deligne’s Hochschild cohomology conjecture, in: *Recent Progress in Homotopy Theory* (Baltimore 2000), Contemp. Math. 293, American Mathematical Society, Providence (2002), 153–193.
- [33] J. E. McClure and J. H. Smith, Multivariable cochain operations and little n -cubes, *J. Amer. Math. Soc.* **16** (2003), 681–704.
- [34] J. E. McClure and J. H. Smith, Cosimplicial objects and little n -cubes. I, *Amer. J. Math.* **126** (2004), 1109–1153.
- [35] R. J. Milgram, Iterated loop spaces, *Ann. of Math. (2)* **84** (1966), 386–403.
- [36] J. R. Munkres, *Elements of Algebraic Topology*, Addison-Wesley, Menlo Park, 1984.
- [37] P. Palacios and M. Ronco, Weak Bruhat order on the set of faces of the permutohedron and the associahedron, *J. Algebra* **229** (2006), no. 2, 648–678.
- [38] M. Salvetti, Topology of the complement of real hyperplanes in \mathbb{C}^N , *Invent. Math.* **88** (1987), 603–618.
- [39] J. H. Smith, Simplicial goup models for $\Omega^n S^n X$, *Israel J. Math.* **66** (1989), 330–350.
- [40] R. Steiner, A canonical operad pair, *Math. Proc. Camb. Phil. Soc.* **86** (1979), 443–449.
- [41] D. E. Tamarkin, Another proof of M. Kontsevich formality theorem, preprint (1998), <https://arxiv.org/abs/math/9803025>.

- [42] D. E. Tamarkin, Formality of chain operad of little discs, *Lett. Math. Phys.* **66** (2003), 65–72.
- [43] A. Tonks, Relating the associahedron and the permutohedron, in: *Operads. Proceedings of Renaissance Conferences* (Hartford/Luminy 1995), *Contemp. Math.* 202, American Mathematical Society, Providence (1997), 33–36.
- [44] V. Tourchine, Dyer–Lashof–Cohen operations in Hochschild cohomology, *Algebr. Geom. Topol.* **6** (2006), 875–894.
- [45] T. Tradler and M. Zeinalian, On the cyclic Deligne conjecture, *J. Pure Appl. Algebra* **204** (2006), no. 2, 280–299.
- [46] A. A. Voronov, Homotopy Gerstenhaber algebras, in: *Conférence Moshé Flato 1999: Quantization, Deformation, and Symmetries. Vol. II* (Dijon 1999), *Math. Phys. Stud.* 22, Kluwer Academic Publishers, Dordrecht (2000), 307–331.
- [47] A. A. Voronov, Notes on universal algebra, in: *Graphs and Patterns in Mathematics and Theoretical Physics*, *Proc. Sympos. Pure Math.* 73, American Mathematical Society, Providence (2005), 81–103.
- [48] B. C. Ward, Cyclic A_∞ structures and Deligne’s conjecture, *Algebr. Geom. Topol.* **12** (2012), no. 3, 1487–1551.
- [49] G. M. Ziegler, *Lectures on Polytopes*, *Grad. Texts in Math.* 152, Berlin, New York, 1995.